Year : 2019

INVOLVEMENTS OF MICROGLIAL POTASSIUM CHANNELS IN NEUROPATHIC PAIN

Gattlen Christophe

UNIL | Université de Lausanne
Faculté de biologie
et de médecine

Centre d'antalgie, service d'anesthésiologie (CHUV)

INVOLVEMENTS OF MICROGLIAL POTASSIUM CHANNELS IN NEUROPATHIC PAIN

Thèse de doctorat ès sciences de la vie (PhD)

Présentée à la

Faculté de Biologie et de Médecine
De l'Université de Lausanne

Par

Christophe GATTLEN

Diplômé en biologie médicale par l'Université de Lausanne

Jury

Prof. Bogdan Draganski, Président
PD. Dr. Marc Suter, Directeur
Prof. Jean-Yves Chatton, Expert
Prof. Stefan Kellenberger. Expert
PD. Dr. Jean-Sébastien Rougier, Expert

Lausanne, 2019

UNIL | Université de Lausanne
Faculté de biologie
et de médecine

Centre d'antalgie, service d'anesthésiologie (CHUV)

INVOLVEMENTS OF MICROGLIAL POTASSIUM CHANNELS IN NEUROPATHIC PAIN

Thèse de doctorat ès sciences de la vie (PhD)

Présentée à la

Faculté de Biologie et de Médecine
De l'Université de Lausanne

Par

Christophe GATTLEN

Diplômé en biologie médicale par l'Université de Lausanne

Jury

Prof. Bogdan Draganski, Président
PD. Dr. Marc Suter, Directeur
Prof. Jean-Yves Chatton, Expert
Prof. Stefan Kellenberger. Expert
PD. Dr. Jean-Sébastien Rougier, Expert

Lausanne, 2019

UNIL | Université de Lausanne

UNIL | Université de Lausanne
Faculté de biologie et de médecine

Ecole Doctorale
Doctorat ès sciences de la vie

Imprimatur

Vu le rapport présenté par le jury d'examen, composé de

Président·e	Monsieur	Prof. Bogdan **Draganski**
Directeur·rice de thèse	Monsieur	Dr Marc **Suter**
Experts·es	Monsieur	Prof. Jean-Yves **Chatton**
	Monsieur	Prof. Stephan **Kellenberger**
	Monsieur	Dr Jean-Sébastien **Rougier**

le Conseil de Faculté autorise l'impression de la thèse de

Monsieur Christophe Gattlen

Maîtrise universitaire ès Sciences en biologie médicale Université de Lausanne

intitulée

Involvements of microglial potassium channels in neuropathic pain

Lausanne, le 13 mars 2019

pour le Doyen
de la Faculté de biologie et de médecine

Prof. Bogdan Draganski

Table of content

Acknowledgments

First, I would like to thank Marc Suter, my thesis director who pushed me to become independent, helping me to sharpen my mind to make new hypothesis and create better experimental designs. Although it was not easy in the beginning since I had a tendency to scatter my attention on many experiments, he really improved my way of thinking in a more structured and efficient way.

I would also like to express my gratitude to Isabelle Decosterd, who invited me in her lab team and allowed me to use her resources to accomplish the research we were dedicated to with Marc. I am also obliged to Violeta Ristoiu who welcomed me in her laboratory in Bucharest, in Romania. As well as her post-doc, also my predecessor Alexandru-Florian Deftu, who taught me the tough and tricky techniques of electrophysiology. More than a mentor, Alex is a friend. I want to thank him for what he made me appreciate both in the biology field and out of the lab. Noroc!

Big thanks for Gil Vantomme whom precious help and patience assisted me through my first steps in electrophysiology back in Lausanne. He also improved a lot my slicing technique. He made me a better scientist. Thanks a lot Gil.

I want to thank Anne Rocher who also assisted to improve and troubleshoot my slice electrophysiology. Her pieces of advice and good mood helped me.

I am grateful to all the members of the lab for their help, teaching, and advice. Their support carried me to where I am today. Especially to Ludovic Gillet, who improved my reasoning and my designs by often challenging me with questions. This pushed me to better understanding and new hypothesis. He also helped me a lot for troubleshooting the electrophysiology setup. He is one of the reasons why I succeeded. So I wish to thank him a lot for that.

Thanks also to Marie Pertin and to Guylène Kirschmann who taught me a lot and were always there when I needed.

I wish to thank Romain-Daniel Gosselin and Romain Cardis for their precious guidance concerning statistics and experimental designs according to good practices in statistics.

I wish to thank my family and friends who supported me, especially through the difficult part of my thesis. Thanks from the bottom of my heart for believing in me - more than I did myself at some times - and for pushing me to accomplish my thesis work.

I also wish to thank all my colleagues of the DNF, with who I shared good times: Yves, Lucas (Cake), Camille, Lara, Michel, Adrian, Ioanna, Susie, Emilie, Dany, Dominique, Frédérique, Elidie, Romain, Georgia, Tamara, Massimo, Salvatore, Céline, Joel, Nadia, Muna, Annick,... the list goes on. Thank you for bringing the joy and laughter that pushed me through the day.

I also thank the fond national Suisse de la recherche scientifique (FNSRS), the European society of anaesthesiology (ESA) and Professor Kern head of the the department of anesthesiology for the fundings that allowed me to do this exciting work.

Abstract

After peripheral nerve injury, erratic nerve influxes generated in sensory neurons sensitize secondary neurons located in the dorsal horn of the spinal cord. This abnormal signaling causes hyperalgesia and allodynia – hallmarks of neuropathic pain. Those injured neurons also release neuronal factors that activate microglia, the immune cells of the central nervous system. Microglia secrete many pro-inflammatory factors such as cytokines and chemokines, which will participate in the sensitization process. Microglia, although non-excitable cells, show important changes in their potassium currents dependent of activation state.

During this thesis, I investigated microglial potassium channels in the context of neuropathic pain using the spared nerve injury (SNI) model. This model imitates a nerve injury and the neuropathic pains that follows. The goal was to determine if potassium channels participate in microglial activation and what physiological function they could influence in these cells. First, I analyzed previous data from the laboratory, which I completed and presented in a manuscript describing the timecourse of microglial activation and lymphocyte T infiltration after SNI.

I investigated for Kv1.3, Kv1.5 and Kir2.1, the main potassium channels described in microglial activation. I could highlight their presence in spinal microglia after SNI.

Then I could demonstrate that potassium currents I identified as Kir2.1-dependent were increased in microglia 2 days following SNI. Besides, the microglial resting membrane potential was hyperpolarized after SNI and could be depolarized using the Kir2.x blocker ML133. I hypothesized that this hyperpolarized resting membrane potential was necessary for microglial proliferation. I then could demonstrate that ML133 strongly reduced proliferation of a BV2 microglial cell line. Following my hypothesis, we collaborated with a former colleague now in the USA, to validate that in vivo. Intrathecal injection of ML133 could reduce microglial proliferation and mechanical hypersensitivity after SNI.

Although there is still much work to do, these results give us a potential novel target for therapy against neuropathic pain based on modulation of the resting membrane potential of microglia.

French summary

Après une lésion nerveuse, des influx électriques erratiques sont générés dans les neurones sensoriels et sensibilisent les neurones de second ordre situés dans la corne dorsale de la moelle épinière. Ce signalement anormal génère de l'hyperalgésie et de l'allodynie – des caractéristiques typiques de la douleur neuropathique. De plus ces neurones endommagés vont libérer des facteurs neuronaux qui activent la microglie, les cellules immunitaires du système nerveux central. Dans cet état, la microglie sécrète de nombreux facteurs pro-inflammatoires tels que des cytokines et chimiokines, qui vont participer au processus de sensibilisation. Les cellules microgliales, bien que n'étant pas des cellules excitables présentent des changements importants dans leurs courants potassiques une fois activées.

Durant ma thèse, j'ai examiné les canaux potassiques de la microglie dans le modèle de douleur neuropathique d'épargne du nerf sural (SNI). Ce modèle induit une lésion nerveuse et la douleur neuropathique qui s'en suit. Le but était de déterminer si les canaux potassiques participaient à l'activation microgliale et quelles conditions physiologiques ils pouvaient influencer. Tout d'abord, j'ai analysé des données obtenues préalablement dans le laboratoire et rédigé un premier article dont le thème était la temporalité de l'activation microgliale et l'infiltration des lymphocytes T après SNI.

J'ai cherché Kv1.3, Kv1.5 et Kir2.1, les principaux canaux potassiques décrits dans l'activation de la microglie. J'ai pu démontrer leur présence dans la microglie de la moelle épinière après SNI. Puis j'ai pu démontrer que suite à l'activation de la microglie induite par le modèle SNI, les courants potassiques provenant de Kir2.1 augmentaient 2 jours après la lésion nerveuse. De plus le potentiel de repos de la membrane des cellules microgliales était hyperpolarisé après SNI et pouvait être dépolarisé en bloquant les canaux Kir2.x avec du ML133. J'ai émis l'hypothèse selon laquelle un potentiel de repos de la membrane hyperpolarisé était nécessaire à la prolifération de la microglie. Le bloqueur a pu fortement réduire la prolifération de lignées cellulaires microgliale (BV2) en culture. Suivant mon hypothèse, nos anciens collègues maintenant aux USA ont pu valider in vivo par injection intrathécale de ML133 la réduction de la prolifération microgliale ainsi que l'hypersensibilité mécanique après SNI.

Bien qu'il reste encore beaucoup de travail, ces résultats mettent en évidence une potentielle nouvelle cible pour la thérapie contre la douleur neuropathique, basée sur la modulation du potentiel de membrane au repos de la microglie.

List of abbreviations

4-AP	4-Aminopyridine
ATP	Adenosine triphosphate
BBB	Blood-brain barrier
BDNF	Brain-derived neurotrophic factor
BrdU	Bromodeoxyuridine
CCI	Chronic constriction injury
CCL1, 2, 3, …	Chemokine CC motif ligand 1, 2, 3, …
CCR1, 2, 3, …	Chemokine CC motif receptor 1, 2, 3, …
CD2, 8, …	Cluster of differentiation 2, 8, …
CFA	Complete Freund's adjuvant
CGRP	Calcitonin gene-related peptide
CNS	Central nervous system
CSF-1/M-CSF	Macrophage colony stimulating factor 1
CX3CL1	Chemokine (C-X3-C motif) ligand 1, also called Fractalkine
CX3CR1	Chemokine (C-X3-C motif) receptor 1
CXCL1, 2, 3…	Chemokine (C-X-C motif) ligand 1, 2, 3, …
DAPI	4',6-diamidino-2-phénylindole
DHi	Dorsal horn ipsilateral (to the treatment)
DRG	Dorsal root ganglion
FACS	Fluorescence-activated cell sorting
GABA	Gamma-aminobutyric acid
GFP	Green fluorescent protein
GPCR	G-protein coupled receptor
IL-6, 10, …	Interleukin 6, 10, …
L3-L5	Region from the lumbar vertebrae 3 to 5
LPS	Lipopolysaccharide
L5Tx	L5 transection
mRNA	Messenger ribonucleic acid
NO	Nitric oxide
P2X4, 7	P2X purinoceptor 4, 7
P(S)NL	Partial (sciatic) nerve ligation
RIN	RNA integrity number
qPCR	Quantitative polymerase chain reaction
RFP	Red fluorescent protein
RMP	Resting membrane potential
ROS	Reactive oxygen species
SCI	Spinal cord injury
SNI	Spared nerve injury
SNL	Spinal nerve ligation
TGF-β	Transforming growth factor beta
TLR 2, 4, …	Toll-like receptors 2, 4, …
TNF-α	Tumor necrosis factor alpha
TEA	Tetraethylammonium
TPA	Tetrapenthylammonium
TrkB	Tropomyosin-related kinase receptor B
TRP	Transient receptor potential
TRPV1	Transient receptor potential V1

Introduction

The awareness of environmental threats is crucial for one's survival. Through the aversive feeling of pain, the peripheral nervous system detects harmful or potentially harmful sources and sends a signal to the central nervous system which is interpreted there as a danger signal. If at first the pain experimented allows an organism to avoid the worst, then the reminiscence of the condition where this aversive signal appears will have the same effect. Pain also has a protective role in the long term. Once an organism is injured, the pain will remind it to be careful until its wounds are healed. Pain is necessary for the survival of organisms. However, in some cases, pain can lose this role. We call these occurrences maladaptive pain.

The study of pain started since long ago. Already scholars of ancient Greece were intrigued by this particular condition. Back then, Aristotle did not describe it as one of the five senses, but rather like an emotion as for pleasure (Dallenbach 1939). There were also other theories, for instance, Hippocrates was convinced that an imbalance of vital human fluids was the cause of pain. Unlike today, people of this era were persuaded that the heart was the organ responsible for the pain sensation (Linton 2005).

In the Middle age, pain was not well understood. As religion had a very strong influence at this time, pain was considered as a punishment from God, a sensation coming from above rather than from the body itself. Its only remedy would be prayers, as a trial for one to reaffirm its faith through piety and suffering (Meldrum 2001).

In the Renaissance, intellectuals such as René Descartes in the Treatise of Man (1644) elaborated the theory that pain would travel along nerve fibers to the brain. This changed the mystical and spiritual vision of pain to a physiological sensation. From this moment on, pain has been seen as a torment that can be cured by medical treatment, instead of supplications.

Today we know that pain is a complex biological phenomenon of signal transmission, modulation and integration. A remarkable circuit of neurons forms the path from the peripheral nerve terminal to the brain. Research has grown in the field showing also involvement of glial cells in the modulation of neuronal excitability.

§1 Pain and Neuropathic pain

i Pain - definition and mechanisms

Pain is an unpleasant sensory and emotional experience associated with actual or potential tissue damage, or described in terms of such damage (IASP).

Stimuli are detected in the periphery by nerve endings. There, mechanoreceptors detect pressure, stretch, vibration or light brush stimuli. Nerve terminals also contain ions channels sensitive to heat, cold or pH. Mechanical stimuli induce action potentials in large fibers (Aα and Aβ, or Aδ for painful mechanical stimuli), while temperature induced stimuli travel along smaller fibers (Aδ, C) (Woolf and Ma 2007, Dubin and Patapoutian 2010) (Figure 1).

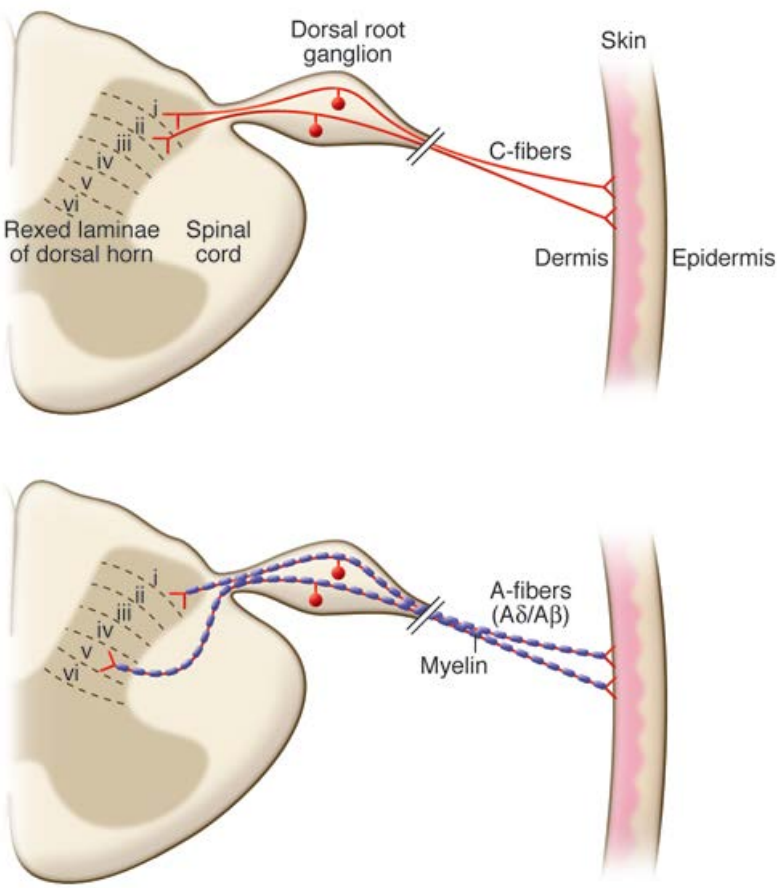

Figure 1: Nociceptive fibers. Representation of the different fibers that will transfer nociceptive information to the spinal cord. These neurons have their cell body in the dorsal root ganglion and connects to second order neurons in different layers of the dorsal horn. Mechanical stimuli are conveyed by myelinated A-fibers (mostly Aδ), while temperature stimuli travel through C-fibers.

Modified from Dubin and Patapoutian (2010)

The transmission of this information occurs via action potentials through sensory neurons whose cell bodies are located in the dorsal root ganglia (DRG). The information is then transferred to second order neuron and relayed to the brain.

Nociceptive neurons are harder to excite but once triggered, they send a burst of action potentials transmitted by both medium thin myelinated (Aδ) and small unmyelinated fibers (C) in the dorsal horn. There, the transmission of the nociceptive information occurs via glutamate, but also via calcitonin gene-related peptide (CGRP) and substance P (Seybold 2009). This information is modulated by local inhibitory interneurons or by neurons descending from the brain in the spinal cord. After modulation, if the signal reaches a certain threshold, it is transmitted by a second order neuron to the brain where this nociceptive information is integrated as pain (Basbaum 2009).

There are four steps necessary for the signaling of pain (Figure 2). First, nociceptors nerve endings detect a noxious stimulus in periphery. There, receptors will transduce it in an electrical signal if the stimuli exceed a certain threshold. For instance neuronal transient receptor potential ion channel V1 (TRPV1) channels in nerve terminals activates if the temperature is greater than 43° (Tominaga and Caterina 2004).

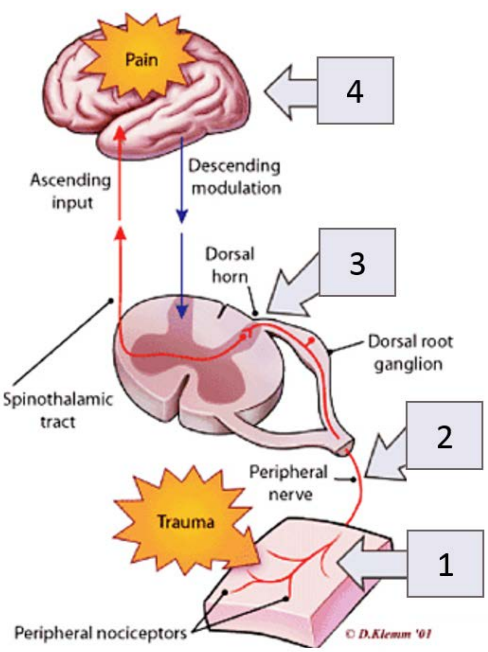

Figure 2: Nociception to pain integration. Representation of the four steps for a nociceptive signal to be integrated as pain.

1) Transduction in electrical signal of the threat.

2) Transmission along the nerve.

3) Modulation in the spinal cord.

4) Integration of the nociceptive information in the brain where it is interpreted as pain.

Modified from Gottschalk and Smith 2001

To generate an action potential, several conditions must be reunited. First, the depolarization of the nerve ending must reach a certain threshold. For instance, following heat stimuli, TRPV1 channels open and allows the entry of Ca^{2+}, Na^{+} and K^{+} as they are non-specific cations channels. This entry of cations will locally depolarize the membrane. (Harriott and Gold 2009). In general, activation of nociceptive receptors is proportional to the intensity of the stimulus, as it happens for heat detection by TRPV1 channels. If enough TRPV1 opens, this local potential becomes higher than the threshold and an action potential is generated through activation of voltage-gated sodium channels. (Caterina et al. 1997)

Secondly, the electric signal is transmitted from the injury site to the spinal cord. through the opening of the voltage-gated sodium channels (Navs). After the transmission, Navs become inactivated for some time before they can be solicited again (refractory period). The propagation of action potential in nociceptive fibers is mediated by Nav1.6, Nav1.7 and Nav1.8 (Woolf and Ma 2007).

In addition, as the soma is more negative than the nerve endings (-70 mV) (Gold et al. 1996), the action potentials transmitted must have a certain power to also depolarize the region of the soma with the T-junction and propagate to the other endings of the nociceptive neurons, located in the spinal cord. Thus, low stimuli are ignored. A burst of action potentials with a certain frequency is required to pass through the T-junction. Interestingly, this filtering is reduced after nerve injury (Gemes et al. 2013).

Thirdly, this signal will be modulated in the spinal cord by different processes. One inhibitory mechanism is called gate control (Figure 3). This theory of pain states the following: non-nociceptive fibers can inhibit the pain signaling. (Melzack and Wall 1965). When a large sensory fiber conveying non-nociceptive information, it modulates nociceptive transmission by the activation of GABAergic inhibitory interneurons. These will act on afferent nociceptor fibers in a presynaptic manner.

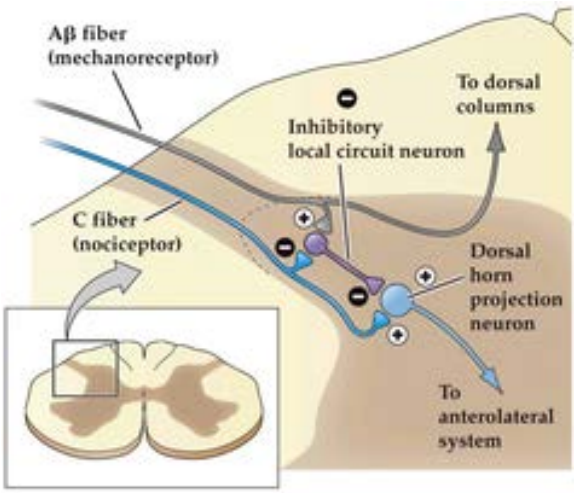

Figure 3: Representation of the Gate control theory. If a sensory stimulation arise at the same time as a nociceptive one, it will activate a spinal inhibitory interneuron that will shut down the simultaneous nociceptive information. The sensory stimulus is transmitted to the brain, but not the nociceptive one.

Image from Glasgow Uni Medicine ILOs

This will reduce the nociceptive signaling during the time a sensory signal is active. Due to this inhibition, the nociceptive information is stopped at the synapse of the DRG neuron located in the spinal cord. As it is not transmitted to the second order neuron, only the sensory information is transferred to the brain. However, if the influx sent is of enough intensity, it will be transferred to the brain (Mendel 2014).

The modulation of the nociceptive information can also occur in the brain stem. The rostral ventral medulla and the periaqueductal gray contribute to the regulation of the spinal nociceptive signal via descending feedback (Basbaum et al 2009).

Fourthly, the signal will be integrated in the brain and interpreted as pain. Following painful stimuli in human, brain activation is detected by functional magnetic resonance imaging in the S1 and S2 area of the somatosensory cortex, the pre-frontal cortex, the anterior cingulate cortex, the insular cortex, the thalamus and the cerebellum (Apkarian et al. 2005). The ascending fibers reach the thalamus, and then the information is relayed to the other cortexes.

Pain can also be modulated after its integration trough descending mechanisms. Projections from the cingulate cortex and amygdala can influence the neurons located in the periaqueductal grey descending through the spinal cord. (Navratilova et al. 2015). This modulation occurs through the noradrenergic and serotoninergic systems (Bannister and

Dickenson 2016). In the context of neuropathic pain, the serotonin-induced analgesia is reduced (Lopez-Alvarez et al 2018).

ii Peripheral and central sensitization

Peripheral and central sensitizations are mechanisms that will increase the gain of the signal along the pain pathway. In the case of inflammation or nerve injury in the periphery, the axon will fire abnormal action potentials. This phenomenon called altered electrogenesis is due to physiological changes of the damaged axon.

Peripheral sensitization

After acute peripheral injuries such as cut or burn, an inflammation is generated due to the substances released by injured cells. This inflammation, further enhanced by activation of immune cells attracted to the injury site. The pro-inflammatory agents they secrete causes sensitization of C and Aδ fibers nociceptive terminals rendering nociceptive neurons more excitable (Pogatzki-Zahn 2018). This peripheral sensitization, named this way as it is generated in the periphery, increases the pain sensation at the damaged location. Sensitization disappears once the inflammation is resorbed and the wound healed (Gold 2010).

In the case of an axotomy (nerve section), the stump of sensory nerve connected to the soma will form an end bulb from where it will sprout in an attempt to reconnect to the cut distal part. In case of failure, it will create a neuroma (Figure 4). This structure is associated with changes in the level of multiple channels involved in the generation of action potentials at the transcriptional, translational and post-translational level.

However the repair process can fail if the fiber is totally removed, such as in amputated body parts, or the gap between the two nerve endings following the cut of the axon is too big to be reconnected by sprouts. In this case, the neuron forms a knot out of the

sprouting nerve fiber. These structures called neuromas are important actors in peripheral sensitization (Fried et al. 1991, Deumens et al. 2010)

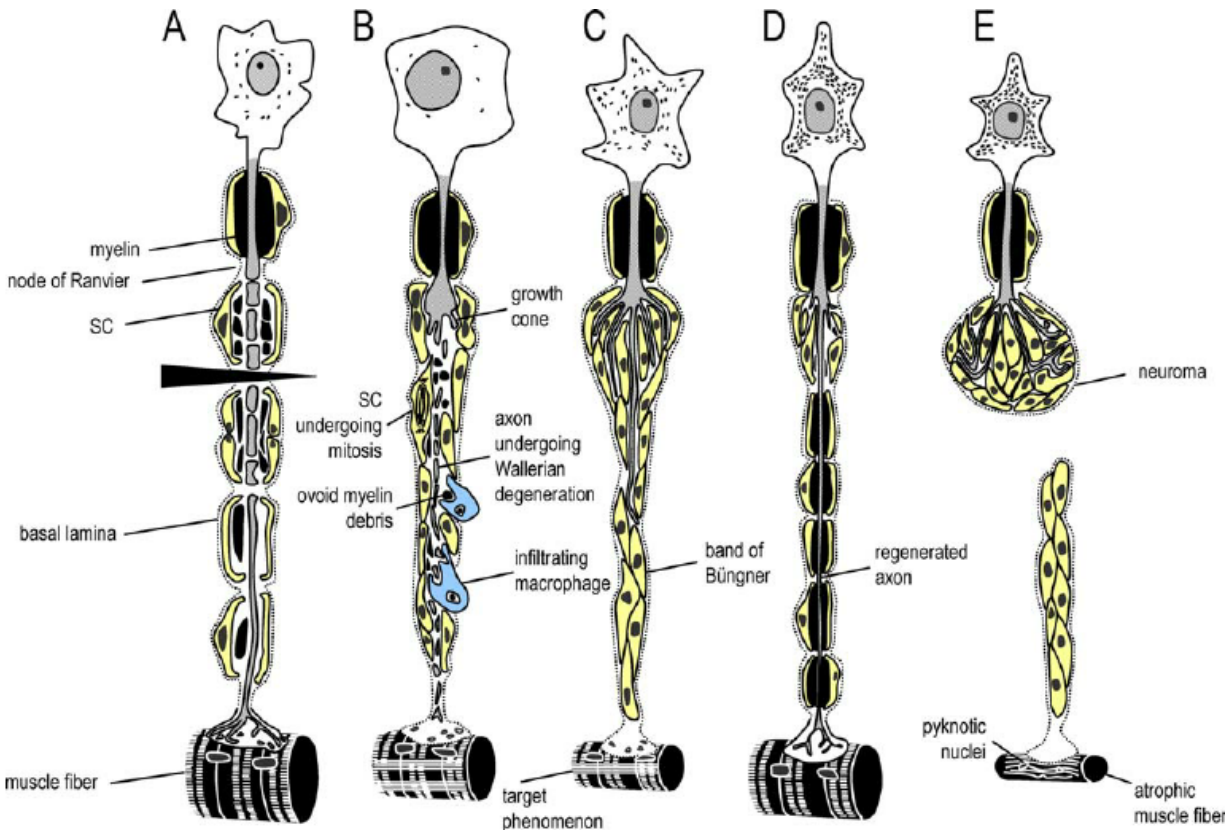

Figure 4: Neuronal regeneration after axotomy. SC is for Schwann cells: cells responsible of myelination of the axon in periphery. **(A):** Early after axonal injury (black arrow), a local degeneration of axon and myelin takes place. **(B):** later, Wallerian degeneration – a degeneration occurring only in the distal part of the axon – is achieved and infiltrating macrophages remove the tissue debris, and the axons generates axonal sprouts. **(C):** Of the many sprouts that enter the injury site, some will cross the injury site. This process can take several weeks. **(D):** Successful axon regeneration: restoration of neurotransmission via the bands of Büngner. The excessive sprouts will retract and a new myelination will occur. (E): Sprouts in this case did not cross the injury. There axon regeneration was not possible and resulted in the formation of a neuroma.

Deumens et al. 2010

Intermediate states can occur when there is a graft. Neurons will reattach to the existent severed axons with little success. Graft recipient get a partial sensation due to the

successful axon reconnections, but also pain due to the unsuccessful ones (Nedelec et al. 2005, Taylor et al. 2010).

Notable spontaneous discharges generated in nerve-end neuromas have been highlighted in several studies (Wall and Gutnik 1974). This erroneous electrical activity can disappear by the removal of the neuromas or by local anesthetics. However, cutting the neuromas only brings a brief relief since a new neuroma can appear at the new site of injury with potentially increased ectopic electrical activity compared to the first neuroma (Govrin-Lipmann and Devor 1978).

Ectopic activity can also be present in mid-nerve location or at the soma. In case of a nerve lesion that would damage neurons without axons cleavage, neuromas-in continuity or micro-neuromas can appear along nerves. Demyelination, the loss of myelin sheath surrounding certain nerve fibers, can also lead to formation of neuroma-like structures. (Burchiel et al. 1980, Calvin et al. 1982, Baker and Bostok 1992, Kajander and Bennet 1992, Wallace et al. 2003). Overall, these ectopic impulse discharges appear after nerve injuries – whatever the type of damage.

Moreover, DRG has a basal activity. Spontaneous firing has been detected even without nerve injury (Wall and Devor 1983, Ma and Lamotte 2007). When healthy patients have all the nerves from a limb blocked, most of them had no feeling - like if they had lost their limb. Yet, they report a non-painful phantom sensation of their limb (Melzack and Bromage 1973).

Following peripheral injury, sensory neurons release neuronal factors such as CGRP and substance P which activate and attracts mast cells, dendritic cells and T lymphocytes at the lesion site, and cause a neuroinflammation. In acute conditions, this recruitment mechanism will facilitate wound healing and improve the immune defense against pathogens entering the damaged site. (Saria 1984, Brain and Williams 1989, Ansel et al. 1993, Mikami et al. 2011, Chiu et al. 2012).

Still, this neuro-immune reaction has deleterious effects in the case of maladaptive pain by amplifying the inflammation (Figure 5).

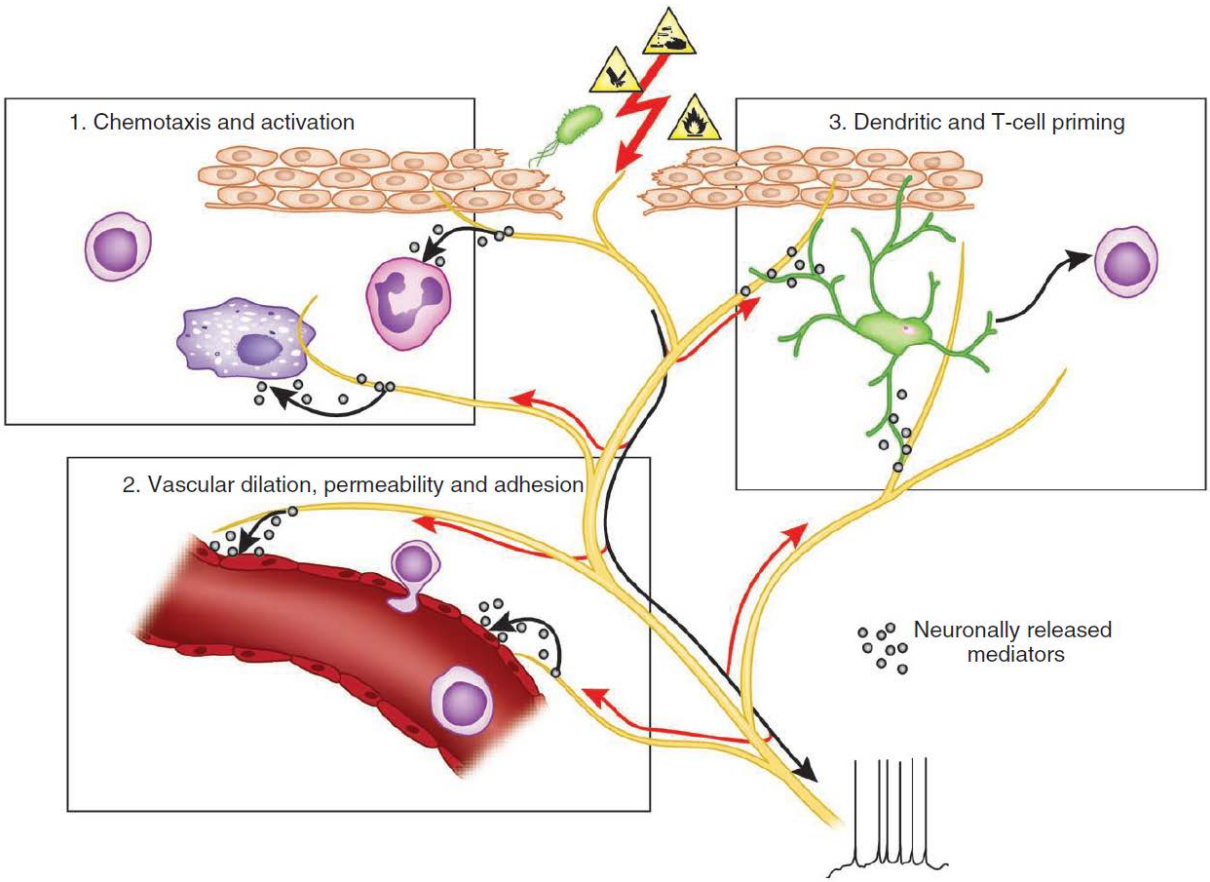

Figure 5: Effects of neuronal factors released by nociceptive neurons after injury. CGRP and BDNF are released by nerve terminals and have several effects. **1)** Activation and attraction of macrophages, neutrophils and lymphocytes to the site of injury. **2)** Vasodilation and increase permeability of blood vessels will permit a better recruitment of immune cells. **3)** Dendritic cells receiving these neuronal messengers will be prepared to trigger an adaptive immune reaction via T-cells.

Chiu, I. M., et al. (2012)

We only spoke of nerve fibers. However, the soma is also involved. Spontaneous firing has also been detected in the DRG. Several studies have shown that the DRG is also responsible of the ectopic electrical activity of damaged nerves. Depending on the lesion the DRG can fire up to 75% of the discharges, the 25% remaining arising from the neuromas. (Babbedge et al. 1996, Liu et al. 2000).

Central sensitization

Central sensitization is defined as a condition where the response to normal stimuli is greatly enhanced. Due to the increased gain of the synapse in the spinal cord, allodynia (lowering of nociceptive threshold) and hyperalgesia (increase of the pain response) appear. In addition, inhibitory modulation is reduced (Woolf 2007) (Figure 6).

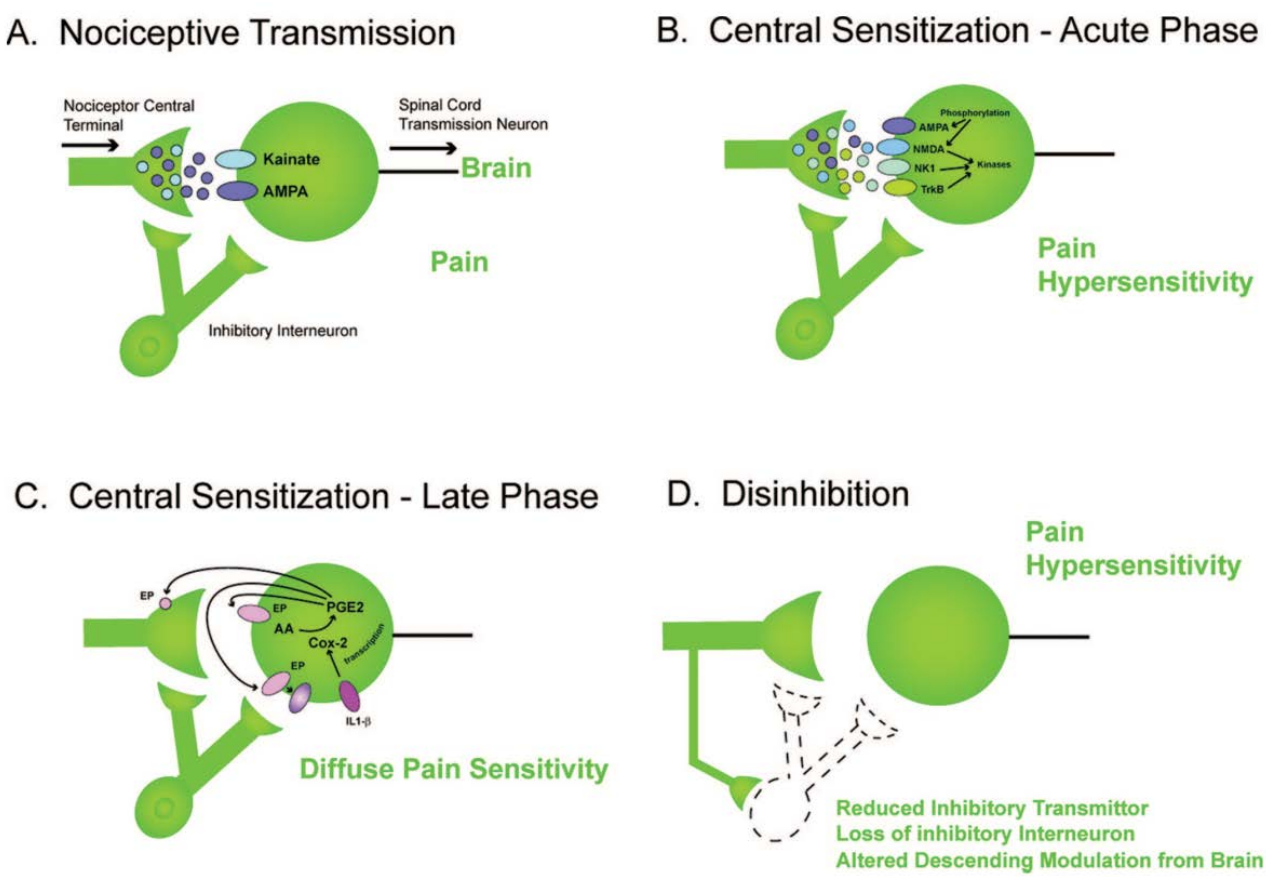

Figure 6. Loss of inhibitory mechanisms. (A) Regular nociceptive transmission. **(B)** Early phase of sensitization. The high amount of neurotransmitter release induces a sort of plasticity. This results in fast and reversible posttranslational modifications of the channels and receptors, which increases the excitability of second order neurons. **(C)** Changes in gene transcription and release of pro inflammatory agents by dorsal horn neurons. **(D)** The consequence of these changes is a reduced activity or death of inhibitory interneurons.

Clifford Woolf (2007)

Following nerve injury, ectopic activity increase of neurotransmitters release from sensory neurons. This will trigger different pathways in the second order neuron, which will secrete new neuromodulators such as prostaglandin E2. These modifications will reduce the activity of inhibitory interneurons, sometimes even a loss of these inhibitory interneurons. Blocking caspase activity involved in interneurons cell death can prevent the loss of this pain inhibition (Scholz et al. 2005).

Similarly to the immune cells in periphery, CNS glial cells will be activated and attracted. Once activated, the glia release pro inflammatory agents, such as tumor necrosis factor alpha (TNF-α), brain-derived neurotrophic factor (BDNF), cytokines such as interleukin-6 (Il-6), chemokines such as CCL2, reactive oxygen species (ROS) such as nitric oxide (NO), prostaglandins, cyclooxygenases, and bradykinins. Neuroinflammation appears and potentiates second order neurons, which will lead to an increased gain of the synapse between 1st and 2nd neuron. This phenomenon amplifies the signal received from the periphery (Devor et al. 1992, Mizumura et al. 2009, Benarroch 2011, Inoue et al. 2018).

As mentioned above, chemical mediators play an important role in sensitization by depolarizing neurons. This would result in a lower neuronal threshold for the firing of action potential, thus an increased firing (Figure 7).

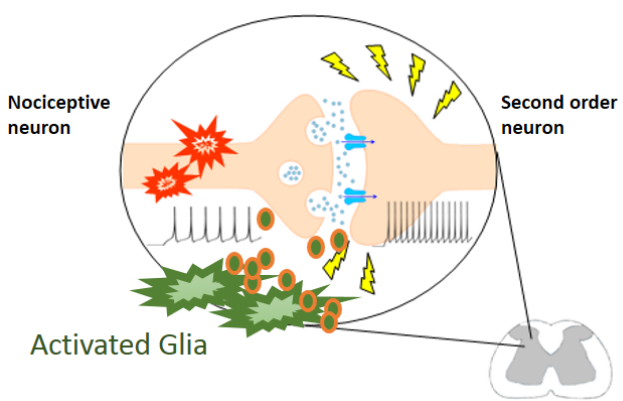

Figure 7: Central sensitization. Representation of the processes taking place in the spinal cord following nerve injury in periphery. Although the damage is on the primary sensory neurons, glia in the spinal cord will be activated by those injured neurons and contribute to the neuroinflammation that will increase the gain of the synapse together with the second order neurons, leading to central sensitization.

Descending inhibition is also altered by nerve injury. To demonstrate this, Rahman and colleagues 2008 used an agonist of the noradrenergic signalling together with the Spinal nerve ligation (SNL) model of neuropathic pain. They show that hypersensibility is reduced in sham animals but not in animals with peripheral nerve injury.

iii Neuropathic pain

Neuropathic pain is a type of pain caused by a lesion or disease of the somatosensory nervous system (IASP).

It arises from a paradox. As Marshall Devor 2013 mentions: "When a telephone cable is cut across, the phone falls silent. Damaged nerves behave differently."

Indeed, when its axon is cut or damaged the nerve cell reacts by electric discharges. These ectopic discharges are the starting point to maladaptive pain such as neuropathic pain.

Nerve lesion can happen after traumas or during surgeries, in metabolic disease such as diabetes mellitus, from infectious agents such as the varicella zoster virus or drugs such as chemotherapeutic or anti-HIV (Nagel and Gilden 2007, Attal et al. 2008). Nerve damages often lead to neuropathic pain because of the consequent changes it can trigger in sensory neurons as well as in the signal processing in the central nervous system.

Patients who suffer from neuropathic pain experiment the sensitization process and all its deleterious effects. One of them is spontaneous pain, which they describe as burning, tingling or as electric discharges. Patients also endure increased pain sensitivity, a low painful stimulus such as needle sting would be perceived as an intense pain. This is called hyperalgesia. Besides this, sensitization of peripheral nervous system (PNS) and central nervous system (CNS) cause allodynia. Non-noxious stimuli such as light touching or a pleasant warm temperature is felt as a painful threat. (Colloca et al. 2015).

Diagnosis of neuropathic pain can be made through a patient history, the help of questionnaires, bed side testing of neurological function, and finally the use of more complex diagnostic techniques (imaging, biopsies, …) (Finnerup et al. 2016).

Current treatment for neuropathic pain is only efficient in one out 3 patients, which is probably due to the complexity of its mechanisms and the targeting of drugs mostly on neuronal pathways.

iv Animal models of Neuropathic pain

There are many different models of neuropathic pain to try to mimic the different causes of this disease in human as diabetic or chemotherapy induced model and mechanical injury models. The latter can target peripheral nerve or the central nervous system. Many peripheral models involve lesion on the sciatic nerve, by transection or by ligation (Figure 8). The ligation can be loose/tight, full or partial. The injury site differs between models. It can be proximal at the level of spinal nerves or more distal, near the sciatic trifurcation.

Often, in these models of neuropathic pain the control group will undergo a sham surgery consisting in performing the surgery of the neuropathic pain model except for the nerve lesion

We use the Spared Nerve Injury (SNI) model of neuropathic pain (Decosterd and Woolf 2000) in mice. It consists in a ligation and section of the tibial and common peroneal nerves just after the trifurcation of the sciatic nerve. After this surgery, a durable development of neuropathic pain-like behavior occurs with strong and robust paw hypersensibility ipsilateral to the surgery.

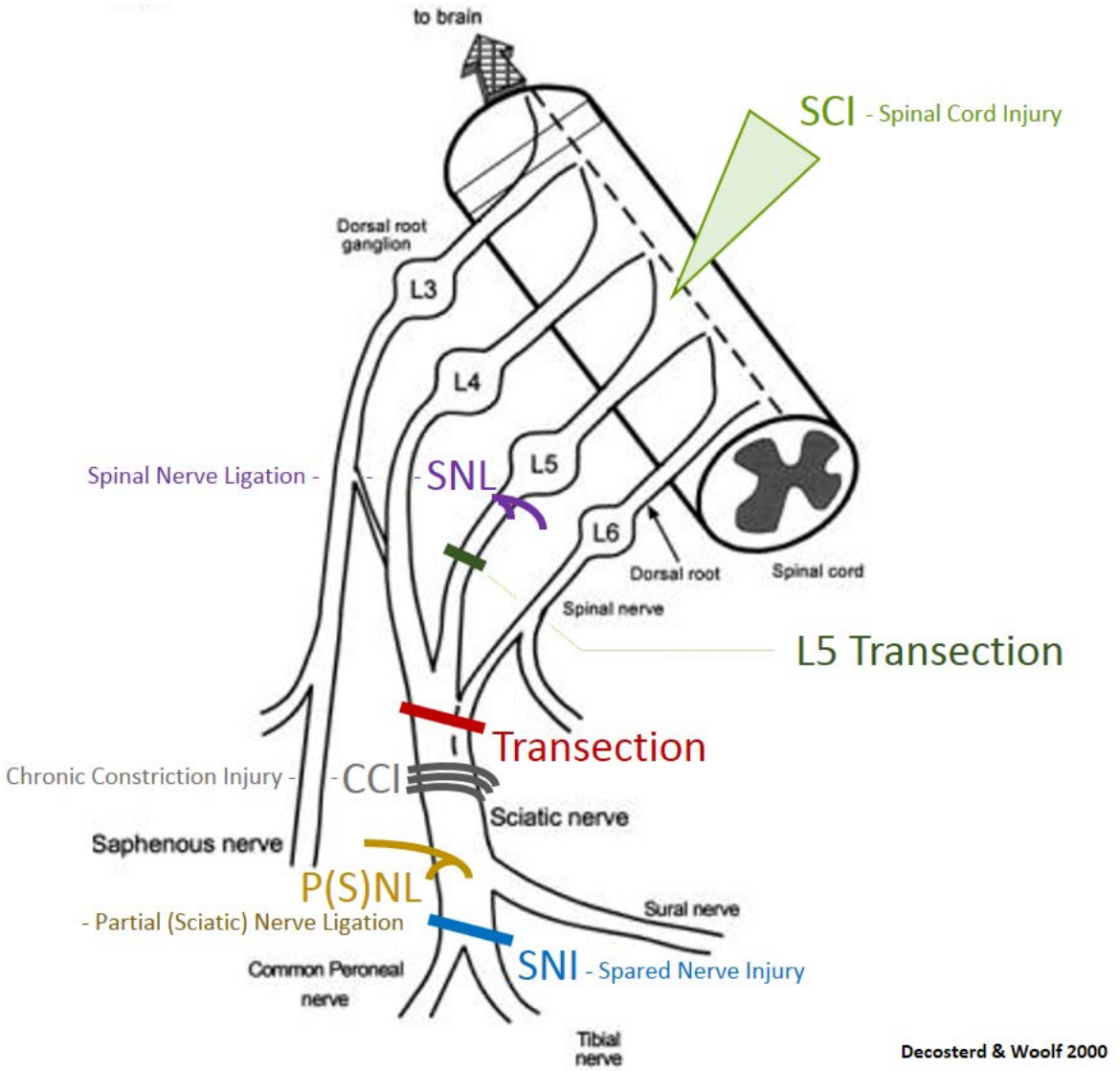

Figure 8: Models of neuropathic pain. Representation of the different neuropathic pain models used on mice and rats, listed here from the most invasive to the less invasive. The **spinal cord Injury (SCI)** consist of letting a mass fall on the spinal cord, crushing it and opening the blood brain barrier. The sciatic **transection** consists of the section of the sciatic nerve. In the **spared nerve injury (SNI)**, 2 out of the 3 nerves are ligated and cut distally to the sciatic trifurcation. The **chronic constriction injury (CCI)** is a ligation of the sciatic nerve. The **partial sciatic nerve ligation (PSNL or PNL)** consists in the ligation of only a part of the sciatic nerve. The **spinal nerve ligation (SNL)** where L5 and sometimes L6 nerves distal to the DRG are ligated and/or cut.

Modified from Decosterd and Woolf 2000

§2 Central nervous system (CNS) and glia

i General organization

The CNS is composed of the brain and the spinal cord and surrounded by meninges and bone (cranium and vertebrae). The meninges are formed by the superposition of three layers of tissue. The first and outer layer, the dura mater is the toughest tissue of the three and is important for mechanical protection, blood supply of the CNS and drainage of cerebro-spinal fluid.

In the middle, the arachnoid called this way because it looks like a spider web, is impermeable to cerebro-spinal fluid and reduces mechanical action on the brain the way a cushion would.

Pia mater, the inner one is tightly attached to the brain and the spinal cord. It follows closely the brain circumvolutions. In the vertebral column, dorsal root ganglia (DRGs) are at the border of the CNS, halfway engulfed in the meninges. The afferent dorsal roots are outside. Still in the periphery, DRGs are the bridge between central and peripheral nervous system for sensory nerve fibers, enclosing the cellular bodies as their axon goes from periphery to the dorsal horn of the spinal cord.

In a cellular approach, we can determine four cell types in the CNS: neurons, astrocytes, oligodendrocytes and microglia (Figure 9).

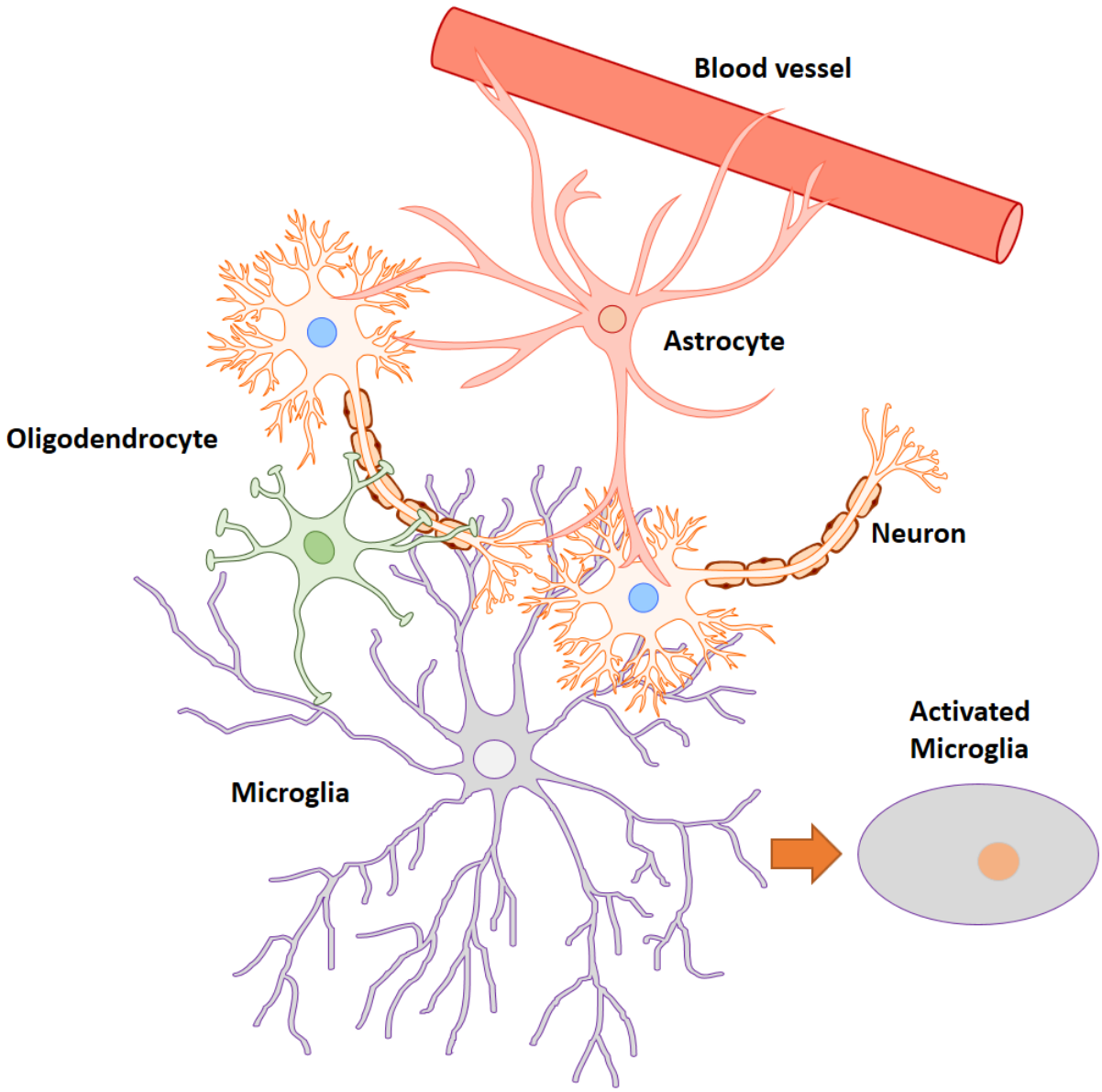

Figure 9: Cellular organization of the CNS. Representation of neurons surrounded by glial cells: astrocytes are forming the blood-brain barrier between blood vessels and neurons (together with endothelial cells and pericytes), oligodendrocyte forming the myelin sheath and microglia surveying the extracellular space, activating their migration and phagocytic state if a threat is detected.

Neurons are composed of a cell body with dendrites, an axon and axon terminals from where electrical messages are transferred to other neurons by neurotransmitters through synapses. Those highly specialized cells became electrically excitable to process and transfer information, allowing by their network for organisms to move and take decisions. However if the capacity acquired by neurons is exceptional, so is their fragility and energy needs. The brain has the highest oxygen and sugar consumption per volume – (consuming 20% of the body glucose for 2% of the body mass) due to the generation and transmission of action potential, requiring a lot of adenosine tri-phosphate (ATP), a molecule storing energy from glucose transformation. ATP in neurons is used essentially to maintain ion gradients and resting membrane potentials via transporters and for the biosynthesis of neurotransmitters. (Mergenthaler et al. 2013)

Moreover, neurons have a very low rate of renewal. A lesion of the brain could not heal as an epithelial tissue would. If the neurogenesis is strong during development of the brain, it is then strongly reduced in adults. Only few regions of the brain keep neurogenesis activities. (Gould et al. 2007, Kokoeva et al. 2007, Feirreira et al. 2018)

The neuronal network is surrounded by glial cells, each of them having important roles in the maintenance of the brain homeostasis. All the CNS cells that are not neurons are categorized as glia. Astrocytes, together with vascular endothelial cells and pericytes, generate the blood-brain barrier (BBB) (Figure 10) (Obermeier et al. 2013).

Gases such as oxygen or carbon dioxide, and small lipophilic molecules can diffuse trough the BBB. Everything else needs a specific transporter, even important ones such as the glucose. This system allows the passage of nutriments and other elements useful to the brain while preventing the entry of potentially toxic agents for neurons travelling in the blood flow (Banks 2009).

In addition of being the main filter of the BBB, astrocytes process glucose into lactate. They deliver it to neurons as a second energy source, but not only. There is a tight cross-talk between neurons and astrocytes. In response of neuronal activity astrocytes increases their lactate production to modulate several neuronal functions such as neuronal plasticity, neuronal excitability as well as memory consolidation (Magistretti et al. 2018). Astrocytes

also recycle used glutamate, the main excitatory neurotransmitter, into glutamine and transfer it to neuron for new biosynthesis and new transmission (Hertz and Zielke 2004).

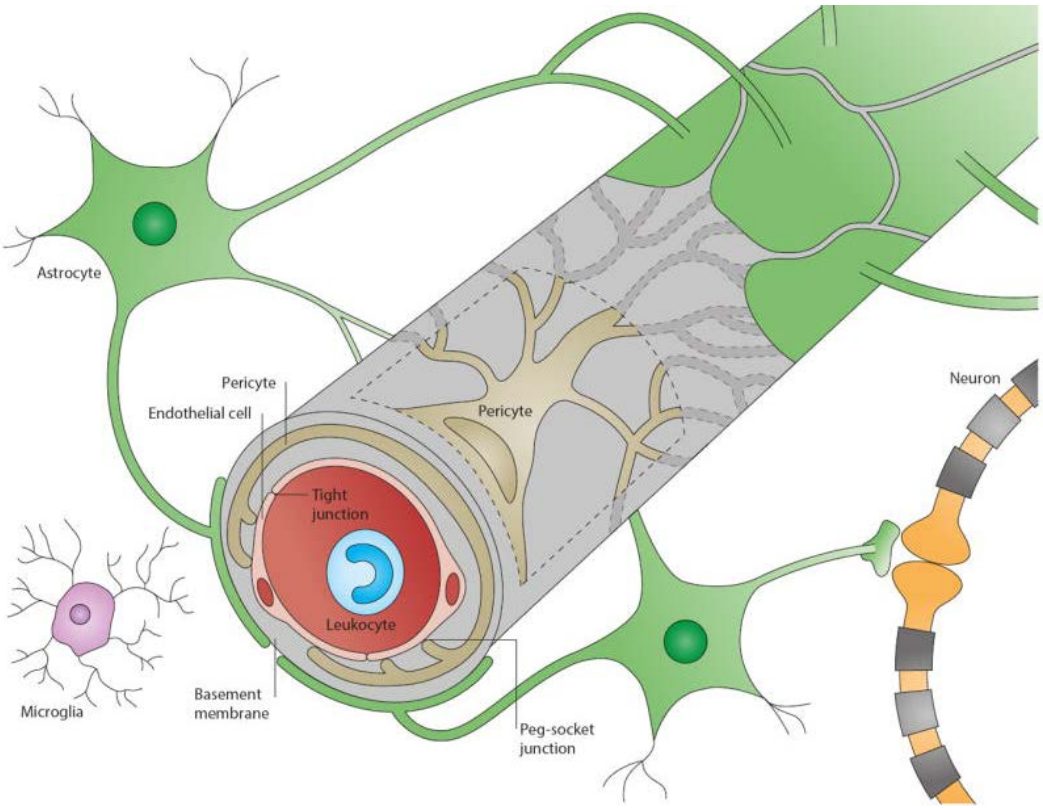

Figure 10: Structure of the blood brain barrier. The blood vessel itself is created by the vascular endothelial cells (in red) linked together by tight junctions. Pericytes (in light brown) wrap blood vessels, embedded in the basal membrane (in grey): a highly specialized extracellular matrix composed of laminin, collagen IV, perlecan and nidogen. Astrocytes (in green) place the final layer on the structure by extending their end foot processes.

Obermeier et al. 2013

Oligodendrocytes are part, with astrocytes, of the macro-glia. Their main function is coat axons with myelin in the CNS, whereas in periphery Schwann cells are coating peripheral axons. The myelin sheath formed of multiple layers of lipid-rich and near waterless membranes isolates the axons. This allows a faster transmission of the information, which is crucial for a rapid reaction of the organism. One oligodendrocyte is able to myelinate up to 50 axons. In charge of axon maintenance, these cells also regulate axons growth or shrinkage (Baumann and Pham-Dinh 2001).

Finally, microglia represent 10% of the CNS cell population (Salter and Beggs 2014). Called this way because they are the smallest cells of the brain, microglia have a very important role, as they are the immune cells of the brain. Deriving from primitive macrophages, they scan and defend the CNS against any type of disturbance. I describe them below in more details.

Note that the proportion of glia increases with the complexity of the organism, suggesting their fundamental function for the fine functioning of brains that are more complex. Glia correspond to 25% of the cells in the fly brain, to 65% in rodent brain and to 90% in human brain (Pfrieger and Barres 1995).

ii Microglia

During the past 20 years, the research on glial cells in the CNS has grown. It appears that microglia have many other functions, yet their pathological activation is difficult to understand. This is illustrated by the many reports showing activation in numerous conditions.

Microglia derive from embryonic macrophages originated in the yolk sac. They migrate and colonize the CNS in a very distinct way. Microglia are not overlapping. Each microglial cell has its own volume. Their network could be compared to a pile of blocks, each block containing one sole microglial cell (Cuadros and Navascuès 1998, Ginhoux et al. 2010).

As resting microglia are constantly scanning their surroundings with their long ramifications, the "microglial grid" structure they form grants a quick and precise detection of any threat or pathogen (Wake et al. 2009). This pattern is found in the whole brain and spinal cord. With their thin and constantly moving processes as well as their remarkable network layout microglia fully scan the brain volume in few hours (Nimmerjahn et al. 2005).

Although surveillance and monitoring is their principal function, microglia have an essential role during the CNS development (Figure 11). They are able to shape the neuronal network by engulfing certain synapses or dendritic spines and eliminating them by phagocytosis. The structure selection criteria of this process called synaptic pruning is still

debated; the current paradigm associates it with neuronal activity and sensory stimuli (Tremblay et al. 2010, Paolicelli et al. 2011).

Still, the importance microglia in synaptic remodeling makes no doubt, as the disruption of the microglial phagocytic pathway via the knockout of complement receptor CR3 causes abnormal synaptic connections (Schafter et al. 2012).

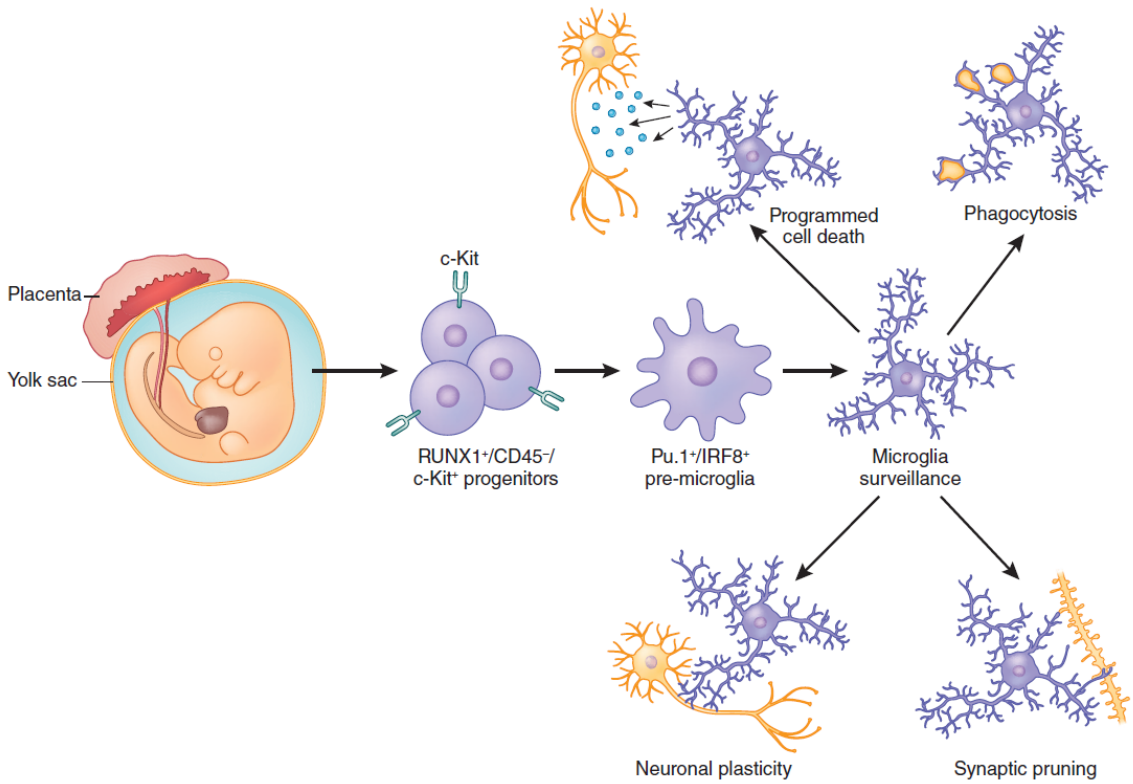

Figure 11: origin and physiological function of microglia. Microglial progenitors migrate from the yolk sac through bloodstream to the developing CNS. At this point, they are more like undifferentiated macrophages. Then Pu.1 and IRF8 lineage genes activation specialize them into microglia. Microglia also play an important role in the development of neuronal network and plasticity by connecting neurons synaptic pruning, programmed cell death and phagocytosis of apoptotic cells.

Salter and Stevens 2017

Another physiological role of microglia consists in phagocytosis and scavenging of neurons in excess targeted by programmed cell death during the development of the CNS. By this process, microglia reduce the neurotoxic impact of apoptosis bodies. Microglial cells can

also be the one triggering programmed cell death via NO, nerve growth factor or TNF-α (Salter and Stevens 2017).

Microglia are known for their migration and phagocytic activity as defenders of the CNS, yet they are also able to modulate electrical activity of the neuronal circuit (Graeber and Streit 2010). For instance, they can reduce the excitability of certain neurons, engulfing them with their processes when attracted by ATP (Li et al 2013, Panatier and Robitaille 2012). Moreover, microglia play a role in neuronal plasticity, more precisely in activity-dependent long-term synaptic plasticity, the mechanism involved in learning and memory. There, microglia participate in activity-initiated synaptic plasticity and adult neurogenesis. If microglia are disrupted - in their fractalkine signaling for instance, the cognitive function of rodents is impaired (Roger et al. 2011, Bachstetter et al. 2011).

§3 Microglial activation

i General characteristics of microglial activation

Microglia are able to change their shape from a sentry state with long ramified prolongations to an amoeboid structure and gains motility to migrate to damaged sites (Figure 12). This occurs when microglia detect pathogens or molecules unusually found in healthy tissues such as pro-inflammatory cytokines or chemokines, ATP, TNF-α, ROS and many others. Microglia are attracted by these chemicals and will trigger an immune response to eliminate threats (Kettenmann et al. 2011).

Among other receptors, pathogens-associated molecular patterns receptors such as Toll-like receptors (TLRs) are found on microglial membranes. Those receptors will trigger a signaling cascade promoting inflammation if they bind to pathogen membrane components such as lipopolysaccharides (LPS) found on the membranes of *E.Coli.* Although LPS will trigger a large part of the TLR family, TLR4 is known to play an important role in the development of glial inflammation (Okun et al. 2011).

Nevertheless, microglia are not always modified in a pro-inflammatory way. Some cytokines such as IL-10 and IL-4 are shaping microglia as anti-inflammatory actors.

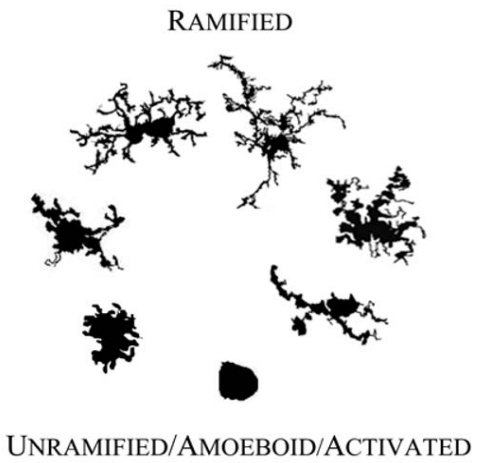

Figure 12: Resting and activated Microglia. Scheme illustrating the morphologic changes of a microglia upon activation.

Karperien et al. 2013

Microglial activation is often characterized in M1 or M2 phenotypes for pro- and anti-inflammatory respectively, mostly depending on the triggering factors (Figure 13) (Fumagalli et al. 2011). Studies indeed described these general phenotypes, but when microglial activation is explored in details, this classification is over simplistic.

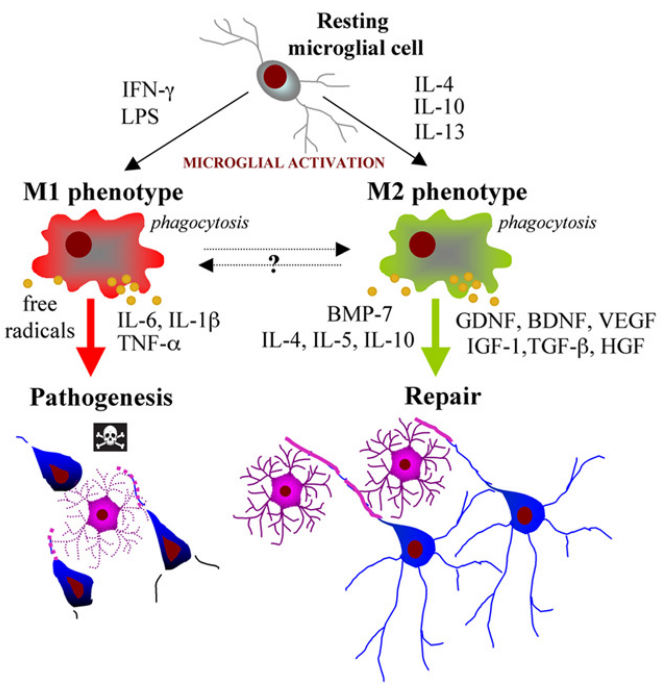

Figure 13: Different activations of microglia. Different chemical agents or proteins have each their effect on microglia. Two main phenotypes have been described: M1 for pro-inflammatory and M2 for anti-inflammatory activation of microglia.

Fumagalli et al. 2011

ii Microglial reactivity in neuropathic pain models

More and more studies highlight the contribution of microglia in neuropathic pain, both in rodents and human. In the case of a nerve injury, damaged sensory neurons will produce macrophage colony stimulating factor 1 (M-CSF or CSF-1), a molecule promoting proliferation of macrophages and microglia (Figure 14). Via axonal transport, CSF-1 is brought from the DRG to the dorsal horn of the spinal cord, causing microglia to activate and proliferate (Guan et al. 2016).

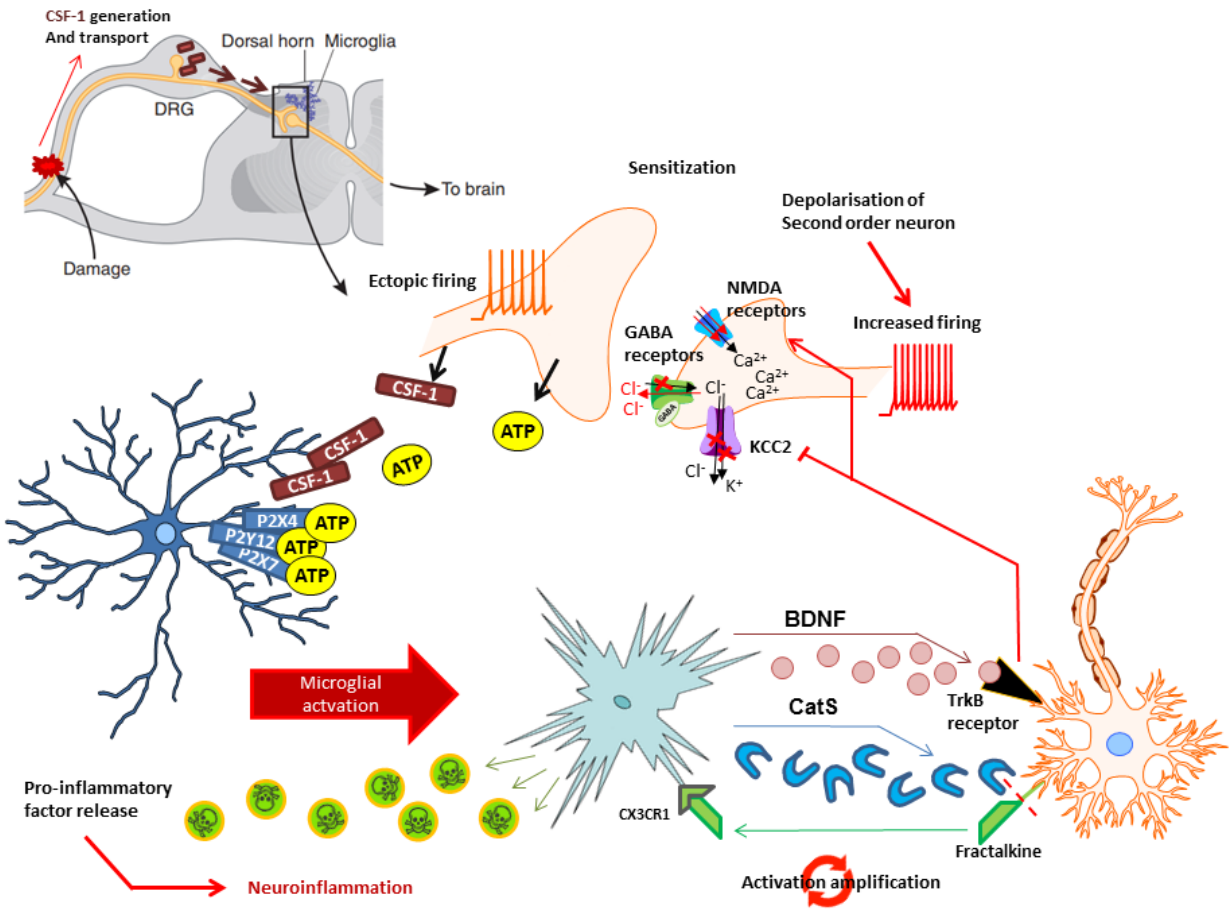

Figure 14: Microglial activation after nerve injury. Representation of the different steps microglia take after a nerve injury. First microglia get activated by ATP and CSF-1. Once activated microglia release many pro-inflammatory cytokines. They maintain and amplify their activation via cathepsin S, cleaving fractalkine from neurons. They also release neurotrophic factors that depolarize second order neuron by changing the activation of synaptic ion channels, increasing their sensitivity.

Modified from Salter and Stevens 2017

In addition, ectopic firing appears in injured neurons. Because of their activity, ATP is released in the extracellular space. (Richler et al. 2008, Khakh and North 2012, Del Puerto et al. 2013). When microglia detect it via purinergic receptors (P2X4, P2X7 and P2Y12), they will migrate to the ATP source (Samuels et al 2010, Madry et al. 2018) and increase their fractalkine receptors (CX3CR1) expression (Tsuda et al. 2003, Chessel et al. 2005, Gu et al. 2016). Yet, no study showed that neurons are responsible for the ATP released in the spinal cord, we can only hypothesize that spinal cord neuron behave as brain neurons once injured.

At this point microglia release cathepsin S, a protease that will cleave fractalkine from neuronal membrane. Fractalkine will then bind on its microglial receptor and in a positive feedback loop with further increase the microglial activation and secretions (Clark et al. 2007).

Simultaneously, the activation of microglial P2X4 leads to the release of BDNF, which will link to its neuronal receptor, the tropomyosin-related kinase receptor B (TrkB). This interaction triggers important synaptic changes. The amount of dendritic spines increases (Parkhurst et al. 2013).

BDNF secreted by microglia potentiate N-methyl-D-aspartate receptors (NMDARs) in synapses, resulting in increased excitability (Hildebrand et al. 2016). BDNF also decreases potassium/chloride cotransporter KCC2 channels in second order neurons which reverses their chloride balance and makes them less sensitive to inhibitory GABAergic stimulation. (Rivera et al. 2002, Coull et al. 2005). This causes neuronal hyperexcitability and pain hypersensitivity.

After nerve injury, microglial activation generates a strong and long lasting inflammation due to numerous pro-inflammatory agents released in the dorsal horn. Cytokines such as interleukins (IL-6, IL18,) are induced by the p38 mitogen-activated protein kinase (p38-MAPK) following fractalkine binding to CX3CR1. TNF-α is induced by the same way. Many other factors such as chemokines (CCL1, CCL2, CCL3, CXCL2, CXCL3, CXCL10), reactive oxygen species (ROS), cyclooxygenases (COX1-2) and prostaglandins (PGE1) are also secreted (Inoue et al. 2018, Penas and Navarro 2018). This neuroinflammation contributes to the neuropathic pain phenotype. There are several model of neuropathic pain.

We observe in almost every model an activation of microglia, although its strength and location may vary depending on the model (Table 1).

For instance in the SNI model, the activation of microglia occurs in L3 to L5 section since sectioned nerve fibers have synapses in the L3 to L5 section (Beggs and Salter 2007). As the sural nerve is not damaged, there is a mix of injured and non-injured neurons in this model. This contrasts with the SNL model where all fibers of the spinal nerve are injured by the ligation or with the transection where all nerves are cut. In L5 transection (L5Tx), as only the nerve distal to the L5 DRG is cut, the damaged neuron ectopic activity and glial reactivity occurs at the L5 level of the spinal cord.

Neuropathic Pain Models	Early - D2	1 week	2 weeks	3 weeks	More than a month	References
SNI	Small ↗ cell number DHi High proliferation Hypersensitivity starts ↗ pro-infl. cytokines ↗ Iba1 ↗ CX3Cr1 ↗ IFN-γ ↗ complement ↗ phospho-p38-MAPK	Large ↗ cell number Proliferation stops Hypersensitivity peaks Slight ↗ CX3CR1 Slight ↘ complement ↘ IFN-γ	Same high cell number Hypersensitivity stays Pro inflammatory back to normal level	Hypersensitivity start to lower ↗ anti-infl.cytokines IFN-γ ↗ to D2 level Slight ↘ complement and ↘ CX3CR1	Hypersensitivity keeps lowering slowly ↘ CX3Cr1 ↘ INF-γ ↘ complement But still higher than naive level	**Gattlen et al. 2016** **Griffin et al. 2007** **Suter et al. 2009**
SNL	strong ↗ CX3CR1 ↗ IFN-γ ↗ complement	Slight ↘ CX3CR1 ↘ IFN-γ ↘ complement		Slight ↘ CX3CR1 Slight ↘ IFN-γ Slight ↘ complement	↘ CX3Cr1 ↘ IFN-γ ↘ complement (D40), still higher than naive level	**Griffin et al. 2007** **Domingez et al. 2008** **Guasti et al. 2009** **Zhuang et al. 2007**
CCI	↗ CX3CR1, IFN-γ ↗ complement ↗ Iba1	↗ GFAP ↗ CD11b and Iba1 – peak ↗ MHC1, CD45 and CD68 Slight ↘ CX3CR1, IFN-γ and complement ↗ phospho-p38-MAPK		Slight ↘ CX3CR1 Slight ↘ IFN-γ Slight ↘ complement	↘ CX3Cr1, IFN-γ and complement (D40), still higher than naive level	**Taves et al 2016** **Griffinet al. 2007** **Hu et al. 2006** **Wei et al.2008**
P(S)NL	Small ↗ cell number (CatS labelled)	Large ↗ cell number (CatS labelled) Hypersensitivity peaks ↗ Iba1 marker, peak ! Small ↗ GFAP	Same high cell number (Iba1 and CatS labelled) small ↘ iba1 ↗ GFAP cells number – peak !	Hypersensitivity stays ↘ Iba1 ↘ GFAP quite back to naive level		**Clark et al 2007** **Zhang et al 2007** **Kobayashi et al 2008**
Transection		↗ GFAP ↗ CD11b				**Hu et al. 2006** **Tozaki-Saito et al. 2008**
L5Tx	Hypersensitivity starts ↗ cell number in Dhi ↗Iba-1, ↗TNF-α	Hypersensitivity peaks	Small ↘ of hypersensitivity	Hypersensitivity stays	Hypersensitivity stays	**Kim et al. 2007** **Cao and De Leo 2008**

Table 1: Microglial activation in different neuropathic pain models in rodents. Abbreviations used in this table: dorsal horn ipsilateral to surgery (DHi), Interferon gamma (IFN-γ), major histocompatibility complex 1 (MHC1), Glial fibrillary acidic protein (GFAP)

iii Microglial activation in inflammatory pain models

Aside from damaged nerves, many factors can activate microglia. Fractalkine (CX3CL1), cytokines, bacterial cell wall molecules such as LPS, capsaicin (the active principle of chili peppers, activating TRPV1 channels) or complete Freund's adjuvant (CFA, a pro-inflammatory cocktail).

Due to the microglial activation, an inflammation takes place. In table 2, I summarize the studies that showed an activation of spinal cord microglia in inflammatory models.

Inflammation Models	Early - D2	1 week	Treatment	Location of activation	References
CX3CL1	I.p. injection caused hypersensitivity already after 1 day, which stayed at D2 ↗ microglial cell number in inected dorsal horn ↗ p-p38-MAPK		Intrathecal injection,	Spinal cord	**Zhuang et al. 2007**
LPS	Spinal cord microglial dissociation after systemic LPS injection ↗IL-1β, ↗ TNF-α, ↗IL-6, ↗ INOS, ↗COX-2 Peak 3h after injection, ↘ after 24h quite back to naive except for TNF-α which continues ↗		Systemic injection	Spinal cord	**Huxtable et al. 2013**
IL-1β, **TNF-α**, IL-6 (Inflammatory agents)	Injection in L5-L6 by spinal cord puncture of IFN-γ , TNF-α and IL-6 All separately ↗ hypersensibility, from 30' to 2h after injection and neurons were positive for pCREB after each injection.		Spinal cord injection by puncture	Spinal cord	**Kawasaki et al. 2008**
Capsaicin	Hypersensitivity already after 1 day peaks at D3 ↗ cell number in Dhi both Iba1 and GFAP cells		Systemic / Intraplantar injection	Spinal cord	**Talbot et al. 2012** **Chen et al. 2008**
Formalin	↗ Iba1+ microglial cells ↗ MHC1 and CD45, but not CD68 ↗ P-SFK and p-p38-MAPK Prostration phase + hypersensibility	Activation by Formalin lasts for 7 days P-SFK still present	Hind paw injection	Spinal cord	**Li et al. 2013** **Tan et al. 2012**
CFA (Complete Freund's adjuvent)	↗ Iba1 already 1 day after hind paw injection ↗IL-1β, ↗ TNF-α, ↗IL-6 ↗NF-κB	↗ of Iba1 – peak Small ↗of GFAP	Hind paw / Intraarticular injection	Spinal cord	**Hu et al. 2018** **Li et al 2013** **Chen et al. 2008**

Table 2: Microglial activation in different inflammation models.

§4 Ion channels in microglia

i Different type of channels - sodium, calcium, chloride, potassium

Additionally to standard ions channels and transporters used for the good function of the cell, microglia cells exhibits many ion channels, although they are not excitable cells.

Kettenmann and colleagues 2011 have described potassium current as the major currents in microglia (Table 3).

Ions	Channels	Impact in the RMP	Fonction associated	Blockers	Upregulated By	References
Potassium	**Kir2.1** (inward rectifying potassium channel)	+++	Maintain the resting membrane potential, plays a role in morphology, proliferation and Ca^{2+} signaling.	ML133 Ba^{2+}, Cs^{2+} CEC	SNI, LPS, CSF-1 (M-CSF)	**Nguyen et al. 2017** **Lam et al 2017-2015** **Eder et al. 1995** **Di Lucente et al. 2018**
	Kv1.1, Kv1.2, Kv1.3, Kv1.5 (voltage gated potassium channels)	+++	Maintain the resting membrane potential, regulates motility, proliferation and ROS release	TEA, 4-AP, CTX, KTX, NTX, MgTX, AgTX-2	TGF-β, LPS	**Nguyen et al. 2017** **Newell et al. 2005** **Fordryce et al. 2005** **Schilling et al. 2000** **Schlichter et al. 1996**
	SK1, SK2, SK3 (Small current-) **IK** (Intermediate current-) **BK** (Big-current- calcium activated potassium channel)	+	Involved in ROS release after microglia activation, their blockade reduced NO release and neuron death	Apamin, PTX Tapamin, Clotrimazole	LPS, resipiratory burst	**Kotecha et al. 1999** **Nguyen et al. 2017** **Schlichter et al. 2010** **Kaushal et al. 2007** **Khanna et al. 2001**
	GIRK (G-protein related potassium channels)	+	Transient strong K+ condution activated by GTPAses	4-AP, PTX	EGF, C2a complement	**Ilschner et al. 1995-6**
Sodium	**Nav1.1, Nav1.6** (TTX-sensitive)	-	Phagocytic activity, migration, release of IL-1 and TNF-α	TTX	LPS EAE, MS Inflamatory models	**Black et al. 2009**
	Nav1.5 (TTX-resistant)	-		Phenytoin		**Craner et al. 2004**
Calcium	**CRAC** (Ca^{2+}-release-activated Ca^{2+} channels)	-	Calcium signaling via depletion of endoplasmic reticulum Ca^{2+}, further increasing microglial activation and factor release	Gd^{3+}, SKF-96365	ATP via P2Y2 channels	**Fereirra et al. 2013** **Ohana et al. 2009** **Färber et al. 2006**
Nonspecific cation channels	**TRPC6** **TRPM2, TRPM4, TRPM7** **TRPV1**	-	TRP activation contributes in microglial Ca^{2+} signaling, Il-6 and ROS production leading to microglial cell death	La^{3+}, Ruthenium red	DBA/2 glaucoma model	**Sappington et al. 2008** **Schilling et al. 2009**
Chloride	**Volume regulated Cl^- Channels (KCCs)**	+++	Involved in microglial resting volume, proliferation, phagocytosis and morphology	Flufenamic acid, DIDS, SITS, DIOA, NPPB, IAA-94	CSF-1	**Zierler et al. 2008** **Furtener et al. 2007** **Newell et al. 2005** **Schlichter et al. 1996**
	CLIC-1 chloride channel	+++	Proliferation and ROS generation.	IAA-94	Amyloid-β	**Novarino et al. 2004**

Table 3: Ion channels in microglia. Abbrevations used in this table : chloroethyclonidine (CEC), tetraethylammonium (TEA), 4-aminopyridine (4-AP), charybdotoxin (CTX), anuroctoxin (KTX), noxiustoxin (NTX), margatoxin (MgTX), Agitoxin-2 (AgTX-2), pertusis toxin (PTX), tetrodotoxin (TTX). Chloride channel blockers: SITS, DIOA, NPPB. Colony stimulating factor 1 (CSF-1).

ii Potassium channels in microglia

Already many studies have illustrated the change of potassium currents in brain microglia following diverse treatments/pathologies. By the use of pharmacological blocking,

different channels could be identified. Outward potassium currents in microglia could be attributed to Kv1.3 and Kv1.5 after blocking channels of hippocampal brain slices with 4-aminopyridine (4-AP), tetraethylammonium (TEA), alpha-dendrotoxin (DTX), margatoxin (MgTX) and agitoxin-2 (AgTx-2) (Menteyne 2009). After the use of chloroethylclonidine (CEC), it was clear for them that inwards currents were caused by Kir2.1 in neonatal mouse brain microglial culture (Muessel et al. 2013).

Microglial potassium channels show different functions. Kv1.3 enhances cytokine production leading to neurotoxic effects in neonatal rat brain microglial culture (Fordyce et al. 2005). Kv1.5 forms heteromers with Kv1.3 to reduce microglial proliferation in neonatal mouse brain microglial culture (Pannasch et al. 2006). Kv1.3, Kv1.5, SK and IK (also called KCa3.1) channels have been identified in neonatal rat brain microglia (Khanna et al. 2001). KCa3.1 is involved in ROS production after microglial activation. (Khausal et al. 2007).

Kir2.1 is involved in cell conformation changes in neonatal mouse brain microglial culture (Muessel et al 2013). Recently, Madry and colleagues 2018 showed the presence the two-pore potassium channel THIK-1 in juvenile rat and mouse brain microglia. This channel responsible of outward currents is involved in surveillance and ramification of microglia. However, we have only little information about those channels in spinal microglia.

§4 Electrophysiology

i Description of the technique

One of the main techniques to understand the physiopathology of excitable cells is electrophysiology, which can also be used on non-excitable cells as microglia. By the use of very thin glass electrodes, it is possible to create a seal with a cell and to record the flux of ions crossing the cell membrane through different channels and to record the membrane potential.

ii Electrophysiology in microglia

Kettenmann et al. 1990 have done the first characterization of microglial current. As they could block the current with potassium blockers such as barium, tetraethyammonium (TEA) or 4-aminopyridine (4-AP), they report that microglia have mainly potassium currents.

As mentioned, when facing changes in the environment by increased cytokines or by the presence of pathogens, microglial activate and their electrophysiological properties are also modified - especially with the potassium balance (Kettenmann et al. 2011) (figure 15).

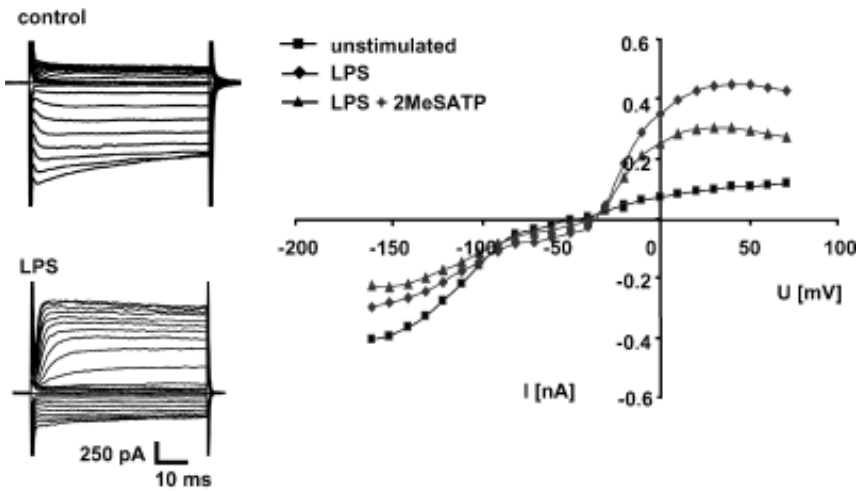

Figure 15: example of microglial currents. The protocol used here is a step protocol from -160 mV to 70 mV in 10 mV increments. **On the left:** Representative voltage step traces of a cell. **On the right:** Representation of the cell population by I-V curves. LPS: lipopolysaccharides, 2MeSATP is a purinergic agonist.

Boucsein et al. 2003

iii Currents in microglia

Several studies have investigated the current expressed by microglia using different drugs or activating agents and recording protocols. In this section, I review the last 30 years of literature on the subject (Table 4). I compared currents and RMP measured in different studies. It appears that age and treatments are the most differencing criteria.

Study and steps	Inward current	Outward Current	RMP	Treatment	Treated: Inward Current	Treated: Outward Current	Treated: RMP	KCl	NaCl	$MgCl_2$	$CaCl_2$	Sol. (mM)	Holding potential	Method and organism
Kettenmann et al. 1990	-500 pA	50 pA	-54 mV	50 mM K^+ ext	-1400 pA	100 pA	-	4.5	160	1	2	EXT	-70 mV	Microglial brain culture, newborn Wistar rats
(steps from -170 to 50 mV)								150	0	2	1	IN		Inward Current strongly reduced by barium and TEA + 4-AP
Nörenberg et al. 1994	-	-	-	LPS (100 ng/ml)	-200 pA	1400 pA	-35 to -70 mV	4.5	160	1	2	EXT	-70 mV	Microglia+astrocyte - brain culture, newborn Wistar rat
(steps from -170 to 50 mV)								150	0	2	1	IN		
Ilschner et al. 1995	-1000 pA	20 pA	-	Remove [Ca]ext	-1200 pA	50 pA	-	5.4	150	1	2	EXT	-70 mV	Note: inward measure taken on the left edge of the steps
(steps from -160 to 20 mV)	-600 pA	40 pA	-	Increase [Ca]in	-80 pA	20 pA	-	130	5	1	1	IN		Measure taken at the right edge, if not mentioned
	-1000 pA	20 pA	-	GTPγS in (100 µM)	-10 pA	200 pA	-							Note: inward measure taken on the left edge of the steps
Cs2+ alone	-60 pA	20 pA	-	ATP (10 µM) + Cs^{2+}	-80 pA	350 pA	-							Microglial brain culture, mouse embryo (E16)
	-120 pA	40 pA	-	TNF-α (1 nM)	-120 pA	360 pA	-							
Schlichter et al. 1996	-	-	-	CSF-1	-300 pA	420 pA	-	5	125 (151)	1	1	EXT	-30 mV or -100 mV	Microglial brain culture, newborn Wistar rats Cultivated with CSF-1 to stimulate proliferation (+ 25 mM $NaHCO_3$, + 1 mM $NaHPO_4$)
(steps from -145 to 35 mV)				CSF-1 + Ba^{2+}	-30 pA	-	-	40 (140)	0 (4)	1	1	IN		(+ 100 mM K-aspartate, + 2 Mm Na_2ATP)
				CSF-1 + MgTx	-	20 pA								
Chung et al. 1998	-120 pA	30 pA	-26 mV	LPS (500 ng/ml)	-190 pA	1550 pA	-48 mV	5	140	3	0	EXT	-80 mV	Microglia+ astrocyte brain culture, 1-3 day old Sprague Dawley rats
(steps from -120 to 40 mV)								140	5	3	0	IN		Ca^{2+} not included to minimise Ca^{2+} dependant currents
				LPS + 4-AP	-190 pA	100 pA	-25 mV							
Chung et al. 1999	-	-	-32 mV	LPS (500 ng/ml)	-600 pA	750 pA	-45 to -70 mV	5	140	3	0	EXT	-60 mV	Microglial brain culture, 1d old Sprague Dawley rats
(steps from -120 to 40 mV)				LPS + Ba^{2+}	-150 pA	750 pA	-45 mV	140	5	3	0	IN		(cells RMPs at -70 mV went back to -45mV with barium block)
Prinz et al. 1999	-650 pA	40 pA	-	PCW	-200 pA	550 pA	-	5.4	150	0	2	EXT	-60 mV	Microglial brain culture, newborn mice (1 day old)
(steps from -160 to 20 mV)	-650 pA	40 pA	-	LPS (100 ng/ml)	-250 pA	450 pA	-	130	0	2	0.5	IN		
	-650 pA	40 pA	-	INFγ (10 ng/ml)	-100 pA	300 pA	-							
Lyons et al. 2000	-120 pA	20 pA	-	MCAO (cerebral artery occulsion)	-750 pA	380 pA	-	2.5 (4.5)	134 (150)	1.3	2	EXT	-70 mV	Brain slice microglia, adult Wistar rats (+ 2 mM K_2HPO_4, + 26 mM $NaHCO_3$)
(steps from -160 to 20 mV)								130	0	2	0.5	IN		
Schilling et al. 2000	-150 pA	10 pA	-	TGF-β	-250 pA	400 pA	-	5	130	1	2	EXT	-60 mV	Cultured brain microglia, newborn NMRI mice
(steps from -150 to 30 mV)								120	0	2	1	IN		
Khanna et al. 2001	0 pA	400 pA	-	AgTx-2	0 pA	100 pA	-	5	0 (145)	1	1	EXT	-90 mV	Cultured brain microglia, 2-3 days old Wistar rats (+ 145 mM Na-aspratate) (outward currents measured at 40 mV) (+ 148 mM K-aspartate)
(steps -60 or-130 to 90 mV)	-100 pA	550 pA		CLT + apamin	-50 pA	100 pA		0 (148)	0	1	0.9	IN		
Visentin et al. 2001	-25 pA/pF	6 pA/pF	-	HIV-Tat (1 µg/ml)	-30 pA/pF	28 pA/pF	-	5	140	1	2.5	EXT	-70 mV	Microglial brain culture, 1-2 day old rats
(steps from -150 to 50 mV)				LPS (100ng ml)	-	21 pA/pF	-	130	0	2	1	IN		Measures were taken near the beginning of traces
				LPS + SN-50	-	8 pA/pF	-							SN-50 is a NF-κB inhibitor
				HIV-Tat + SN-50	-	9 pA/pF	-							

Study and steps	Inward current	Outward Current	RMP	Treatment	Treated: Inward Current	Treated: Outward Current	Treated: RMP	KCl	NaCl	$MgCl_2$	$CaCl_2$	Sol. (mM)	Holding potential	Method and organism
Boucsein et al. 2003	-100 pA	60 pA	-75 mV	Only characterization	-	-	-	2.5 (5)	134 (150)	1.3	2	EXT	-70 mV	Brain slice microglia, adult (6-8 weeks old) C57BL/6 mice (+ 1.25 mM K_2HPO_4, +26 mM $NaHCO_3$)
(steps from -160 to 70 mV)								130	0 (2)	1.3	2	IN	or - 20mV	(+ 2mM Na-ATP) (if mean of RMP, around -34 mV)
	-450 pA	100 pA	-29	LPS (100 ng/ml)	-260 pA	470 pA	-							Cultured brain microglia, newborn mice
			-61	LPS + ATP	-300 pA	400 pA	-							(if mean of RMP, around -41 mV)
	-500 pA	100 pA	-	LPS + ATPγS	-150 pA	200 pA	-							
	-400 pA	80 pA	-	LPS + 2MeSATP	-250 pA	300 pA	-							
Schilling et al. 2004 (steps from -90 to 60 mV)	-20 pA	100 pA	-45	LPC (15 µM)	-450 pA	780 pA	-17 mV (transient)	5	130	1	2	EXT	0 mV	BV2 murine brain microglia cell line
							Then -70	120	0	2	1	IN		
(steps : -120 to 30), low Ca^{2+} in	-80 pA	20 pA	-	LPC (15 µM), low Ca^{2+} in	-360 pA	850 pA	-							
(steps : -120 to 30), low Ca^{2+} in	-80 pA	20 pA	-	LPC + CTX, low Ca^{2+} in	-600 pA	100 pA	-							
Fordyce et al. 2005	-	100 pA	-	LPS (100 ng/ml)	-	200 pA	-	5	125 (151)	1	1	EXT	-100 mV	Microglial brain culture, newborn Wistar rats (day 2-3) (+ 25 mM $NaHCO_3$, + 1 mM $NaHPO_4$)
(steps from -80 to 40mV)								40 (140)	0 (4)	1	1	IN		(+ 100 mM K-aspartate, + 2 Mm Na_2ATP)
Yi et al. 2005	-30 pA	250 pA	-	LPS (100 ng/ml)	-100 pA	500 pA	-	5	140	1	1	EXT	-80 mV	Microglial brain culture, Sprague Dawley rat embryo (E18)
(steps from -120 to 40 mV)								140	10	0	1	IN		
Glucosamine	-30 pA	125 pA	-	LPS + glucosamine	-50 pA	300 pA	-							
			-	LPS + Agtx-2	-10 pA	60 pA	-							
Pannash et al. 2006	-250 pA	200 pA	-	LPS (100 ng/ml)	-150 pA	2700 pA	-	5.4	150	1	2	EXT	-70 mV	Microglial brain culture, newborn mice (1d old)
(steps from -160 to 70 mV)								130	0 (2)	2	0.5	IN		(+ 2 mM Na-ATP)
De Simoni et al. 2008	-100 pA	600 pA	-18	LPS (1 µg/ml)	-300 pA	1000 pA	-	2.4	126 (151)	2	2.5	EXT	-23 mV	Brain slice microglia, juvenile mice (day 21) (+ 26 mM $NaHCO_3$, + 1 mM NaH_2PO_4)
(steps from -63 to 88 mV)								130	4 (4.5)	0 (2)	0	IN		(+ 2 m M MgATP, +0.5 mM NaGTP)
Cheung et al. 2009	-300 pA	60 pA	-	Muscimol (100µM)	-500 pA	50 pA	-	5.4	150	1	2	EXT	-70 mV	brain slice microglia, newborn mice (6-8days old)
(steps from -170 to 50 mV)	-150 pA	40 pA	-	Increase in $[K^+]$ext	-850 pA	50 pA	-	130	0	2	0.5	IN		Microglial brain culture, newborn mice
Menteyne et al. 2009	-30 pA	100 pA	-	Status epilepticus	-480 pA	600 pA	-	3	124 (151.25)	1	2	EXT	-70 mV	brain slice microglia, adult mice (30-40 days old) (+ 26 mM $NaHCO_3$, +1.25 NaH_2PO_4)
(steps from -150 to 30 mV)								0 (132)	0	4	0	IN		(+ 132 mM K-gluconate)
Moussaud et al. 2009	-600 pA	800 pA	-	LPS (1 µg/ml)	-300 pA	600 pA	-	5.5	140	1	1.8	EXT	-60 mV	C4-B8 microglial cell line
(steps from -150 to 30 mV)								140	20	2	2.5	IN		
Dries 2010 (thesis)	-50 pA	60 pA	-	LPS (100 ng/ml)	-120 pA	600 pA	-	5	145	1.4	2	EXT	-60 mV	Microglial brain culture, newborn Wistar rat (day 1 -2)
(steps from -140 to 40 mV)				LPS + minocycline	-340 pA	120 pA	-	130	5	2	1	IN		

Study and steps	Inward current	Outward Current	RMP	Treatment	Treated: Inward Current	Treated: Outward Current	Treated: RMP	KCl	NaCl	$MgCl_2$	$CaCl_2$	Sol. (mM)	Holding potential	Method and organism
Seifert 2011 (thesis)	-500 pA	150 pA	-	LPS (100 ng/ml)	-200 pA	400 pA	-	2.4 (4.8)	134 (160)	1.3	2	EXT	-70 mV	Microglial brain culture, newborn mice (day 0-3) (+ 1.2 mM K_2HPO_4, + 26 mM $NaHCO_3$)
(steps from -160 to 70 mV)	-220 pA	250 pA	-	LPS (100 ng/ml)	-200 pA	300 pA	-	130	0	2	0.5	IN		juvenile (day 22)
	-125 pA	180 pA	-	LPS (100 ng/ml)	-100 pA	350 pA	-							and adult mice (day 49-54)
	-50 pA	30 pA	-	Stab wound	-180 pA	250 pA	-							Brain slice microglia, adult mice
Konno et al. 2012	-8 pA/pF	15 pA/pF	-	Arachidonic acid (AA)	-30 pA/pF	75 pA/pF	-	2	140	2	2	EXT	-70 mV	Microglial brain culture, newborn Wistar rat (day 0-1)
(steps from -100 to 100 mV)				AA + ruthenium red	-8 pA/pF	10 pA/pF	-	20 (140)	0	0 (4)	0	IN		(+120 mM K-gluconate, + 4 mM Mg-ATP)
Scheffel et al. 2012	-500 pA	120 pA	-	LPS (100 ng/ml)	-180 pA	300 pA	-	5.4	150	1	2	EXT	-70 mV	Microglial brain culture, Iba1-GFP newborn mice (d0) (+ 2 mM Na-ATP)
(steps from -160 to 50 mV)	-280 pA	280 pA	-	LPS (100 ng/ml)	-200 pA	350 pA	-	130	0 (2)	2	0.5	IN		Day 21
	-100 pA	200 pA	-	LPS (100 ng/ml)	-100 pA	400 pA	-							Day 49
Liu et al. 2013	-160 pA	20 pA	-	HIV-Tat (200 ng/ml)	-400 pA	1050 pA	-	4.5	150	1	2	EXT	-70 mV	Microglial brain culture, newborn Sprague Dawley rat (d1)
(steps from -170 to 50 mV)				HIV-Tat (1 µg/ml)	-180 pA	1200 pA	-	150	0	1	1	IN		
Muessel et al. 2013	-500 pA	20 pA	-	Chloroethyl-clonidine (CEC)	-50 pA	20 pA	-	5	134	1	1	EXT	-40 mV	Microglial brain culture, CD1 mice (day 2-4)
(steps from -120 to 10 mV)				SDF-1	-700 pA	40 pA	-	40 (124)	0 (0.1)	1 (3)	0	IN		(+ 84 mM K-gluconate, + 2 mM Mg-ATP, +0.1 mM Na-GTP)
	-400 pA	120 pA	-	LPA	-50 pA	50 pA	-							
Tsai et al. 2013	-300 pA	100 pA	-62 mV	Memantine (MEM) (10µM)	-150 pA	110 pA	-55 mV	5.4	136.5	0.53	1.8	EXT	-50 mV	BV2 murine brain microglia cell line
(steps from -140 to 40 mV)				MEM (30µM)	-	-	-47 mV	20 (151)	0 (3.2)	1	0	IN		(+ 130 mM K-aspartate, + 1 mM KH_2PO_4, + 3 mM Na-ATP, +0.1 mM Na_2GTP)
Ferreira et al. 2014	-300 pA	60 pA	-	IL-4 (20 ng/ml)	-50 pA	450 pA	-	5	125	1	1	EXT	-70 mV	Microglial brain culture, newborn Sprague Dawley rat (d1)
(steps from -100 to 80 mV)				IL-4 + NS309	-40 pA	800 pA	-	40 (140)	0	1 (3)	4.3	IN		(+ 100 mM K-aspartate, + 2 mM Mg-ATP)
				IL-4 + TRAM-34	-30 pA	150 pA	-							
Arnoux et al. 2014	-75 pA	125 pA	-	Minocycline	-50 pA	75 pA	-	2.5	126 (153.25)	1	2	EXT	-70 mV	In vivo recordings, cortex of P8 mice (CX3CR1-eGFP) (+ 26 mM $NaHCO_3$, + 1.25 NaH_2PO_4)
(steps from -175 to 75 mV)								0 (132)	0	4	0	IN		(+132 mM K-gluconate)
Komm et al. 2014	-	-	-56 mV	Glycine (Gly,5 mM)	-	-	-20 mV	5.6	140	1.5	2.5	EXT	-60 mV	BV2 murine brain microglia cell line
(zero current clamp patch)				Gly , 0 Na^+ ext	-	-	-59 mV	10 (150)	10	4	2	IN		(+ 70 mM K_2SO_4)
Peng et al. 2014	-	100 pA	-	Irradiation (30 Gy)	-	200 pA	-	4.5	160	1	2	EXT	-80 mV	Microglial brain culture, 6 to 8 week-old Balb/c mice
(one sole step, voltage NA)								0 (160)	0	2	0	IN		(+ 160 mM KF)
Richter et al. 2014	-80 pA	40 pA	-25 mV	Glioma implantation	-130 pA	150 pA	-38 mV	2.5 (5)	134 (160)	1.3	2	EXT	-70 mV	Brain slice microglia, adult (8-10 w old) (+ 1.25 mM K2HPO4, +26 NaHCO3)
(steps from -160 to 50 mV)				Stab wound	-300 pA	100 pA	-40mV	120	4	4	0.5	IN		Cx3Cr1-GFP mice

Study and steps	Inward current	Outward Current	RMP	Treatment	Treated: Inward Current	Treated: Outward Current	Treated: RMP	KCl	NaCl	$MgCl_2$	$CaCl_2$	Sol. (mM)	Holding potential	Method and organism
Chen et al. 2015	-40 pA	30 pA	-	MCAO (cerebral artery occulsion)	-180 pA	230 pA	-	4.5	160	1	2	EXT	Ramps	Microglial brain culture, 7 day old C57BL/6 mice
(ramps from -120 to 40 mV)				MCAO + TRAM-34	-50 pA	80 pA	-	0 (165)	0	2	8.5	IN	NA	(+ 145 mM K-aspartate, + 10 mM K_2EGTA)
				LPS	-50 pA	400 pA	-							
				LPS + TRAM-34	-50 PA	250 pA	-							
Lam et al. 2015	-600pA	0 pA	-	ML133	-20 pA	0 pA	-	5	120	1	1	EXT	0 mV	Microglial brain culture, day 1-2 Sprague Dawley rats
(steps from -160 to 10 mV)				IL-4	-580 pA	20 pA	-	40 (140)	0	1 (3)	0	IN		(+ 100 mM K-aspartated, + 2 mM MgATP)
				IL-10	-500 pA	0 pA	-							
Schilling et al. 2015	-220 pA	20 pA	-37 mV	Old animal	-450 pA	80 pA	-54 mV	3	129 (151.8)	0 (3)	1.6	EXT	-60 mV or -20 mV	Brain slice microglia of adult (8-12w old) or old (19-24 month old) C57BL/6 mice
(steps from -160 to 10 mV)								120	0	2	1	IN		(+ 1.8 mM $NaHCO_3$, + 21 mM $NaH2PO_4$, + 3 mM $MgSO_4$)
Blomster et al. 2016	-80 pA	180 pA	-18 mV	NS309 (500 nM)	-100 pA	380 pA	-76 mV	4	140	1	2	EXT	-90 mV	Human neocortex microglial culture, from epilepsy patients
(steps from -120 to 30 mV)			-	NS309 + NS6180	-120 pA	40 pA	-25 mV	109	0	1.4	5.2	IN		NS309 is a KCa channel activator
	-100 pA	450 pA	-	IL-4	-200 pA	1000 pA	-							Both Il-4 and LPS conditions had outward current
	-120 pA	350 pA	-	LPS	-150 pA	780 pA	-							strongly reduced by the Kca3.1 blocker NS6180
Gu et al. 2016 (steps from -100 to 80 mV)	-10 pA (sham)	40 pA (sham)	-22 mV	SNT D3	-20 pA	240 pA	-	2.5	125 (152.25)	1	2	EXT	-20 mV for traces	Spinal cord slices, 6 to 8 weeks old CX3R1-eGFP mice (+ 1.25 mM NaH_2PO_4, + 26 mM $NaHCO_3$)
(P2Y12-KO sham)	-10 pA	50 pA	-21 mV	SNT D3, P2Y12-KO	-10 pA	80 pA	-	0 (120)	5 (5.3)	1	0	IN	-60 mV for I-V curve	(+ 120 mM K-gluconate, +0.1 mM Na_3GTP)
Lam et al. 2017	-400 pA	220 pA	-	IFN-γ + TNF-α	-250 pA	660 pA	-	5	125	1	1	EXT	-105 mV	Microglial brain culture, newborn Sprague-Dawley rat (P1–P2)
(steps from -175 to 45 mV)			-	Il-4	-160 pA	550 pA	-	40 (140)	0	1 (3)	0.5	IN		(+ 100 mM K-aspartate, + 2 mM MgATP) ML133 fully blocked inward currents in all conditions
Note : outward measures			-	Il-10	-320 pA	400 pA	-							Agtx-2 fully blocked outward currents in all conditions
Taken on left edge	-500 pA	280 pA	-	IFN-γ + TNF-α	-250 pA	550 pA	-							Microglial brain culture, newborn C57BL/6 mice (P0–P2)
			-	Il-4	-360 pA	300 pA	-							
			-	Il-10	-180 pA	120 pA	-							
Nguyen et al. 2017	-40 pA	50 pA	-	LPS	-60 pA	550 pA	-	4.5	0 (160)	1	2	EXT	Ramps	Microglial brain culture, newborn C57BL/6 mice (+ 160 mM Na-aspartate)
(ramps from -120 to 40 mV)			-	LPS + IFN-γ	-20 pA	350 pA	-	0 (145)	0	2	1	IN	NA	(+ 145 mM K-aspartate)
			-	IL-4	-380 pA	40 pA	-							PAP-1 fully blocked LPS and LPS+ IFN-γ outward currents
			-	IFN-γ	-50 pA	50 pA	-							
			-	ATP	-180 pA	80 pA	-							

Study and steps	Inward current	Outward Current	RMP	Treatment	Treated: Inward Current	Treated: Outward Current	Treated: RMP	KCl	NaCl	$MgCl_2$	$CaCl_2$	Sol. (mM)	Holding potential	Method and organism
Deftu et al. 2018	-580 pA	300 pA	-	CXCL1 (intrathecal injection) (1.5 mM)	-1100 pA	300 pA	-	5	120	1	2	EXT	-60 mV	Microglial spinal cord culture, adult CX3R1-eGFP mice
(steps from -160 to 100 mV)				20 mM K^+	-1080 pA	300 pA	-12 mV	130	5	2	1	IN		
				CXCL1 + 20 mM K^+	-2400 pA	380 pA	-46 mV							
Di Lucente et al. 2018 (ramps from -120 to 40 mV)	-40 pA	150 pA	-	LPS injection	-100 pA	600 pA	-	4.5	160	1	2	EXT	Ramps	Microglial brain culture, adult C57BL/6 mouse
Kv1.3-KO	-60 pA	40 pA	-	LPS injection	-160 pA	60 pA	-	0 (160)	0	2	0	IN	NA	PAP-1 strongly reduced outward currents (+ 160 mM KF)
Madry et al. 2018	-10 pA	20 pA	-35 mV	ATP injection	-10 pA	90 pA	-68 mV	2.5	140 (141)	1	2	EXT	NA	brain slice microglia, adult C57BL/6 mouse (+ 1 mM NaH_2PO_4)
(steps from -160 to 40 mV)				(100 µM)				125	4	0	1	IN		
				Laser damage	-15 pA	90 pA								
			-38 mV	TPA (50 µM)	-10 pA	20 pA	-15 mV							
			-40 mV	Isoflurane	-10 pA	20 pA	-17 mV							
			-39 mV	High [K^+] injection (140 mM)	-	-	-16 mV							
Maezawa et al. 2018	-10 pA	20 pA	-	Amyloid-β	-80 pA	150 pA	-							Microglial brain culture, adult C57BL/6 mouse and APP/PS1
(steps from -80 to 100 mV)				(50 nM)										
Gattlen et al. 2019	-120 pA (sham D2)	60 pA (sham D2)	-17 mV	SNI D2	-290 pA	120 pA	-44 mV	5	120 (156.25)	1	2	EXT	-60 mV	Spinal cord Slice microglia, adult CX3R1-eGFP mice
(steps from -160 to 40 mV)	-120 pA (naive)	60 pA (naive)	-20 mV	SNI D7	-100 pA	80 pA	-28 mV	130	5	2	1	IN		(+25 mM $NaHCO_3$, + 1.25 mM Na_2HPO_4)
20 mM K^+ext	-170 pA (naive)	20 pA (naive)	-21 mV	SNI D2, 20 mM K^+ext	-620 pA	30 pA	-37 mV	20	120	1	2	EXT	-60 mV	Microglial spinal cord culture, adult CX3R1-eGFP mice
20 mM K^+ext				SNI D2 + ML133	-40 pA	30 pA	-9 mV	130	5	2	1	IN		20 mM K^+ in extracelluluar solution
5 mM K^+ext	-90 pA (naive)	20 pA (naive)	-27 mV	SNI D2, 5 mM K^+ext	-230 pA	30 pA	-49 mV	5	120	1	2	EXT	-60 mV	5 mM K^+ in extracelluluar solution
5 mM K^+ext				SNI D2 + ML133	-80 pA	30 pA	-5 mV	130	5	2	1	IN		

Table 4 : Electrophysiology in microglia. Abbreviations used in this table: tumor necrosis factor alpha (TNF-α), interferon gamma (IFN-γ), lipopolysaccharide (LPS), Lysophosphatidylcholine (LPC), pneumococcal cell walls (PCW), sciatic nerve transection (SNT), spared nerve injury (SNI), middle cerebral artery occlusion (MCAO), charybdotoxin (CTX), margatoxin (MgTX), not available (NA), tetrapentylammonium (TPA). GTPγS, ATPγS: inactive forms of GTP and ATP respectively. 2MeSATP: purinergic receptor agonist. NS309: KCa channel activator, NS6180: KCa3.1 channel inhibitor. SN-50: NF-κB inhibitor. Muscimol: $GABA_A$ receptor agonist. Agitoxin-2 (AgTx-2) and PAP-1: Kv1.3 inhibitor.

Co-culture of microglia and astrocytes

In newborn rat brain microglia co-cultured with astrocytes there is a clear inward current but little outward current (Nörenberg et al 1992, Chung et al. 1998). After LPS activation, both studies show a slight increase of inward and a great increase of outward microglial current (up to 1500 pA at 40 mV). This outward current was successfully blocked by 4-AP, a blocker of Kv1.x and Kv3.x channels.

Embryos and neonatal microglia

Brain microglia cultured from mouse embryo (E16) shows similar pattern: a rather strong inward current with very low outward current. (Ilschner et al. 1995). Sprague Dawley rat embryo (E18) microglia have a resting pattern with low inward and intermediate outward currents. Yet their activated pattern with LPS is similar to mouse with low inward currents and high outward currents (500 pA at 40 mV) (Yi et al. 2005).

When we look at the situation of neonatal brain microglia culture in mice and rat. In the majority of studies the inward current ranges between -250 and -500 pA, this current is a bit lower inward in rats. All studies find low outward currents in resting state, with 100 pA in average. Even though microglia are activated in many different ways, quite all studies show a clear increase of outward current.

Pathogen intrusion mimicked by LPS or pneumococcal cell walls (PCW), or HIV-Tat proteins cause similar patterns of activation in most of the studies: a lowering of inward current and a strong increase of outward current in mice (Prinz et al. 1999, Boucsein et al. 2003, Pannash et al. 2006, Seifert 2011, Scheffel et al. 2012 and Nguyen et al. 2007) and rats (Chung et al. 1999, Visentin et al. 2001 Fordryce et al. 2005, Dreies 2010, Konno et al. 2012 and Liu 2013). Activation by TNF-α and INF-γ induces the same reaction (Lam et al. 2017), but hypoxia induced by middle cerebral artery occlusion (MCAO) generated both inward and outward currents (Chen et al. 2015). CSF-1 activated microglia also display both inward and outward currents (Schlichter et al. 1996).

Cheung et al. 2009 managed to record microglia from 8 day old mice brain slices. They recorded rather low inward currents (-150 pA) and very low outward current from resting

microglia (40 pA). Using muscimol, a GABAergic receptor agonist, they elicited notable microglial inward currents (-500 pA). However, these current were not caused by a microglial response but to an increase of extracellular potassium concentration coming from other cells reacting to muscimol.

In vivo electrophysiology on cortical microglia of 7 days old mice revealed small microglial currents in resting state, between -100 and -125 pA. Those current could be reduced by half with minocycline (Arnoux et al. 2014).

Juvenile mice microglia exhibit the same kind of increased inward current as newborn when activated by LPS, whether they are in brain slice or culture. However, their resting state is very variable between studies (De Simoni et al. 2008, Seifert 2011, Scheffel et al. 2012).

Adult microglia

In adult brain microglia so far, every study note an increase of outward potassium currents - both in mouse and rats, and both in culture and slice microglia. Interestingly those cells have quite low inward currents in resting state compared to younger microglia. All of the 12 studies show currents between -10 to -220 pA. Unless activated, outward currents in adult microglia are merely of 10 to 180 pA. Now for the inward currents, it appears that most of them are increased during microglial activation, differentially depending on the activation stimuli. While LPS only cause a mild increase but damaged tissue via stab wound, hypoxia (MCAO) or status epilepticus generated remarkable inward currents (Lyons et al. 2000, Menteyne et al. 2009, Seifert 2011, Richter et al. 2014)

Other

In older mice, 19 to 24 month, Schilling and colleagues 2015 showed an increase inward current (-450 pA) compared to adult animals (-220 pA) in resting state. Ageing induced current similar to activation of microglia.

In human brain microglia Blomster and colleagues 2016 showed low currents for the resting state. Yet, human microglia displayed strong outward current once activated by IL-4 or LPS, and slightly increased inward currents.

Microglia have been less studied in the spinal cord. There Deftu et al. 2018 highlighted high inward and mild outward current in resting state microglia. Activation of microglia by the CXCL1 chemokine increased remarkably inward currents while outward currents remained at the same level. In spinal cord slices the resting microglial current measured by Gu. et al 2016 were much lower, and the activation of microglia with the spinal nerve transection model of neuropathic pain did increase the outward current much more than the inward current this time.

In culture cell lines, there are too few studies to see a general pattern.

Summary of the table 4 – regarding methodology and conclusions of studies.

From table 4, some studies have characterized currents of microglia. Kettenmann et al. 1990 first explored the subject with newborn rat brain microglial cultures, determining K^+ as the main microglial current by barium, 4-AP and TEA blockade. Khanna et al. 2001 replicated this and highlighted the involvement of SK and KCa3.1 channels in microglial potassium currents. Also in newborn rats, Schlichter et al. 1996 evaluated currents in CSF-1 cultured brain microglia with different K^+ channel blockers. In addition, they showed that blocking K^+ as well as Cl^-channels reduced the CSF-1 induced microglia proliferation. In mice brain cultured microglia, Muessel et al. 2013 characterized K^+ current and highlighted that Kir2.1 modulation by small GTPases regulates microglial morphology. Boucsein et al 2003 showed electrophysiological properties of microglia mice brain culture and slices and report P2X and P2Y purinergic receptors in microglial activation. Moreover, microglial physiology has been studied in adult and old mice, where Schilling et al. 2015 showed an activated-like phenotype for older animal unchallenged microglia. In human, Blomster et al. 2016 characterized currents of microglia from the cortex of epilepsy patients, where they showed the involvement of KCa3.1 channels.

Several studies have challenged microglia with different pro-inflammatory agents:

Nörenberg et al. 1994 (LPS) Ilschner et al. 1995 (TNF-α), Chung et al. 1998-9 (LPS), Prinz et al. 1999 (LPS, PCW, INFγ), Schilling et al 2000 (TGF-β), Visentin et al. 2001 (HIV-Tat proteins), Bouscein et al. 2003 (LPS + ATP), Schilling et al. 2004 (LPC), Yi et al. 2005 (LPS),

Fordyce et al. 2005 (LPS), Pannash et al. 2006 (LPS), De Simoni et al. 2008 (LPS), Moussaud et al. 2009 (LPS), Dries 2010 (LPS), Seifert 2011 (LPS), Scheffel et al. 2012 (LPS), Konno et al. 2012 (Arachidonic acid), Liu et al. 2013 (HIV-Tat proteins), Chen et al 2015 (LPS), Lam et al. 2017 (TNF-α + INFγ), Nguyen et al 2017 (LPS, INFγ, LPS + INFγ), Deftu et al. 2018 (CXCL1), Di Lucente et al. 2018 (LPS), Maezawa et al 2018 (Amyloid-β)

Or investigated microglial reactivity in injury models:

Lyons et al. 2000 (MCAO), Seifert 2011(stab wound), Richter et al. 2014 (glioma implantation, stab wound), Chen et al. 2015 (MCAO), Gu et al. 2016 (SNT), Madry et al 2018 (laser damage), Gattlen et al. in preparation (SNI)

Some studies used anti-inflammatory agents on microglia:

Ferreira et al. 2014 (IL-4), Lam et al. 2015-17 (IL-4, IL-10), Blomster et al. 2016 (IL-4), Nguyen et al. 2018 (IL-4)

Other types of activations were used:

Ilschner et al 1995 (ATP + Cs^{2+}), Peng et al. 2014 (irradiation), Komm et al. 2014 (glycine), Blomster et al. 2016 (NS309 – KCa channels activator), Nguyen et al. 2017 (ATP), Madry et al. 2018 (ATP injection)

Many studies observed microglial inhibition:

Fordyce et al. (Kv channels blockers, minocycline), Yi et al. 2005 (glucosamine), Konno et al. 2012 (TRPV4 agonists), Liu et al 2013 (Kv channels blockers), Arnoux et al. 2014 (minocycline, yet deleterious during CNS development), Peng et al. 2014 (Kv1.3 peptide inhibitor), Chen et al. 2015 (TRAM-34 – Kca3.1 inhibitor, doxycycline), Madry et al. 2018 (TPA, isoflurane), Di Lucente et al. 2018 and Maezawa et al. 2018 (PAP-1 - Kv1.3 blocker)

In addition, several studies pushed the reasoning further, determining key players in microglial activation, or in microglial physiology:

Schlichter et al. 1996 highlighted the importance of Kir and Cl- channels in CSF-1 induced microglial proliferation. Blockade of such channels inhibited microglial proliferation. Schilling et al. 2000 first mentions Kir2.1 and Kv1.3 as responsible for inward and outward microglial currents respectively. Khanna et al. 2001 shows the involvement of microglial SK channels as wells as Kv1.3 in respiratory burst. Later, Schlichter et al. 2010 determined SK3 as the main SK channel contributing to the neurotoxic microglial phenotype. Vistenin et al. 2001 showed that LPS or HIV-Tat protein microglial involved the NF-κB pathway.

Fordyce et al. 2005 showed p-p38 MAPK pathway activation and reactive oxygen species release via INOS in LPS activated microglia. In addition, they could reduce neuronal death by using minocycline or Kv channels blockers. Yi et al. 2005 proved that glucosamine could inhibit LPS activated microglia by reducing calcium influx and TNF-α expression.

Konno et al. 2012 discovered that depolarizing microglia with TRPV4 agonists suppressed TNF-α expression, a hallmark of microglial activation. Liu et al. 2013 showed that Kv current inhibition abrogated the neurotoxic effect of HIV-Tat protein activated microglia.

Peng et al. 2014 showed that Kv1.3 selective peptide inhibitor reduced microglial inflammation after brain irradiation. Chen et al. 2015 exposed that blockade of microglial KCa3.1 channels ameliorates neuroinflammation after MCAO. Lam and Schlichter 2015 revealed that Kir2.1 is involved in cell migration, chemotaxis and proliferation of anti-inflammatory primed microglia. Gu et al. 2016 demonstrated the crucial role of P2Y12 in microglial activation in the SNT neuropathic pain model.

Ngyuen et al. 2017 highlighted the involvement of Kv1.3 and KCa3.1 in both IL-4 and LPS activated microglia. Di Lucente et al. 2018 showed that Kv1.3 is necessary for M1 pro inflammatory activation of microglia in vivo. Madry et al. 2018 discovered the two-pore potassium channel THIK-1 as a regulator microglial ramification and surveillance. Finally, Maezawa et al. 2018 presented Kv1.3 blockade as a potent therapeutic option against amyloid-β microglial activation in Alzheimer's disease.

iv Resting membrane potential (RMP) in microglia

The membrane potential is the charge difference between the inner and the outer part of the cell membrane. The resting membrane potential is measured when no current is injected in the cell. This potential depends on the difference in concentration of ions inside and outside of the cell in a resting state. The RMP is influenced by the channels active in the cell. The Goldmann-Hodgkin-Katz equation (1) can predict it given the permeability and concentration inside and outside the cell for each ions across the membrane, mainly K^+, Na^+, and Cl^-.

$$V_m = \frac{RT}{F} \ln\left(\frac{p_K[K^+]_o + p_{Na}[Na^+]_o + p_{Cl}[Cl^-]_i}{p_K[K^+]_i + p_{Na}[Na^+]_i + p_{Cl}[Cl^-]_o} \right) \quad (1)$$

Vm: membrane potential

P_K : permeability of K^+ ions

R: the gas constant (8.315 J mol^{-1} K^{-1})

F: Faraday's constant (96480 C mol^{-1})

T: absolute temperature (20 °C = 293 K)

$[K^+]_o$, $[K^+]_i$: K^+ ion concentrations outside and inside cell

ln: natural logarithm

As cells are more permeable to potassium, the RMP often tend to values close to the K^+ equilibrium potential. Ion diffusion across the membrane is defined by 2 driving forces: the concentration gradient and the electrical force. At the K+ equilibrium potential the K^+ ion, those forces balance each other. However, channels gating in the cell membrane is tightly regulated, thus the RMP of the cell is different from ions equilibrium potential.

After reviewing the literature, I observed that RMP of resting microglia is around -25 mV. If concentration of cations (K^+, Na^+, Mg^{2+}, and Ca^{2+}) rises in the cell it will push the RMP toward less negative values, depolarizing it. The opposite will happen if their concentration drops inside the cell. There the potential will reach more negative value, hyperpolarizing it. For anions (Cl^-), it is the opposite. The direction of ion trafficking depends on their equilibrium potential for each ion. From the Nernst equation (2), we could determine the K^+ equilibrium potential with the conditions of our experiments at -83.40 mV with 5 mM of extracellular potassium at 24°C.

$$E_m = \frac{RT}{zF} \ln \frac{[K^+]_o}{[K^+]_i} \quad (2)$$

Em: equilibrium potential

R: the gas constant (8.315 J mol^{-1} K^{-1})
T: absolute temperature (20 °C = 293 K)
z: charge on the ion (*z*=1 for K^+)
F: Faraday's constant (96480 C mol^{-1})
$[K^+]_o$, $[K^+]_i$: K^+ ion concentrations outside and inside cell
ln: natural logarithm

This means that if the RMP of microglia is less negative (depolarized) than the potassium equilibrium potential and if there is enough permeability for K^+ , K^+ would exit the cell trying to reach its equilibrium potential.

As for currents measured in microglial studies, I summarized the observations concerning microglial RMP in the literature.

Co-culture of microglia and astrocytes

Microglial RMP has been measured in different conditions. Adult mice brain microglia co-cultured with astrocytes show a mean RMP of -26 mV. Once exposed to LPS their RMP shifts to -48 mV, but Kv channels blockade by 4-AP rescued the RMP to values comparable to resting microglia (Chung et al. 1998).

Embryos and neonatal microglia

Another study from Chung and colleague (1999) investigated the microglial RMP in brain culture of newborn Sprague Dawley rat (1 day old). They measured -32 mV in resting microglia and a range from -45 to -70 mV after LPS activation. Interestingly, cells with a RMP of -70 mV went back to -45 mV after inward current blockade by barium.

In newborn mice, microglia cultured from brain showed a mean RMP in a range of -20 to -80 mV with peaks at -29 and -61 mV. In adult mice (6-8 weeks old), brain slice microglia had a RMP in a range of -10 to -80 mV with peaks at -23 and -52 mV (Boucsein et al 2003). Out of these values, I calculated means of -41 mV for cultured cells and -34 mV for slice microglia.

In juvenile mice (21 days old), brain slices resting microglia exhibited -18 mV as resting membrane potential. (De Simoni et al 2008).

Adult microglia

Richter and colleagues 2014 have observed similar RMP in adult (8-10 weeks old) mouse brain slice microglia, with a mean value of -25 mV. Once activated by glioma implantation or stab wound in this study, microglia have a hyperpolarized RMP of -38 and -40 mV respectively.

This RMP shift toward hyperpolarized values upon activation is also observed in human microglial culture. Human microglia RMP goes from a mean of -18 mV to -76 mV once activated. There also, the blockade of KCa3.1 currents reversed the effect to -25 mV (Blomster et al. 2016).

Although most studies were performed in newborn or adult mice, Schilling and colleagues 2015 shed the light on the situation in adult older mice. It appears that resting membrane potential is hyperpolarized in old mice. It shifts from -37 mV in adult mice (8-12 weeks old) to -54 mV in old mice (19-24 months old).

In spinal cord slice, we only have the RMP value of resting microglia observed at -22 mV in adult mouse (6-8 weeks old) (Gu et al. 2005). In dissociated spinal cord microglia, the RMP of -12 mV was measured in 20 mM extracellular potassium condition. Although this condition slightly shifts the K^+ equilibrium potential toward more positive values, the activation of microglia – here by injection of the CXCL1 chemokine – did hyperpolarize microglial RMP to -46 mV (Deftu et al. 2017).

Cell line

The murine brain microglial cell line BV2 shows different patterns of RMP: a more hyperpolarized RMP than primary or slice microglia has been measured. -45 mV, -62 mV and -56 mV by Schilling et al. 2004, Tsai et al. 2013 and Komm et al. 2014 respectively. Still once activated by LPC, the team of Schilling measured a hyperpolarized RMP with a mean of -70 mV. They managed to block outward currents with charybdotoxin but did not measure the RMP at this point. However, Tsai and colleagues observed a depolarization of the RMP from -62 to -47 mV using memantine against Kir2.1-like currents.

Overall, it seems that every time microglia are activated they display either inward or outward currents (when voltage steps are applied at respectively negative and positive voltages) or both currents. The channels responsible for these ion fluxes allow hyperpolarization of the microglial RMP, because when they are blocked, we observe a rescue of the RMP toward resting microglia level.

§5 Aim of the thesis

There is low success in the treatment of neuropathic pain. Treatments currently used target neurons, yet glia has an important role in the development of the pathology. More specifically microglia, which are responsible of neuroinflammation, rapidly cleanse the CNS of pathogens or certain noxious substances but can aggravate the situation in the case of neuropathic pain. Thus, modulating microglial reactivity is a promising strategy to reduce neuropathic pain.

As several studies showed, microglial currents of higher amplitudes are observed once microglia is activated. Reducing of such currents through modulation of microglial ion channels could be an option to reduce microglia-induced neuroinflammation. The general goal of this project is to find a novel target on microglia to potentially improve neuropathic pain treatment by looking at electrophysiological properties of these cells after peripheral nerve injury.

I aimed here for a better understanding of potassium channels changes in microglia following peripheral injury and their implication in the pathophysiology of pain, by the study of inward (Kir2.1) and outward (Kv1.3 and Kv1.5) potassium currents as well as microglial RMP. My hypothesis is that the blockade of activated microglial currents could reduce microglial reactivity.

Results

Unpublished study

Introduction

In literature, Kv1.3, Kv1.5 and Kir2.1 potassium channels have been identified as the main actors causing microglial currents. These channels contribute to microglial functions such as inflammation (Kv1.3 and Kv1.5 Pannasch et al. 2006), cell morphology (Kir2.1 Muessel et al. 2013), migration (Kv1.3 and Kir2.1 Lam et al. 2017) or proliferation (Kv1.3, Kv1.5 Fordryce et al. 2005 and Kir2.1 Schilling et al. 1996). Yet no study have investigated them in the field of neuropathic pain.

Aim

The goal of this project was to highlight the presence of such channels in microglia before and after SNI, and to evaluate their mRNA and protein expression in the spinal cord. I hypothesized that one of those potassium channel might change its expression after SNI and be involved in microglial activation and be an interesting target to modulate microglial reactivity.

Results and discussion

I first investigated the main voltage gated potassium channels implicated in microglial potassium currents. As expected from literature, Kv1.3, Kv1.5 and Kir2.1 were present in the microglia we studied (Figure 16).

It turned out from our electrophysiology results that the Kv1.3 and Kv1.5 had very little impact in our currents. As we observed no increase in outward current when applying voltage step in the positive range. Instead, we measured increased inward current after SNI when applying lower voltage steps that we determined as generated by Kir2.1, as further developed in the second article.

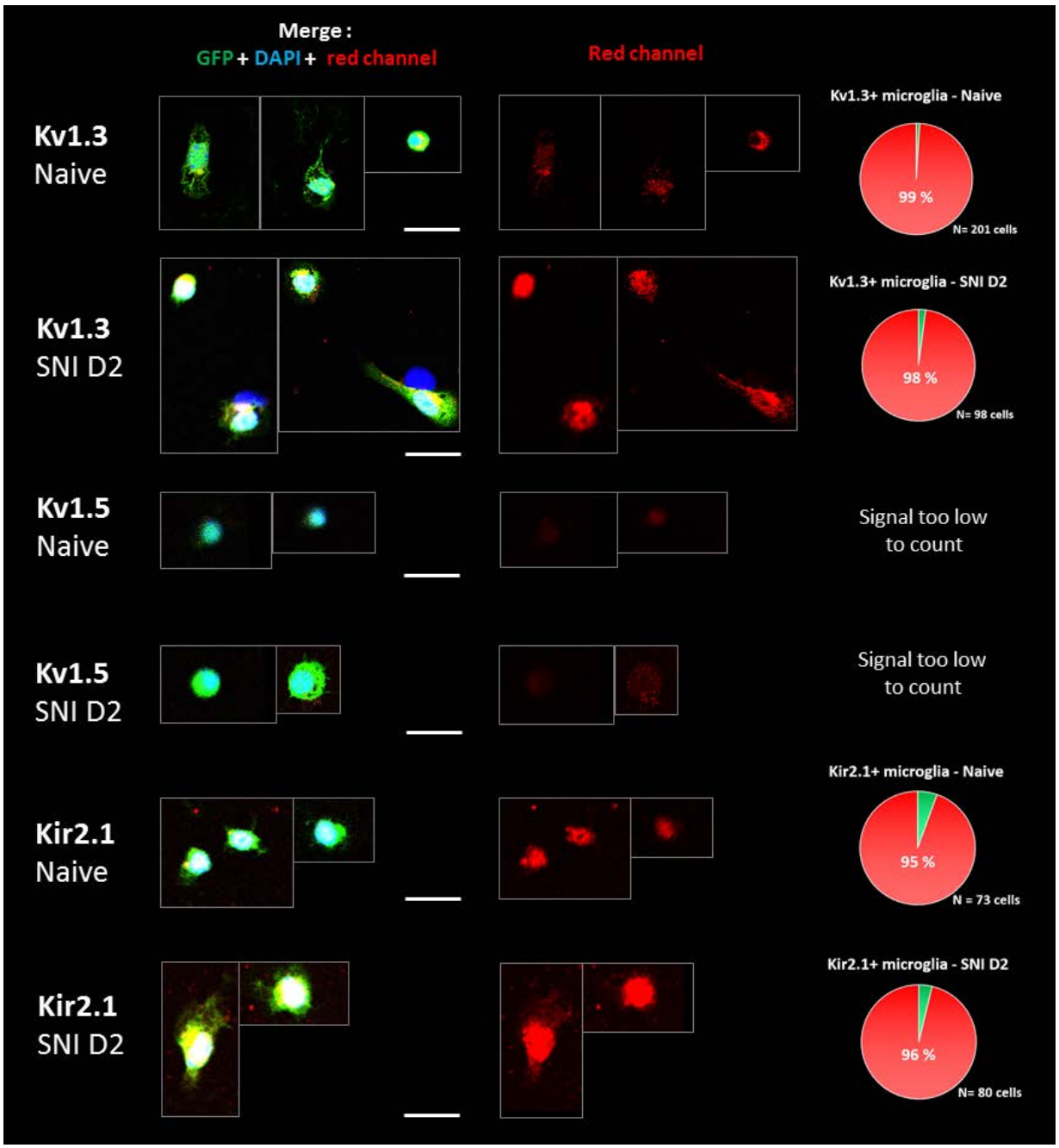

Figure 16: Kv1.3, Kv1.5 and Kir2.1 presence in freshly isolated spinal cord microglia. Microglia isolated from the dorsal horn ipsilateral to the surgery. Immunostaining of Kv1.3, Kv1.5 and Kir2.1 in naive and SNI D2 animals. The proportion of stained cells out of GFP+ cells is shown on the right. For Kv1.5 the signal was so low that it was impossible to count. Thus, no proportion is shown. The scale bars all represent 20 µM per images.

To confirm the validity of these staining, we transfected HEK cells with Kv1.3, Kv1.5 and Kir2.1. We then stained them with our antibodies to determine their specificity (Figure 17).

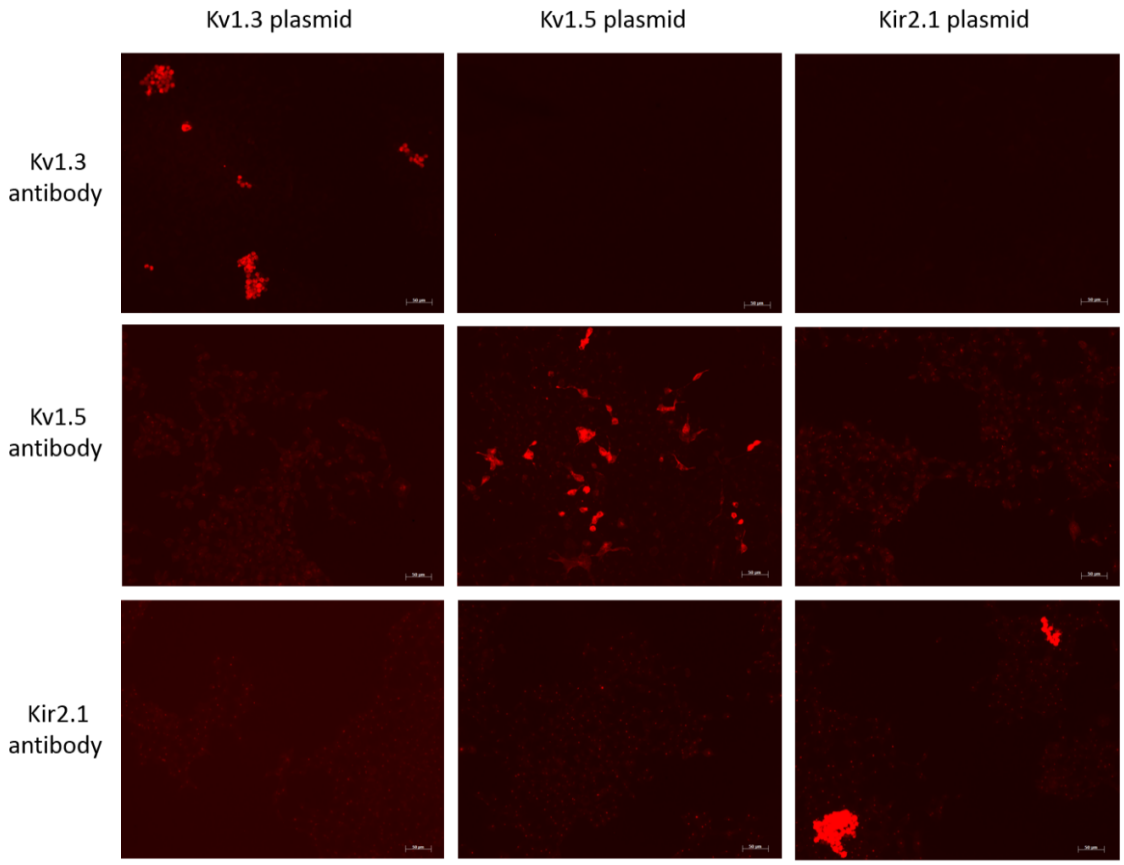

Figure 17: Positive control for antibody on transfected HEK cells. Potassium channels Kv1.3, Kv1.5 and Kir2.1 were transfected in HEK cells. Two days after, the HEK cells were fixed and stained with corresponding antibodies.

We examined the quarters of spinal cord corresponding to the dorsal horn ipsilateral to the SNI surgery (DHi), wherethe microglial activation appears after nerve injury (Figure 18).

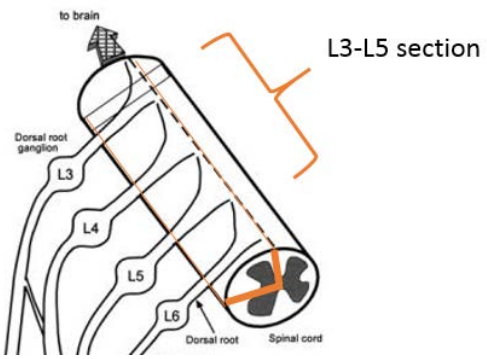

Figure 18: Section of the spinal cord used for qPCR and western blots. After SNI surgery, nerves arriving via the dorsal roots in the section corresponding to the lumbar vertebrae 3 to 5 (L3-L5) are damaged. Microglia in the dorsal horn is activated where the injured nerve afferents arrive. This is the section we study.

By qPCR, we evaluated the expression of Kv1.3, Kv1.5 and Kir2.1 in the dorsal horn ipsilateral to SNI surgery in a timecourse (Figure 19). We used six animals per condition. Our inclusion criteria were to have low RNA degradation after extraction (RNA integrity number (RIN) > 6) and a clear specific melting peak.

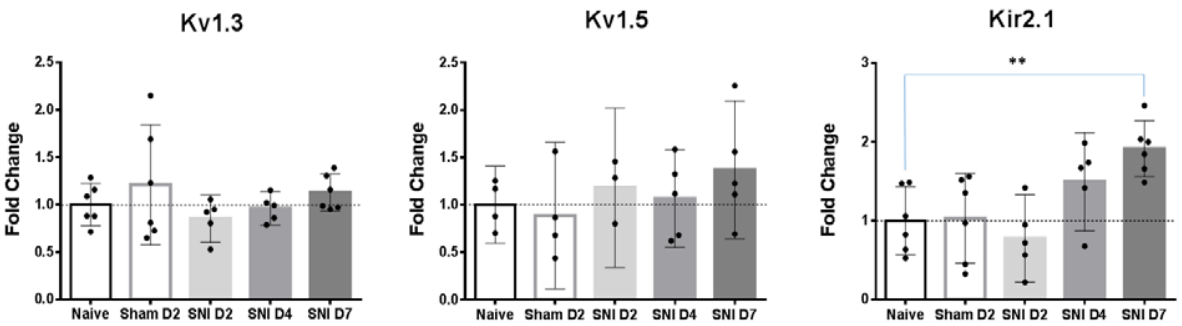

Figure 19: Kv1.3 Kv1.5 and Kir2.1 mRNA expression in the dorsal horn (DHi). Values normalized by mean of naive samples. Values expressed as mean ± SD. One way ANOVAs – post-hoc tests Sidak corrected, **: $p < 0.005$

Except an increase in Kir2.1 seven days after SNI compared to naive animals, no significant difference was found. Moreover, this increase does not correspond to the changes in electrophysiology of microglial cells. As quarter of spinal cord were used, other cells might have contributed to this increase.

I thus hypothesized that the regulation in microglia was at the protein level, and went for western blots. Only the time points of interest with modification in electrophysiology were tested, ie day 0, 2 and 4 with 3 animals per condition.Protein expression of Kv1.3, Kv1.5 and Kir2.1 (Figure 20) was evaluated with western blots. We could not detect any increase of expression two days after SNI, nor could we see difference in protein expression.

The HEK Kv1.3 positive control band was found at a lower molecular weight than expected. It appeared by sequencing that it was truncated in the N-terminal region. As the C-terminal region corresponding to the binding region of our Kv1.3 antibody epitope was intact, this was not noticed by immunofluorescence. Quantifications after normalization to reference protein (GAPDH, Tubulin, β-actin) are shown on the right. The outlier in Kir2.1 naive is caused by a bad binding of the reference gene antibody at the edge of the membrane.

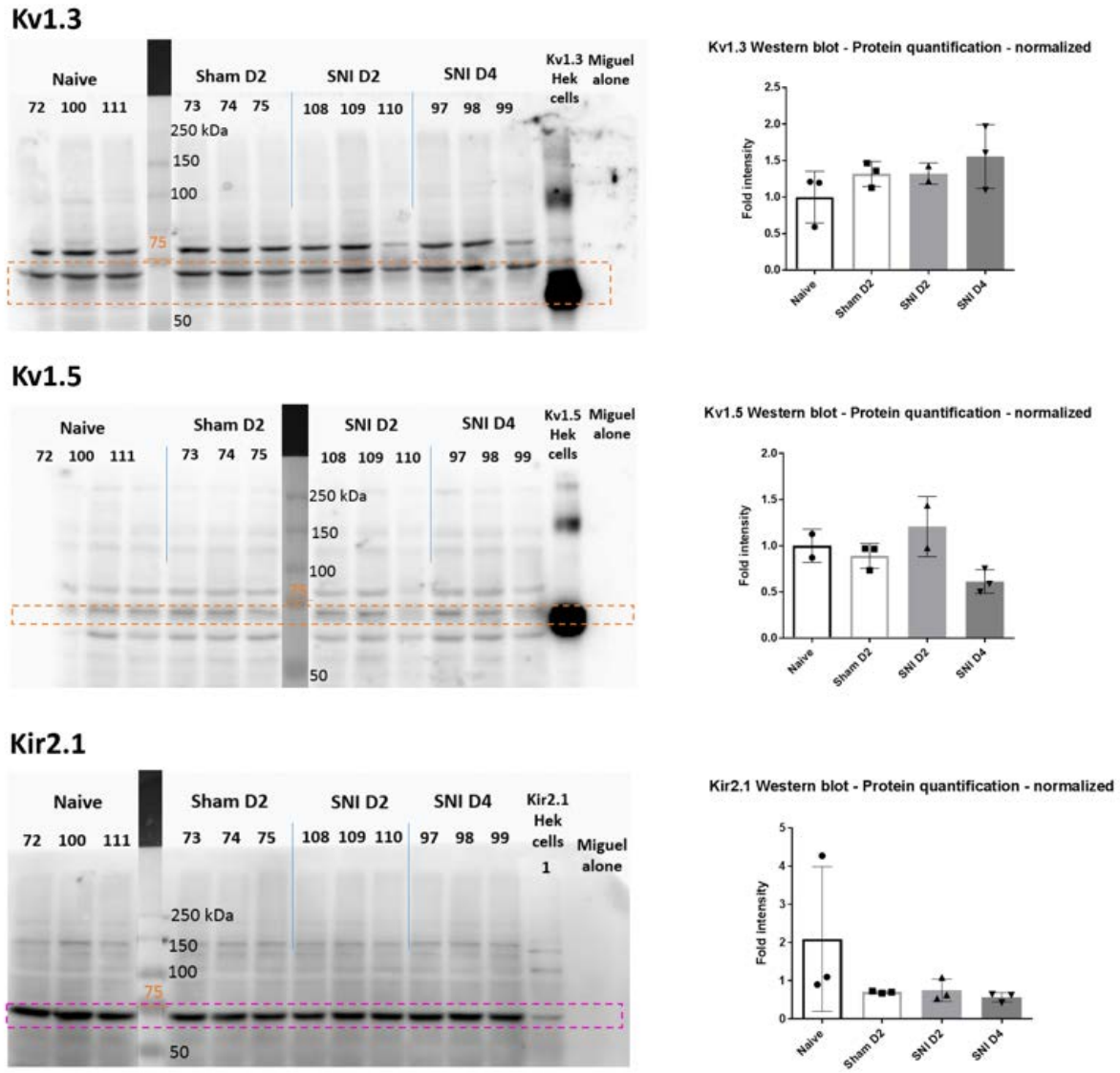

Figure 20: Kv1.3, Kv1.5 and Kir2.1 protein expression in the dorsal horn (DHi). Quantification shown on graphs are normalized to proteins of reference genes. Values expressed as mean ± SD. One way ANOVAs – post-hoc tests Sidak corrected. No significant differences when compared to naive or to sham D2

Interestingly, Fordyce and colleague 2005 observed no increase in Kv1.3 or Kv1.5 proteins after LPS or PMA (respiratory burst) treatment in neonatal rat brain cultured microglia. The D7 time point was not investigatd here as no difference was found in the early timepoints that showed differences in electrophysiology results. The same problem of sampling as in qPCR above, quarter of spinal cord without specifically collecting microglia could have diluted a change in microglia.

To detect specific regulations in microglia, I tried to select only these cells by fluorescence activated cell sorter (FACS) as CX3CR1-eGFP transgenic mice (with GFP-labelled microglia) were used (Figure 21).

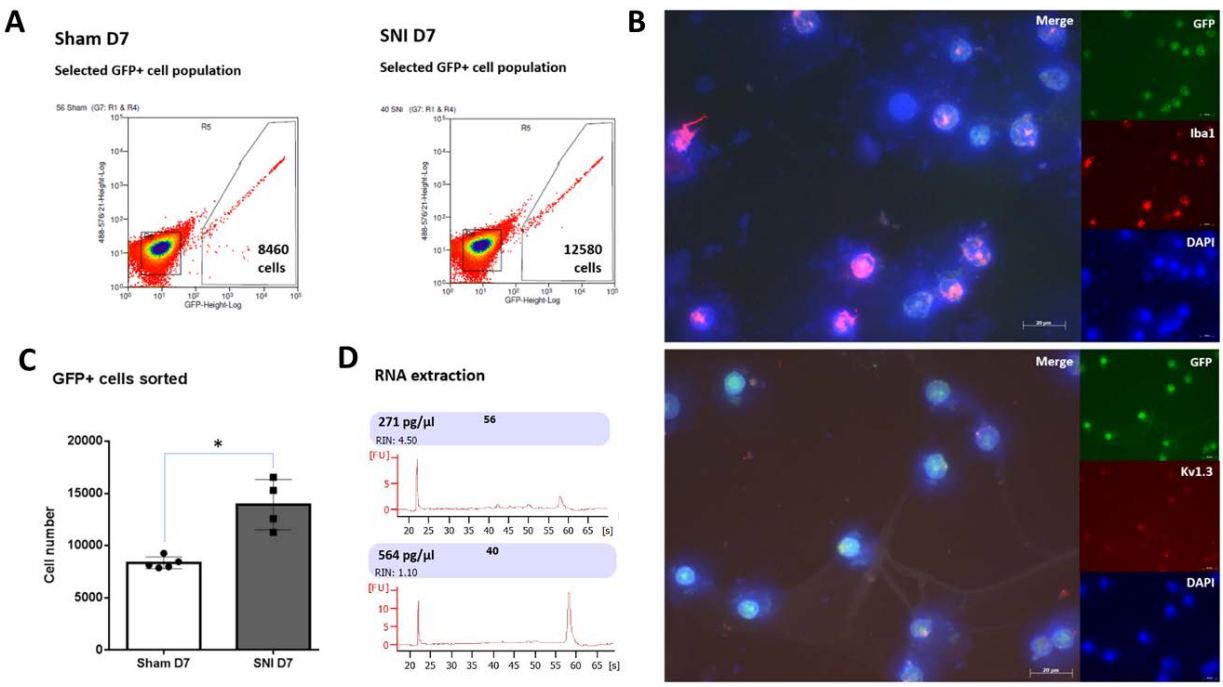

Figure 21: FACS sorting of microglia. **(A)** Representative FACS sortings for sham and SNI animals. **(B)** SNI D7 immunofluorescence to verify that our cells are microglia with labelling of Iba1 (microglial marker) and Kv1.3 (channel of interest – specific to microglia). **(C)** Number of GFP positive cell sorted. Values expressed as Mean ± 95% CI. Student's T-test, *: $p<0.05$. **(D)** Amount with RIN of RNA extracted from sham and SNI depicted in (A).

After sorting, only less than nanograms of RNA could be extracted, with RIN values around 4, not acceptable for good qPCR standards. Several FACS optimizations and RNA extraction kit were tried without significantly improving the results. One solution would be to increase the number of animals, but too many animals would need to be used.

As meanwhile, the membrane expression of Kir2.1 after nerve injury via Kir2.1 antibodies against extracellular epitope gave satisfying results to answer the question of the origin of the increased current, the FACS experiment was not continued.

Methods

Male CX3CR1-eGFP mice were lethally anesthetized by intraperitoneal injection of pentobarbital. The spinal cord was removed and the quarter of spinal cord corresponding to L3-L5 was extracted (Figure 18). This tissue was used for RNA extraction for qPCR, for protein extraction for western blots, or dissociated and plated on 8-well slides for immunofluorescence.

For the dissociation, cells were incubated 30' at 30°C in 2mg/ml papain and separated by pipet trituration in DMEM with 10% fetal bovine serum and 1% penicillin-streptomycin. Cells were then centrifuged at 400g for 5 minutes and the supernatant was removed. Cells were resuspended in 200µl and plated in the 8-well chamber or filtered in a tube and brought to the FACS.

For the qPCR, quarter of L3-L5 spinal cord region were rapidly dissected and placed in ice cold Qiazol (Qiagen). Total RNA was extracted with Zymo Direct-zol RNA kit. Amount and quality of RNA was verified by gel migration using RNA 6000 Nano LabChip with the Agilent Bio-analyzer. RNA was then reverse transcribed using Omniscript reverse transcriptase kit (Qiagen), Quantitative real-time PCR was performed using SYBR-green qPCR with the MyiQ Single Color real-time PCR System or CFX96 Real-Time System (Bio-Rad, Reinach, Switzerland). Primer sets were either taken from literature or designed on Primerblast (NCBI). Specific PCR product amplification was confirmed using dissociation protocol and melting curve and checked by gel migration. All experiments were made in experimental triplicates with N=6 animals per condition. Fold changes were determined by the ΔΔCT method. Glyceraldehyde-3-phosphate dehydrogenase (GAPDH) and hypoxanthine phosphoribosyltransferase 1 (HPRT1) were used as reference genes since their expression in spinal cord is not altered by SNI surgery. The following primer were used:

Gene	Forward primer	Reverse Primer
Kv1.3	CTCCTTTGAGCTTCTGGTGC	CTGCCCATTACCTTGTCGTT
Kv1.5	CCGGGTTTCCCGAATCTTCA	AGAAGTGCGACCCCTGATTG
Kir2.1	CAGTGTCTTGGGAATTCTCAC	ACCTTAGTAACTCAGCTGAC
GAPDH	TCCATGACAACTTTGGCATTG	CAGTCTTCTGGGTGGCAGTGA
HPRT1	ACTGGAAAGAATGTCTTGATTGTTG	CATTTTGGGGCTGTACTGCTT

For immunofluorescence, please refer to the methods of the second article for the experimental procedure. In this part, the following primary antibodies were used:

Antibody	Source	Target	Concentration
Rabbit anti-Kv1.3	Alomone Labs, Israel	Kv1.3	1:300
Rabbit anti-Kv1..5	Alomone Labs, Israel	Kv1.5	1:300
Rabbit anti-Kir2.1 extracellular	Alomone Labs, Israel	Kir2.1	1:300
Rabbit anti-Iba1	Wako, USA	Iba1 – Microglial marker	1:750

The secondary antibody was Cy3-labelled donkey anti-rabbit with a concentration of 1:500 from Jackson. DAPI was used to stain the nucleus both in immunofluorescence and in the FACS to determine the viability of our cells.

For western blots, protein samples were prepared from quarter of L3-L5 spinal cord region by homogenization in a lysis buffer containing protease and phosphatase inhibitors (Sigma-Aldrich). 160 µg (for Kv1.3 and 1.5) or 80 µg (for Kir2.1) of proteins were separated on 10 % SDS–PAGE gel and transferred to nitrocellulose blots. The blots were blocked and incubated overnight at 4 °C with antibodies against Kv1.3, Kv1.5 and Kir2.1 intracellular (Alomone, all diluted at 1:300). These blots were incubated further with HRP-conjugated secondary antibody and developed in ECL solution (Thermo Fisher). Specific bands were evaluated by apparent molecular sizes. The intensity of the selected bands was analyzed using NIH ImageJ software. For normalization, the reference gene with the best signal was used: GAPDH for Kv1.3, tubulin for Kv1.5 and β-actin for Kir2.1.

Study I

Spinal Cord T-Cell Infiltration in the Rat Spared Nerve Injury Model: A Time Course Study

Christophe Gattlen, Christine B. Clarke, Nicolas Piller, Guylène Kirschmann,
Marie Pertin, Isabelle Decosterd, Romain-Daniel Gosselin and Marc R. Suter

Int J Mol Sci 2016 17(3): 352.

Synopsis

The immune system participates in development of neuropathic pain following nerve injury. In particular, T-lymphocytes infiltration of the spinal cord following peripheral nerve injury was described as contributor to sensory hypersensitivity.

In the dorsal horn ipsilateral to SNI, Iba1 and bromodesoxyuridine (BrdU) immunostainings revealed the microglial activation and proliferation, attesting neuroinflammation with various time-courses. The expression of the microglial marker Iba1 peaked at D4 and D7 respectively at the mRNA and protein level. Proliferation, revealed by BrdU stainings, occurred almost only in Iba1 positive cells and peaked at D2.

Overall changes of gene expression with a time-course RT-qPCR array were invetigated. An increase in the regulation of genes related to inflammatory and later anti-inflammatory cytokines, the toll like receptors and their downstream cascade as well as genes coding for complement components was observed. Most of these genes groups can be related to microglial activation.

Some upregulated cytokines are also lymphocytes attractors and T-cell infiltration was investigated byimmunofluorescence with CD2/CD8 antibodies. There were few CD2/CD8 positive lymphocytes in the dorsal horn ipsilateral to SNI surgery.

Spinal cord injury (SCI) model, consisting in dropping a blunt stick with a definite strength onthe exposed spinal cord, was used as a positive control. There a clear infiltration of the CD2+ or CD8+ T-cells was observed. This validated our negative results after SNI. It

seems that T-lymphocyte infiltration is greatly increased when the blood-brain barrier is mechanically damaged. This could explain why we have little infiltration in the SNI model.

Although we can clearly see the microglial reactivity, and find upregulated genes correlating our results with other studies, we could not find T-lymphocyte infiltration in the SNI model of neuropathic pain, despite the findings of other groups. This discrepancy is discussed in the article.

Aim

With this study, we first wanted to investigate and characterize gene regulation of nearly 100 genes in a time course after SNI. The goal was to determine the crucial timepoints in the microglial activation as well as the important genes involved in the process. Secondly, as the acquired-immune system could play a major role in certain case of neuroinflammation, we decided to evaluate its impact in the context of neuropathic pain by assessing lymphocyte infiltration.

This study was the starting point of my thesis. As we concluded that lymphocyte had little impact in the SNI model, we decided to concentrate our efforts on microglial reactivity. With the time course and the gene regulation as a basis to study - and with the aim to modulate - microglial activation.

Author Contributions: Christophe Gattlen analyzed data and drafted the first manuscript. Nicolas Piller designed and performed the RT-qPCR array and timecourse. Christine B. Clarke performed immunohistochemical studies, data analysis, imaging participated in the study design and drafted the manuscript. Guylène Kirschmann did the animal surgery and prepared the tissue. Marie Pertin performed immunohistochemistry, prepared tissue, performed staining and imaging. Isabelle Decosterd supervised the experiments and the final manuscript. Romain-Daniel Gosselin supervised and designed the experiments and the statistical analysis. Marc R. Suter supervised and designed the experiments and wrote the final manuscript. All the authors read and approved the final manuscript.

Article

Spinal Cord T-Cell Infiltration in the Rat Spared Nerve Injury Model: A Time Course Study

Christophe Gattlen [1,2,*], Christine B. Clarke [1,2,†], Nicolas Piller [1,2], Guylène Kirschmann [1,2], Marie Pertin [1,2], Isabelle Decosterd [1,2], Romain-Daniel Gosselin [1,2] and Marc R. Suter[1,2,*]

[1] Pain Center, Department of Anesthesiology, Lausanne University Hospital (CHUV) and University of Lausanne, 1011 Lausanne, Switzerland; Nicolas.Piller@chuv.ch (N.P.); Guylene.Kirschmann@unil.ch (G.K.); Marie.Pertin@unil.ch (M.P.); Isabelle.Decosterd@chuv.ch (I.D.); rdg@biotelligences.com (R.-D.G.)

[2] Department of Fundamental Neurosciences, University of Lausanne, 1005 Lausanne, Switzerland

* Correspondence: christophe.gattlen@unil.ch (C.G.); marc.suter@chuv.ch (M.R.S.); Tel.: +41-21-314-11-11 (C.G. & M.R.S.)

† This author passed away.

Academic Editor: Irmgard Tegeder

Received: 7 December 2015; Accepted: 29 February 2016; Published: date

Abstract: The immune system is involved in the development of neuropathic pain. In particular, the infiltration of T-lymphocytes into the spinal cord following peripheral nerve injury has been described as a contributor to sensory hypersensitivity. We used the spared nerve injury (SNI) model of neuropathic pain in Sprague Dawley adult male rats to assess proliferation, and/or protein/gene expression levels for microglia (Iba1), T-lymphocytes (CD2) and cytotoxic T-lymphocytes (CD8). In the dorsal horn ipsilateral to SNI, Iba1 and BrdU stainings revealed microglial reactivity and proliferation, respectively, with different durations. Iba1 expression peaked at D4 and D7 at the mRNA and protein level, respectively, and was long-lasting. Proliferation occurred almost exclusively in Iba1 positive cells and peaked at D2. Gene expression observation by RT-qPCR array suggested that T-lymphocytes attracting chemokines were upregulated after SNI in rat spinal cord but only a few CD2/CD8 positive cells were found. A pronounced infiltration of CD2/CD8 positive T-cells was seen in the spinal cord injury (SCI) model used as a positive control for lymphocyte infiltration. Under these experimental conditions, we show early and long-lasting microglia reactivity in the spinal cord after SNI, but no lymphocyte infiltration was found.

Keywords: peripheral nerve injury; SNI (spared nerve injury); SCI (spinal cord injury); microglia; lymphocytes; neuropathic pain

1. Introduction

Neuropathic pain is a type of chronic pain, arising as a consequence of a lesion or disease of the somatosensory nervous system. It affects up to 10% of the global population [1] and, therefore, represents a major challenge for the medical community. Although the lesion occurs in neurons, glial and immune cells (such as astrocytes, microglia, infiltrating macrophages or lymphocytes) are implicated in chronic pain in both the periphery and in the central nervous system (CNS) [2–5].

When a peripheral nerve is injured, an immune reaction occurs, with an initial activation of neuroglial cells in the dorsal horn of the spinal cord, ipsilateral to the injury. In particular, microglia (the CNS macrophages) proliferate and change their morphology and gene expression (such as an up-regulation of Iba1) [3–5]. Following peripheral nerve injury, microglia activation is often described as early and transient participating in the development of pain-related behavior, whereas the response of

other immune-mediating cells, such as astrocytes, begins later and contributes to the maintenance of the chronic pain [5]. Using chimera mice with a partial sciatic nerve ligation (PSNL), Zhang *et al.* showed that a number of cells expressing microglia markers were of hematogenous monocytic origin, infiltrating the spinal cord before proliferating there [6]. Leukocyte trafficking through the blood–brain barrier has also been reported after L5 spinal nerve transection in rats [7]. Many studies have been performed using different neuropathic pain models, including chronic constriction injury (CCI) [8], L5 spinal nerve transection [9], and spared nerve injury (SNI) [10] in the investigation of lymphocyte infiltration, but this phenomenon was not observed in all studies and therefore remains somewhat controversial [11,12]. The exact contribution of infiltrating lymphocytes in neuropathic pain needs further study.

Here, we aim to characterize some specific features of neuroimmune reactivity in the spinal cord following peripheral nerve injury in rats. For this study, we used the SNI model of neuropathic pain in Sprague Dawley adult male rats to assess proliferation, and/or protein/gene expression levels for microglia (Iba1), T-lymphocytes (CD2) and cytotoxic T-lymphocytes (CD8). We observed the reaction of the immune system over a prolonged time course performing an array study of inflammatory markers as well as immunostainings of lymphocyte infiltration into the spinal cord.

2. Results

2.1. SNI Upregulates Genes Related to Microglial Reactivity

Microglial reactivity was assessed using a gene expression time course of the microglial markers CD11b and Iba1 in the lumbar section of adult male Sprague Dawley rats 2, 4, 7, 10, 14 and 21 days after SNI compared to naive animals. We observed an upregulation of CD11b at day 2, 4, 10, 14 and 21, and an upregulation of Iba1 at day 2, 4, 10, 14 and 21 (non-overlap of 95% CI method compared to D0 [13], Figure 1, no sham group was used for each time point to lower the number of animals needed).

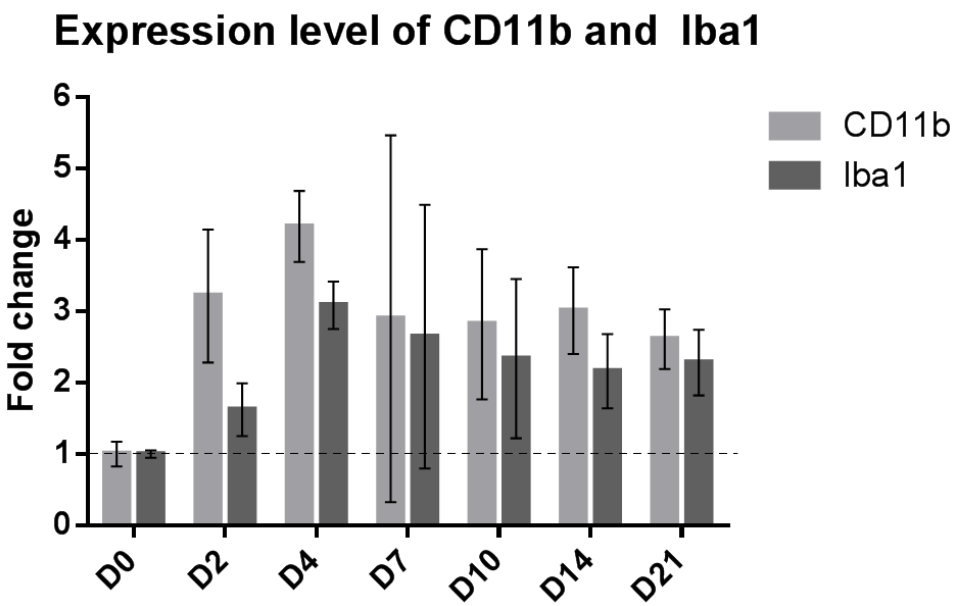

Figure 1. Upregulation of microglial markers after SNI. Bar graph showing the mRNA fold change in rat ipsilateral dorsal horns of the microglial markers CD11b (light gray) and Iba1 (dark gray) compared to naive animals. Values are expressed as mean ± 95% CI. $N = 3$ for each time point.

We also assessed the change over time of Iba1 at the protein level using immunofluorescence on the ipsilateral dorsal horn of the spinal cord: the time course of Iba1 protein expression follows that of mRNA but with a few days delay, peaking at day 7 (Figure 2). At both the mRNA and protein level we observe a prolonged increase in microglial reactivity.

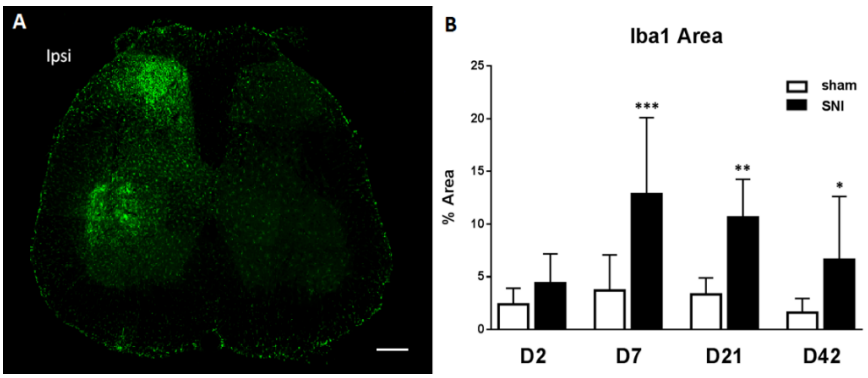

Figure 2. Neuroinflammation in the spinal cord after SNI. (**A**) Immunofluorescence of a lumbar section seven days after injury showing the microglial activation marker Iba1 in green (**B**) Time course of the percentage of Iba1 positive area by immunostaining in the ipsilateral dorsal horn. $N = 4$/group. Values are expressed as mean ± 95% CI, 2-way ANOVA with Sidak correction, sham *vs*. SNI. * $p < 0.05$, ** $p < 0.01$, *** $p < 0.001$. Scale bar represents 200 μm.

2.2. SNI Induces Microglial Activation and Proliferation

We also investigated microglial proliferation as an indicator of microglial reactivity. Using immunofluorescence, we performed an expression time course of the proliferation marker BrdU (bromodeoxyuridine) on rat spinal cord lumbar sections combined with the cellular marker Iba1 (Figure 3). We observed a peak of the BrdU signal at D2. BrdU signal almost fully (95.5%) colocalized with Iba1 (Figure 3F).

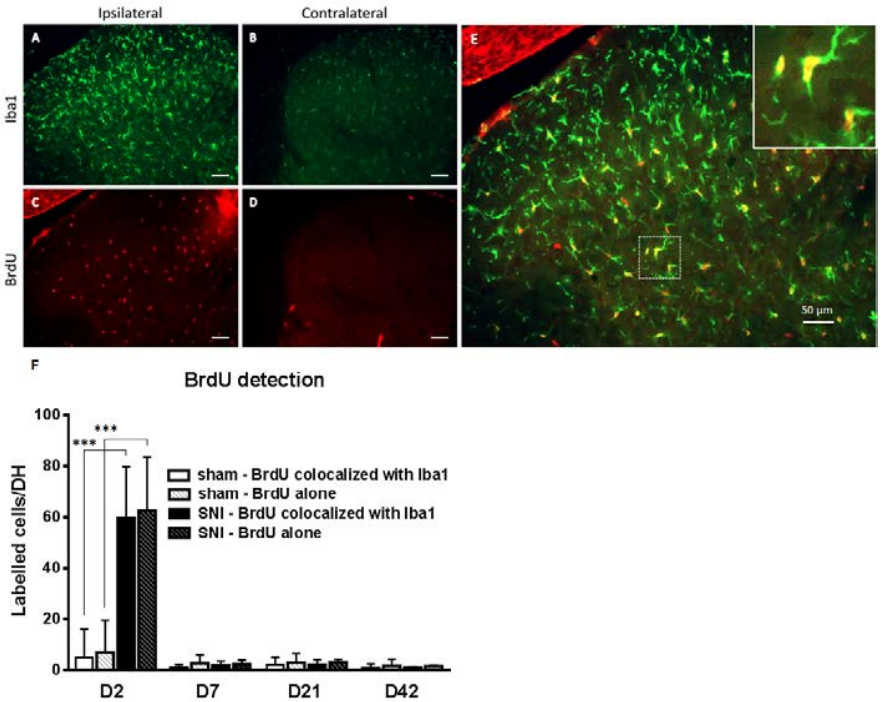

Figure 3. Colocalization of the proliferation marker BrdU with Iba1 in the ipsilateral dorsal horn two days after SNI. (**A**–**D**) Iba1 (green) and BrdU (red) in the ipsilateral (**A**,**C**) and contralateral (**B**,**D**) dorsal horn two days after SNI surgery. There is a marked microglial reaction on the ipsilateral side (**E**) Merge of Iba1 and BrdU ipsilateral showing the colocalization of the two markers indicating microglial proliferation following peripheral nerve injury. Insert: magnification (**F**) Time course of BrdU positive cells in dorsal horn, colocalized or not with Iba1. *N* = 4/group. Values are expressed as mean ± 95% CI, 2-way ANOVA with Sidak correction, *** $p < 0.001$. DH, dorsal horn. Scale bar represents 50 µm.

The time course of proliferation, with a sharp increase only observed at day 2, is in stark contrast to the prolonged increase of the markers Iba1 and CD11b. This highlights the necessity to specify how microglial reactivity is defined. Using only proliferation as a marker of reactivity could lead to the misleading idea that microglial activation is restricted to early time points after peripheral nerve injury.

2.3. Inflammatory Genes Are Regulated after Peripheral Nerve Injury

Based on the Iba1 expression time course (Figure 1), we selected four time points (2, 4, 10 and 21 days) at which to assess the mRNA expression changes of 96 genes of interest in the lumbar spinal cord of adult male Sprague Dawley rats in SNI compared to naive animals (Figure 4). Sham animals were only tested for 2 and 4 day and are shown in the supplemental data. These are the time points with the highest chances to demonstrate modification caused by inflammation. Differences for TLR1 and Iba1 in sham D2 and for CCL12 in sham D4 were significant. Long term changes might have been missed by not performing sham D10 and D21. Exact p-values are available in Table S1.

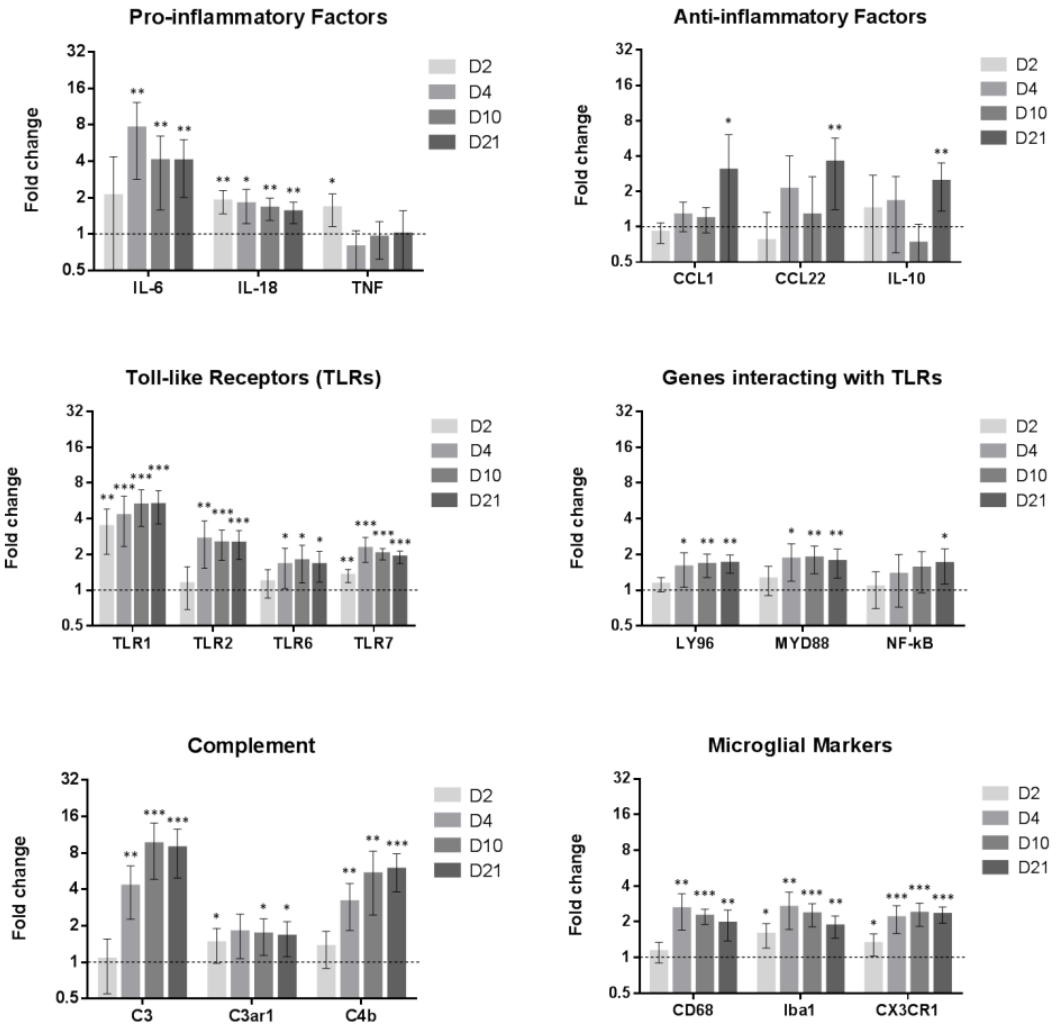

Figure 4. Gene regulation in the spinal cord following SNI. RT-qPCR array with fold change of gene expression in adult male rat ipsilateral dorsal horns at D2, D4, D10 and D21 after SNI compared to naive animals. Values are expressed as mean ± 95% CI. Dotted line at one fold regulation (naive animals). * $p < 0.05$, ** $p < 0.01$, *** $p < 0.001$. Student's *t*-test: naive (not shown) vs SNI. $N = 6$ for each time point (D2, D4, D10 and D21).

Genes were associated in clusters:

Prototypical pro-inflammatory factors such as TNF-α or IL-6 [14] were upregulated at early time points. At later time points, such as day 21, we noticed the upregulation of more "anti-inflammatory factors" such as IL-10, CCL1 or CCL22 which could play a role in the resolution of inflammation [15,16].

Most of the toll-like receptors (TLRs) are upregulated during the whole time course (see in Supplementary Figure S2).Genes involved in the complement system are also upregulated following nerve injury. We observed, in this study, changes in C3 and C4b expression, confirming previous studies [17]. The expression of the microglial markers Iba1, CD68 and CX3CR1, used to indicate microglial reactivity, were also assessed. Their mRNA was upregulated over the full time course (Supplementary Figures S2 and S3. The full array data are available at figshare [18]).

As Lymphocyte/T-lymphocyte attractors [19], such as CCL12 [20], CXCL11 [21] or CD74 [22], were upregulated (Figure 5A), we wanted to further investigate if there was indeed an infiltration of lymphocytes through the blood–spinal cord barrier. Counting regions have been defined in Supplementary Figure S1. Injured nerve regions have been verified with isolectin B4 (see Supplementary Figure S6).

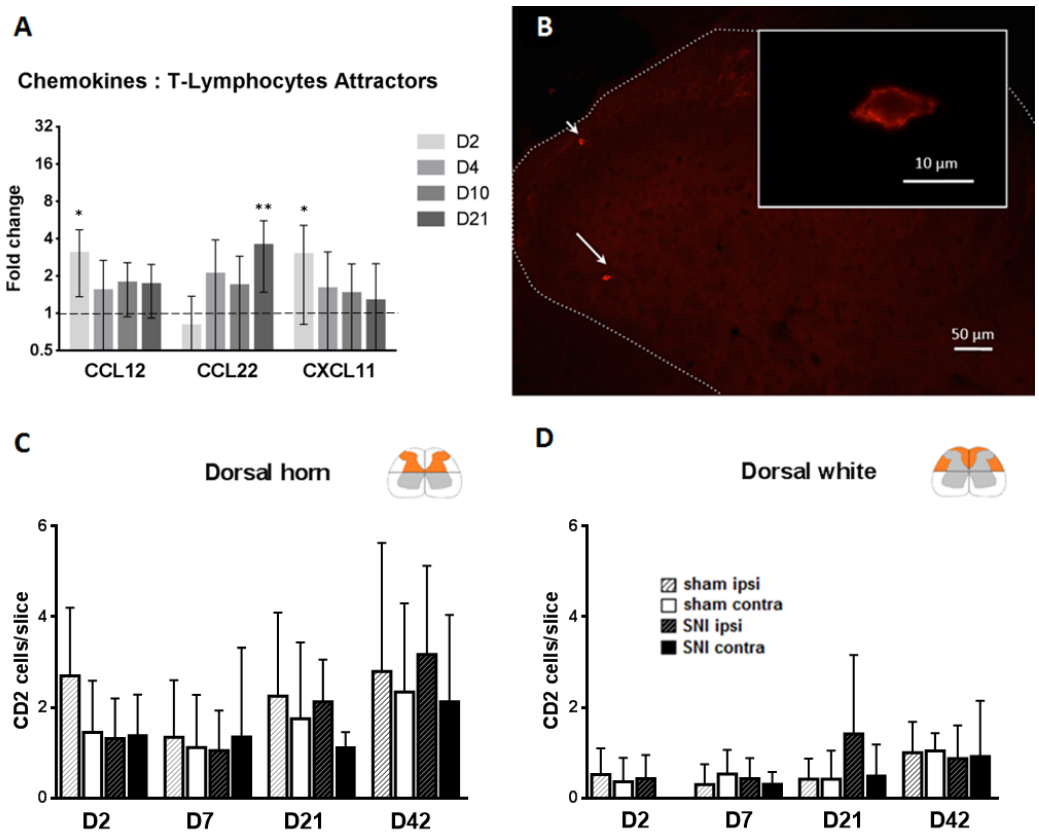

Figure 5. CD2-positive T-cell infiltration in the lumbar spinal cord. (**A**) Expression of genes of T-cells attractors in the spinal cord of rats following SNI from the RT-qPCR array showing the upregulation of gene expression of T-lymphocytes attractors. * $p < 0.05$, ** $p < 0.01$. Student's *t*-test: naive (not shown) *vs.* SNI. $N = 6$ for each time point (D2, D4, D10 and D21); (**B**) Immunofluorescence of the ipsilateral dorsal horn showing CD2+ cells (pointed by arrows) in the spinal cord seven days after SNI; Insert: Magnification of the cell pointed by the longest arrow (**C**,**D**) Bar histograms showing the number of CD^{2+} cells detected in sham or SNI at days 2, 4, 10 and 21 in the ipsilateral or contralateral side to SNI. Two regions of spinal cords were analyzed: **C**, the dorsal horn and **D**, the dorsal white matter. $N = 4$/groups. Values are expressed as mean ± 95% CI. No significant difference, 2-way ANOVA with Sidak correction.

2.4. T-Cells Do Not Infiltrate the Spinal Cord after SNI

To detect T-cell infiltration after SNI, we counted either CD2, a general marker for T-lymphocytes or CD8 a marker of cytotoxic T-lymphocytes in different parts of the dorsal cord using immunofluorescence (Figure 5B–D and Supplementary Figure S5). There were only very few CD2-positive T-cells in our slices. We did not find a significant difference between the ipsilateral and the contralateral side of the dorsal horn at any time point. The only significant difference between sham and SNI was found in the dorsal white matter,

with an absolute number of 1.5 cells per slice. Under our experimental conditions, there was no T-cell infiltration into the dorsal horn after SNI.

2.5. T-Cells Infiltrate the Spinal Cord after SCI

To confirm whether we were actually able to observe T-cell infiltration, we applied the same methodology to the spinal cord injury model (SCI), which consists of a direct mechanical injury to the spinal cord. We could indeed observe CD2 and CD8-positive cells following a 200 kdyn force injury and a high number of these cells following the 250 kdyn injury (Figure 6A–C).

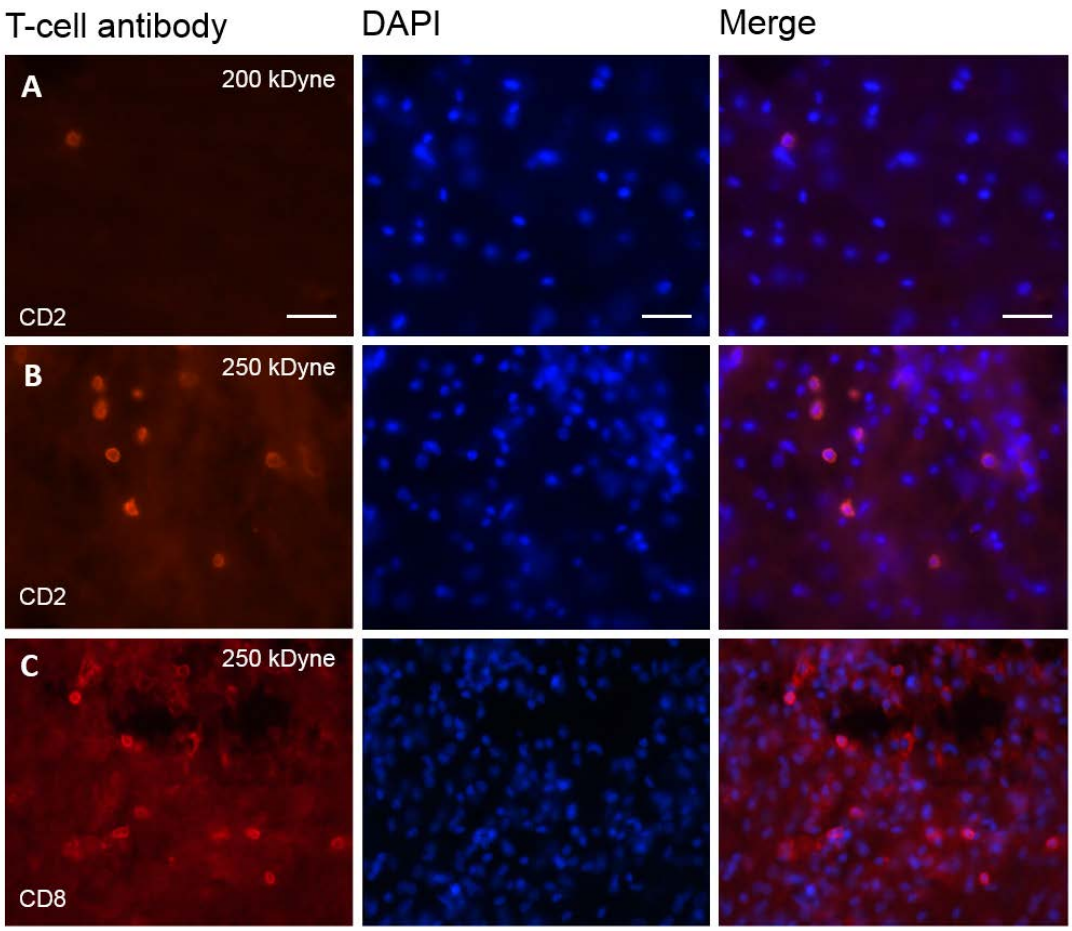

Figure 6. Infiltration of the spinal cord by T-cells after SCI. (**A**,**B**) Immunofluorescence of $CD2^+$ T-cells seven days after a SCI induced with a strength of 200 and 250 kdyn, respectively (machine range: 30–300 kdyn); (**C**) Immunofluorescence of $CD8^+$ T-cells after a SCI induced with a strength of 250 kdyn. We observe a clear T-cell infiltration with both CD2 and CD8 antibodies at 250 kdyn SCI. Scale bar represents 50 μm.

3. Discussion

We here show novel findings in inflammatory changes in the spinal cord after peripheral nerve injury. We first show a prolonged increase in microglial markers at the mRNA (Iba1, CD11b) and protein level (Iba1). However, proliferation of microglia is only increased at day 2. We observed a switch from pro-

inflammatory factors upregulated early, to anti-inflammatory factors later. Finally, we did not detect lymphocyte infiltration in the spinal cord.

Different classifications of microglia reactivity were attempted, mostly paralleling the classifications used for circulating macrophages. They vary from simply dichotomizing between a classical M1 and alternative M2, to much broader description of a continuum of phenotypes using immunological markers as well as functional aspects (phagocytosis, antigen presentation, cytokine secretion) [16,23,24]. Iba1 and CD11b are cell markers not usually used to discriminate between any subtypes. CD68 is a lysosomal marker indicative of microglial phagocytic activity [25]. CX3CR1 is the receptor for fractalkine (CX3CL1) solely expressed in microglia in the central nervous system and participating in the pathophysiology of pain following nerve injury [26]. These microglial markers show a longstanding increase over at least 21 or 42 days. The pro-inflammatory cytokines IL-1β, TNF-α and IL-6 have been shown to increase excitability in lamina II neurons of the spinal cord [27]. These cytokines were also shown to modulate the phenotype of microglia. Interestingly, IL-10 and IL-6 were shown to modulate towards alternative phenotypes. This highlights the ambiguous aspect of IL-6, which is upregulated until day 21 in our array and might have a dual role in neurons and microglia [28]. For the more classical anti-inflammatory IL-10, which has recently been shown to be responsible for decreased neuropathic pain in rat pups compared to adults [29] and used successfully to treat neuropathic pain [30], the increase in the late phase could correspond to a switch from M1 to alternative phenotype. The cell-type responsible for the regulation is unknown in whole tissue samples, which is a limitation of the array study part of our work.

Nociceptive information is relayed by many mechanisms including pattern recognition systems, such as Toll-like receptors (TLRs) [31]. TLRs play an important role in microglial activation following the detection of danger or damage-associated molecules. These can be exogenous (such as bacterial lipopolysaccharides (LPS), viral glycoproteins, bacterial peptidoglycan, or parasitic/viral RNAs) or endogenous (such as proteins like fibronectin, polysaccharides like heparan sulphate, nucleic acids and phospholipids) released upon tissue damage or cell death [32]. TLRs allow, via a downstream cascade, the release of pro-inflammatory factors including IL-1β, IL-6, IL-18, and TNF-α [33]. Many of these factors were upregulated after SNI in our study (Figure 4). TLR2 is an important microglial activator, using both ERK and NF-κB pathways [34], TLR4 and TLR7 also contribute to the process by allowing the release of pro-inflammatory factors such as IL-1β, TNF-α through the NF-κB pathway [33,35].

The complement cascade has been shown to be activated after peripheral nerve injury and to play a role in hypersensitivity through the release of the anaphylatoxin peptide (C5a) by the terminal membrane attack complex (MAC) complement, itself induced by C3 activity [17]. We observe an increase in complement factors which confirms this literature and supports our array data.

We only used sham animals at day 2 and 4, to follow the 3Rs recommendations. We thought that inflammatory changes in sham animals, if they occur, would be present at the early time points (shown in Supplementary Figure S3). We acknowledge the limitation that later changes in sham animals could have been missed.

Lymphocyte infiltration into the spinal cord after a peripheral injury is still debated. We do not find relevant CD2, neither CD8 positive lymphocytes infiltration following SNI. The only significant difference between sham and SNI is seen at day 21 in the dorsal part of the white matter for CD2 positive cells, with less than 1.5 cells/slice. Our study differs from others, where different model/species were used, such as the sciatic nerve transection or the CCI in rats [8] or spinal nerve transection in mice [10], and where immune cells infiltration through the blood spinal cord barrier [8,10] was indeed detected. However, no T-cells were observed after PSNL in mice (11) or CCI in rats (12) in line with our results. Costigan *et al.* used the same model, time point, rat strain and gender, and antibodies as we did [10], and demonstrated the infiltration of CD2 positive cells into the spinal cord. Our detection technique differed slightly from that used in the Costigan study. However, we demonstrated our ability to detect both CD2 and CD8 positive cells using the SCI model, minimizing the risk of a false negative, due to a different lot of antibody. We sampled spinal

cord sections regularly across the spinal cord where IB4 staining was lost and we therefore reduced the risk of missing the part of interest [3]. Recently, gender has been surprisingly reported as a major driver for different immune reactions following nerve injury [36]. In that study, female mice were using adaptive immunity, likely T-lymphocytes, and not male mice. They did not quantify infiltration but show higher levels of CD3e, CD4 and CD8a mRNA in female mice than in male mice. Conceptually, this paper underlines the fact that different pathways are involved in pain development which can replace one another as shown by the different paradigms they test when changing the hormonal status of their animals. We can therefore hypothesize that other factors, not yet identified, could explain the differential results compared to the data of Costigan *et al.* Housing conditions influence microglia phenotype through the germ prevalence or [37,38]. Differences in handling, stress or food could also be contributing factors.

To conclude, we identified an early expression of pro-inflammatory factors and a later expression of anti-inflammatory markers in the spinal cord after SNI. Finally, despite showing an increase in lymphocyte-attracting chemokines, we did not observe an increase in CD2 and CD8 positive cells in the spinal cord following SNI. We have shown that there is a longstanding upregulation of microglial reactivity markers (CD11b and Iba1) up to 42 days, whereas proliferation is only observed shortly. This highlights that when microglia reactivity is mentioned, it has to be defined very specifically as it varies over time. Further research should focus on specific changes in microglia, and try to understand not only the early pro-inflammatory reaction, but also the active switch to resolution of inflammation.

4. Materials and Methods

4.1. Animal Surgery

Adult male Sprague Dawley rats (250–350 g) were anesthetized by isoflurane. We used the spared nerve injury (SNI) model of neuropathic pain [39]: After an incision through the skin and muscle and the visualization of the sciatic trifurcation, the sural nerve was left intact and the two other sciatic nerve branches (the common peroneal and the tibial nerve) were ligated, cut distally with a few millimeters removed. The wounds were then closed separately for muscle and skin and rats were placed back in their cage. The same procedure was followed for sham surgery, but the nerves were not cut; instead, a silk was laid next to the trifurcation of the sciatic nerve. Spinal cord injury (SCI) was performed under aseptic conditions and general anesthesia: a partial laminectomy was made at the L4–L5 lumbar level of spinal cord and a 250 or 200 kdyn (1 dyn = 10 μN) contusion injury was applied using a force-controlled spinal cord impactor (IH-0400 Impactor, Precision Systems and Instrumentation (Nottinghill, VA, USA) [40], using a holding device [41]. All procedures were approved by the committee on animal experimentation for the canton of Vaud, Switzerland, in accordance with Swiss federal law on animal welfare and guidelines of the international association for the study of pain (IASP) [42].

4.2. Immunohistochemistry

We injected intraperitoneally (i.p.) 25mg of bromodeoxyuridine (BrdU) in phosphate buffered saline (PBS) + 0.007 N NaOH 2 h before sacrifice. Rats were lethally anesthetized by a 50 mg i.p. injection of pentobarbital and perfused with ice cold PBS for 1 min followed by 4% paraformaldehyde (PFA) PBS for 4 min.

The ipsilateral sciatic nerve was dissected and exposed up to the L4–L5–L6 spinal nerves, then the spinal cord was exposed and the L4-L5 lumbar section was collected and post-fixed in 4% PFA at 4 °C overnight. Samples were then transferred into 20% sucrose overnight for cryoprotection and then rapidly frozen. Using a cryostat, 30 μm slices were cut and stored in 30% glycol and 30% glycerol PBS. For immunofluorescence, slices were incubated for 30 min in blocking solution: 10% goat serum (NGS), 0.05% triton in 0.05% azide PBS, and overnight with the primary antibody (Table 1).

Table 1. Primary antibodies used for immunofluorescence.

Antibody	Source	Target	Concentration
Mouse anti-CD2	Serotec, UK	T-cells	1:250
Mouse anti-CD8	Abcam, USA	CD8+ T-cells	1:250
Rabbit anti-Iba1	Wako, USA	Activated microglia	1:2000
Mouse anti-GFAP	Millipore, USA	Activated astrocytes	1:1500
Rat anti-BrdU	Abcam, USA	Proliferating cells	1:500

After washing in PBS, slices were incubated in the blocking solution for one hour at room temperature with secondary antibody (Table 2). Diamidinophenylindole (DAPI) was applied on the slices for nuclear labelling before the final PBS wash. Lumbar spinal cord sections were then mounted on slides with mowiol mounting medium and stored at 4 °C.

Table 2. Secondary antibodies used for immunofluorescence.

Antibody	Source	Concentration
Alexa 488-labelled goat anti-mouse	Molecular Probes, UK	1:500
Alexa 488-labelled donkey anti-rabbit	Molecular Probes, UK	1:500
Cy3-labelled donkey anti-mouse	Jackson, USA	1:500
Cy3-labelled donkey anti-rat	Jackson, USA	1:500

To verify that the part of the spinal cord corresponds to the topographic region of lumbar dorsal horn occupied by the central terminals of afferent injured nerves, a staining with isolectin (Griffonia simplicifolia) B4 FITC conjugated has been performed [3]. One of each 5 slices has been stained. After blocking the slice for half an hour, the IB4 was incubated for 2 h, the slices were then washed in PBS and mounted in mowiol.

Thymi and neuromas were also collected for positive controls for antibody testing (See Supplementary Figure S4).

For cell counting and signal quantification, six sections from each animal were stained by immunofluorescence for CD2 and CD8 as described above. Fluorescent cells in each region as illustrated in Supplementary Figure 1 were counted by an investigator blinded to the sample identity, using an Axio Imager Z1 fluorescence microscope (Zeiss, Oberkochen, Germany). Sections were viewed with the 20× objective and the counting was made "on view" directly at the microscope.

Pictures of three Iba1-labelled lumbar sections for each SNI and sham operated animals were taken with the 20× objective, keeping the same fluorescence intensity and exposure for every picture. For Iba1 signal quantification, the contrast of images was enhanced using GNU Image Manipulation Program software (www.gimp.org). The labelled area was quantified and expressed as a percentage of total area using ImageJ software.

4.3. RT-qPCR and RT-qPCR Array

For RNA samples, rats were terminally anesthetized by a 50 mg i.p. injection of pentobarbital and transcardially perfused with NaCl 0.9%. The L4 and L5 ipsilateral dorsal horns of the spinal cord were dissected and rapidly frozen. The tissues were homogenized and total RNA was extracted with RNeasy Plus Mini Kit (Qiagen®, Hombrechtikon, Switzerland). The obtained RNA, was purified by the Minelute Reaction Cleanup Kit (Qiagen®), then analyzed by the RNA 6000 Nano Assay (Agilent®,Basel, Switzerland), and reverse transcribed into cDNA with Omniscript RT Kit (Qiagen®), if RNA integrity number (RIN) was over 7.5. The RT-qPCR amplification was performed with ROX SYBR Green on an ABI 7900 HT (Bio-Rad®, Reinach, Switzerland).

4.4. Statistics

All data are represented as mean ± 95% CI. For the RT-qPCR of the initial time course, the non-overlap of 95% CI method was used [13]. No other statistical test was performed on these data due to the small sample size (3 animals/group). Two-way ANOVA was used for Iba1 immunohistochemistry, BrdU time course, and T-lymphocyte counts. A p-value <0.05 was considered significant. The RT2 profiler PCR array data analysis version 3.4 from SABiosciences (Qiagen®) was used for the array (6 animals/group for each SNI time point and 4/group for sham D2 and D4). It does not apply any correction for multiple testing and a p-value of 0.05 is proposed as significant. We however also provide the exact p-values of the array data if the reader prefers to apply more conservative statistics (Table S1). For the four time points time course, a p-value <0.0125 could be taken as significant (Bonferroni correction). All RT-qPCR data were analyzed with the delta C_t method.

Supplementary Materials: Supplementary materials can be found at http://www.mdpi.com/1422-0067/17/3/xx/s1.

Acknowledgments: We dedicate this publication to Christine B. Clarke, who contributed to this study during her work towards a Masters in Medicine. She sadly passed away in 2014, but we remember her for her dazzling personality and her songs (see http://www.ladyslamenco.com/). We thank Christian Kern, Head of department of anesthesiology, Lausanne University Hospital (CHUV), for his support, Grégoire Courtine and Simone Duis from the International Paraplegic Foundation Chair in Spinal Cord Repair, Center for Neuroprosthetics and Brain Mind Institute, Swiss Federal institute of technology (EPFL), for providing the animals with spinal cord injury as a positive control. This study is supported by the Swiss National Science Foundation grants 310030A_124996 (ID) and 33CM30-124117 (MRS and ID), the 2011 IASP Early Career Grant funded by the ScanDesign Foundation BY INGER & JENS BRUUN (MRS), the Swiss Society of Anesthesiology (MRS) and the European Society of Anaesthesiology ESA Project Grants 2014 (MRS)

Author Contributions: Christophe Gattlen analyzed data and drafted the first manuscript. Nicolas Piller designed and performed the RT-qPCR array and timecourse. Christine B. Clarke performed immunohistochemical studies, data analysis, imaging, participated in the study design and drafted the manuscript. Guylène Kirschmann did the animal surgery and prepared the tissue. Marie Pertin performed immunohistochemistry, prepared tissue, performed staining and imaging. Isabelle Decosterd supervised the experiments and the final manuscript. Romain-Daniel Gosselin supervised and designed the experiments and the statistical analysis. Marc R. Suter supervised and designed the experiments and wrote the final manuscript. All the authors read and approved the final manuscript.

Conflicts of Interest: The authors declare no conflict of interest.

Abbreviations

BrdU	Bromodeoxyuridine
CI	Confidence interval
CCI	Chronic constriction injury
CHUV	Centre Hospitalier Universitaire Vaudois
CNS	Central nervous system
LPS	Lipopolysaccharides
MAC	Membrane attack complex
MDPI	Multidisciplinary Digital Publishing Institute
mRNA	Messenger ribonucleic acid
PBS	Phosphate buffer saline
PSNL	Partial sciatic nerve ligation
RT-qPCR	Real-time quantitative polymerase chain reaction
SNI	Spared nerve injury
SCI	Spinal cord injury

TLR Toll-like receptor

References

1. Van Hecke, O.; Austin, S.K.; Khan, R.A.; Smith, B.H.; Torrance, N. Neuropathic pain in the general population: A systematic review of epidemiological studies. *Pain* **2014**, *155*, 654–662.
2. McMahon, S.B.; Russa, F.L.; Bennett, D.L. Crosstalk between the nociceptive and immune systems in host defence and disease. *Nat. Rev. Neurosci.* **2015**, *16*, 389–402.
3. Beggs, S.; Salter, M.W. Stereological and somatotopic analysis of the spinal microglial response to peripheral nerve injury. *Brain Behav. Immun.* **2007**, *21*, 624–633.
4. Suter, M.R.; Berta, T.; Gao, Y.J.; Decosterd, I.; Ji, R.R. Large A-fiber activity is required for microglial proliferation and p38 MAPK activation in the spinal cord: Different effects of resiniferatoxin and bupivacaine on spinal microglial changes after spared nerve injury. *Mol. Pain* **2009**, *5*, 53.
5. Gosselin, R.D.; Suter, M.R.; Ji, R.R.; Decosterd, I. Glial cells and chronic pain. *Neuroscientist* **2010**, *16*, 519–531.
6. Zhang, J.; Shi, X.Q.; Echeverry, S.; Mogil, J.S.; de Koninck, Y.; Rivest, S. Expression of CCR2 in both resident and bone marrow-derived microglia plays a critical role in neuropathic pain. *J. Neurosci.* **2007**, *27*, 45.
7. Sweitzer, S.M.; Hickey, W.F.; Rutkowski, M.D.; Pahl, J.L.; DeLeo, J.A. Focal peripheral nerve injury induces leukocyte trafficking into the central nervous system: Potential relationship to neuropathic pain. *Pain* **2002**, *100*, 163–170.
8. Hu, P.; Bembrick, A.L.; Keay, K.A.; McLachlan, E.M. Immune cell involvement in dorsal root ganglia and spinal cord after chronic constriction or transection of the rat sciatic nerve. *Brain Behav. Immun.* **2007,** *21*, 599–616.
9. Cao, L.; DeLeo, J.A. CNS-infiltrating $CD4^+$ T lymphocytes contribute to murine spinal nerve transection-induced neuropathic pain. *Eur. J. Immunol.* **2008**, *38*, 448–458.
10. Costigan, M.; Moss, A.; Latremoliere, A.; Johnston, C.; Verma-Gandhu, M.; Herbert, T.A.; Barrett, L.; Brenner, G.J.; Vardeh, D.; Woolf, C.J.; *et al*. T-cell infiltration and signaling in the adult dorsal spinal cord is a major contributor to neuropathic pain-like hypersensitivity. *J. Neurosci.* **2009**, *29*, 14415–14422.
11. Kim, C.F.; Moalem-Taylor, G. Detailed characterization of neuro-immune responses following neuropathic injury in mice. *Brain Res.* **2011**, *1405*, 95–108.
12. Austin, P.J.; Kim, C.F.; Perera, C.J.; Moalem-Taylor, G. Regulatory T cells attenuate neuropathic pain following peripheral nerve injury and experimental autoimmune neuritis. *Pain* **2012**, *153*, 1916–1931.
13. Cumming, G. The new statistics: Why and how. *Psychol. Sci.* **2014**, *25*, 7–29.
14. A. Ellis1, D.L. H. Bennett. Neuroinflammation and the generation of neuropathic pain. *Br. J. Anaesth.* **2013**, *111*, 26–37.
15. Opal, S.M.; de Palo, V.A. Anti-inflammatory cytokines. *Chest* **2000**, *117*, 1162–1172.
16. Mosser, D.M.; Edwards, J.P. Exploring the full spectrum of macrophage activation. *Nat. Rev. Immunol.* **2008** *8*, 958–969.
17. Griffin, R.S.; Costigan, M.; Brenner, G.J.; Ma, C.H.; Scholz, J.; Moss, A.; Allchorne, A.J.; Stahl, G.L.; Woolf, C.J. Complement induction in spinal cord microglia results in anaphylatoxin C5a-mediated pain hypersensitivity. *J. Neurosci.* **2007**, *27*, 8699–708.
18. Figshare. Available online: http://figshare.com/s/e1a0e64486fd11e5b72906ec4b8d1f61 (accessed on 5 November 2015).
19. Jia, G.Q.; Gonzalo, J.A.; Lloyd, C.; Kremer, L.; Lu, L.; Martinez, A.C.; Wershil, B.K.; Gutierrez-Ramos, J.C. Distinct expression and function of the novel mouse chemokine monocyte chemotactic protein-5 in lung allergic inflammation. *J. Exp. Med.* **1996**, *184*, 1939–1951.
20. Ford, L.B.; Cerovic, V.; Milling, S.W.; Graham, G.J.; Hansell, C.A.; Nibbs, R.J. Characterization of conventional and atypical receptors for the chemokine CCL2 on mouse leukocytes. *J. Immunol.* **2014**, *193*, 400–411.
21. Muller, M.; Carter, S.; Hofer, M.J.; Campbell, I.L. Review: The chemokine receptor CXCR3 and its ligands CXCL9, CXCL10 and CXCL11 in neuroimmunity—A tale of conflict and conundrum. *Neuropathol. Appl. Neurobiol.* **2010**, *36*, 368–387.

22. Hsieh, C.Y.; Chen, C.L.; Lin, Y.S.; Yeh, T.M.; Tsai, T.T.; Hong, M.Y.; Lin, C.F. Macrophage migration inhibitory factor triggers chemotaxis of $CD74^{+}CXCR2^{+}$ NKT cells in chemically induced IFN-γ-mediated skin inflammation. *J. Immunol.* **2014**, *193*, 3693–3703.
23. Salter, M.W.; Beggs, S. Sublime microglia: Expanding roles for the guardians of the CNS. *Cell* **2014**, *158*, 15–24.
24. Chhor, V.; Le Charpentier, T.; Lebon, S.; Ore, M.V.; Celador, I.L.; Josserand, J.; Degos, V.; Jacotot, E.; Hagberg, H.; Savman, K.; *et al*. Characterization of phenotype markers and neuronotoxic potential of polarised primary microglia *in vitro*. *Brain Behav. Immun.* **2013**, *32*, 70–85.
25. Walker, D.G.; Lue, L.F.; Immune phenotypes of microglia in human neurodegenerative disease: Challenges to detecting microglial polarization in human brains. *Alzheimers Res. Ther.* **2015**, *7*, 56.
26. Clark, A.K.; Malcangio, M. Microglial signalling mechanisms: Cathepsin S and Fractalkine. *Exp. Neurol.* **2012**, *234*, 283–292.
27. Kawasaki, Y.; Zhang, L.; Cheng, J.K.; Ji, R.R. Cytokine mechanisms of central sensitization: Distinct and overlapping role of interleukin-1beta, interleukin-6, and tumor necrosis factor-alpha in regulating synaptic and neuronal activity in the superficial spinal cord. *J. Neurosci.* **2008**, *28*, 5189–5194.
28. Saijo, K.; Collier, J.G.M; Li, A.C.; Katzenellenbogen, J.A.; Glass, C.K. An ADIOL-ERβ-CtBP transrepression pathway negatively regulates microglia-mediated inflammation. *Cell* **2011**, *145*, 584–595.
29. McKelvey, R.; Berta, T.; Old, E.; Ji, R.R.; Fitzgerald, M. Neuropathic pain is constitutively suppressed in early life by anti-inflammatory neuroimmune regulation. *J. Neurosci.* **2015**, *35*, 457–466.
30. Milligan, E.D.; Penzkover, K.R.; Soderquist, R.G.; Mahoney, M.J. Spinal interleukin-10 therapy to treat peripheral neuropathic pain. *Neuromodulation* **2012**, *15*, 520–526.
31. Kato, J.; Svensson, C.I. Role of extracellular damage-associated molecular pattern molecules (DAMPs) as mediators of persistent pain. *Prog. Mol. Biol. Transl. Sci.* **2015**, *131*, 251–279.
32. Yu, L.; Wang, L.; Chen, S. Endogenous toll-like receptor ligands and their biological significance. *J. Cell. Mol. Med.* **2010**, *14*, 2592–2603.
33. Nicotra, L.; Loram, L.C.; Watkins, L.R.; Hutchinson, M.R. Toll-like receptors in chronic pain. *Exp. Neurol.* **2012**, *243*, 316–329.
34. Kim, D.; Kim, M.A.; Cho, I.H.; Kim, M.S.; Lee, S.; Jo, E.K.; Choi, S.Y.; Park, K.; Kim, J.S.; Akira, S.; *et al*. A critical role of toll-like receptor 2 in nerve injury-induced spinal cord glial cell activation and pain hypersensitivity *J. Biol. Chem.* **2007**, *282*, 14975–14983.
35. Rosenberger, K.; Derkow, K.; Dembny, P.; Kruger, C.; Schott, E.; Lehnardt, S. The impact of single and pairwise Toll-like receptor activation on neuroinflammation and neurodegeneration. *J. Neuroinflamm.* **2014**, *11*, 166.
36. Sorge, R.E.; Mapplebeck, J.C.; Rosen, S.; Beggs, S.; Taves, S.; Alexander, J.K.; Martin, L.J.; Austin, J.S.; Sotocinal, S.G.; Chen, D.; Yang, M.; *et al*. Different immune cells mediate mechanical pain hypersensitivity in male and female mice. *Nat. Neurosci.* **2015**, *18*, 1081–1083.
37. Kierdorf, K.; Erny, D.; Goldmann, T.; Sander, V.; Schulz, C.; Perdiguero, E.G.; Wieghofer, P.; Heinrich, A.; Riemke, P.; Holscher, C.; *et al*. Microglia emerge from erythromyeloid precursors via Pu.1- and Irf8-dependent pathways. *Nat. Neurosci.* **2013**, *16*, 273–280.
38. Erny D.; Hrabe de Angelis, A.L.; Jaitin D.; Wieghofer P.; Staszewski O.; David, E.; Keren-Shaul, H.; Mahlakoiv, T.; Jakobshagen, K.; Buch, T.; *et al*. Host microbiota constantly control maturation and function of microglia in the CNS. *Nat. Neurosci.* **2015**, *18*, 965–977.
39. Decosterd, I.; Woolf, C.J. Spared nerve injury: An animal model of persistent peripheral neuropathic pain. *Pain* **2000**, *87*, 149–158.
40. Nishi, R.A.; Liu, H.; Chu, Y.; Hamamura, M.; Su, M.Y.; Nalcioglu, O.; Anderson, A.J. Behavioral, histological, and *ex vivo* magnetic resonance imaging assessment of graded contusion spinal cord injury in mice. *J. Neurotrauma* **2007**, *24*, 674–689.
41. Scheff, S.W.; Rabchevsky, A.G; Fugaccia, I.; Main, J.A.; Lumpp, J.E., Jr. Experimental modeling of spinal cord injury: Characterization of a force-defined injury device. *J. Neurotrauma* **2003**, *20*, 179–193.
42. Zimmermann, M. Ethical guidelines for investigations of experimental pain in conscious animals. *Pain* **1983**, *16*, 109–110.

Study II

Kir2.1 blockade reduces hypersensibility by regulating spinal microglial proliferation trough membrane potential modulation in the SNI model of neuropathic pain

C. Gattlen, A. Deftu, T. Raquel, V. Ristoiu, T. Berta, I. Decosterd, M.R. Suter

To be submitted to the EMBO journal

Synopsis

Following nerve injury, erratic action potentials from sensory neurons sensitize secondary neurons located in the dorsal horn of the spinal cord generating hypersensibility and allodynia – hallmarks of neuropathic pain. There microglia, the immune cells of the central nervous system, get activated and participate in the sensitization process by releasing cytokines and chemokines and reactive oxygen species. Microglial cells can change their potassium currents once activated. I investigated in the context of neuropathic pain using the spared nerve injury (SNI) model if potassium channels participate in microglial activation and what physiological function they could influence in these cells.

In this study, *CX3CR1^{eGFP}* transgenic male mice (background C57BL/6) were used. CX3CR1 is expressed in macrophages, but is specific to microglia in the CNS. The GFP reporter co-expressed with CX3CR1 allowed patching microglia under fluorescence microscope.

Electrical response of microglia after SNI was measured and an increase of inward current 2 days after SNI in freshly dissociated microglia was observed. The current went down at D4 and to a level similar to naive at D7. This was confirmed in spinal cord slices.

To determine the source of this current, several strategies were used. First, the extracellular concentration of potassium was changed. The SNI D2 current measured gradually decreased with reduction of extracellular K^+ concentration and increased when its concentration was raised. Then, a current reduction in a dose-dependent way for the 2 broad range K^+ channel blockers barium and cesium was observed. Finally, a dose-dependent block of the K^+ currents was measured with ML133, a specific Kir2.x blocker. A full block of the current was reached with 50 µM of ML133. I therefore demonstrated that Kir2.1 generates

potassium currents in microglia, as no other Kir2.x family members have been described in those cells.

Interestingly the current is not the only component modified by the SNI or ML133. Two days after SNI, microglial resting membrane potential (RMP) was hyperpolarized and went back to naive levels at D4 and D7. ML133 depolarized both SNI D2 and naive cells to a level beyond the naive RMP. The current from Kir2.1 is an inward current at lower voltage steps (-160 to -50 mV) and an outward current in the voltage range of microglial RMP (-45 to -20 mV). The latter explains the hyperpolarization of microglial RMP at SNI D2. When ML133 is applied, Kir2.1 is blocked and the membrane potential gets depolarized. This suggests that Kir 2.1 regulates the microglial membrane potential.

As shown in the unpublished results section, RNA and protein expression of Kir2.1 seemed not to be changed. We investigated the membrane expression of Kir2.1 to explain the current/RMP differences observed. When using a Kir2.1 antibody against an intracellular epitope, most microglia were stained, in both naive and SNI D2 conditions with permeabilization. An antibody against the extracellular epitope of Kir2.1 was used without permeabilization of the cells and only 23.2 % of naive microglia were stained. However, in SNI D2 microglia more than twice more cells stained (49.3 %) showing that Kir2.1 is present at the membrane more often 2 days after SNI. When we permeabilized the cell membrane, Kir2.1 extracellular epitope stained over 97% of microglial cell. The pattern observed with non-permeabilized Kir2.1 extracellular epitope is matching our electrophysiology experiments: both SNI D4 and SNI D7 cells have similar Kir2.1 membrane expression as naive condition.

Microglial activation in the ipsilateral dorsal horn after SNI was assessed by counting CX3CR1-GFP positive cells. Proliferation was assessed more specifically by staining spinal cord slices with Ki-67 antibody. There is a continuous increase of microglial cells after SNI surgery compared to naive or sham D7. An increasing number of cells was observed from D2 to D7 with peak in their amount at D7 (Fig. 7 A). The Ki-67 proliferation marker, counted only out of the GFP+ cells, peaked 2 days after SNI, decreased at D4 and was no more visible in SNI D7 slices. It was not detectable in naive and sham D7. This pattern temporally coincides with

the changes in electrophysiology. I therefore hypothesized a link between these 2 phenomena.

The effect of ML133 on proliferation of an immortalized murine microglial cell line (BV2) was tested by culturing them with and without 50 µM ML133, the same concentration used for electrophysiology. A strong reduction of the microglial proliferation, by counting the number of cells as well as the ratio of proliferating cells was observed, after both 2 and 4 days in culture. The effect of ML133 was finally tested in vivo by intrathecal injection and a reduction could be seen in microglial proliferation at SNI D2 associated with a reduction of neuropathic pain-related behavior.

To conclude, we observed that Kir2.1 currents, Kir2.1 channels membrane expression and proliferation of microglia all peak at the same timepoint, 2 days after SNI. Moreover inhibiting Kir channels in BV2 cell line impedes proliferation. Finally inhibiting Kir2.1 channels in vivo reduces microglial proliferation and pain behavior.

We therefore propose that the increase of Kir2.1 at the cell membrane is responsible for hyperpolarization, leading to proliferation of microglia following peripheral nerve injury, which participates in pain behavior. Targeting membrane potential of microglia could be a new way to modulate microglial reactivity and pain behavior.

Aim

The main goal of this study was to characterize electrophysiological modification in a time course after SNI, as well as the possible variations of RMP. The second goal was to determine that specific impact of electrophysiological changes on microglial physiology and reactivity. Finally, the last goal was to validate the findings in vivo as potential targets in the context of neuropathic pain.

In this study which was the main part of my thesis; I managed to unravel a new description of microglial reactivity, opening a new path for microglial modulation in the context of neuropathic pain.

Author Contributions: Christophe Gattlen designed the experiments, performed the electrophysiology, immunostainings except for the in vivo part, analyzed data and drafted the first manuscript. Alexandru F. Deftu designed and performed electrophysiology experiments. Violeta Ristoiu designed and supervised the electrophysiology experiments. Raquel Tonello designed and performed the behavior and immunostaining. Temugin Berta and Isabelle Decosterd supervised the experiments and design and corrected the manuscript. Marc R. Suter designed and supervised the experiments and the whole study and wrote the final manuscript.

Kir2.1 blockade depolarizes microglia, reduces its proliferation and attenuates neuropathic pain

C. Gattlen[1], A. F. Deftu[1,3], R. Tonello[4], Y. Ling[4,5], T. Berta[4], V. Ristoiu[3], I. Decosterd[1,2], M.R. Suter[1]

[1] Pain Center, Department of Anesthesiology, Lausanne University Hospital (CHUV) and Faculty of Biology and Medicine (FBM) University of Lausanne (UNIL), Switzerland
[2] Department of Fundamental Neurosciences, Faculty of Biology and Medicine (FBM), University of Lausanne (UNIL), Switzerland
[3] Department of Anatomy, Animal Physiology and Biophysics, Faculty of Biology, University of Bucharest, Romania
[4] Pain Research Center, Department of Anesthesiology, University of Cincinnati Medical Center, Cincinnati, USA.
[5] Pain Research Laboratory, Institute of Nautical Medicine, Jiangsu Key Laboratory of Neurodegeneration, Nantong University, Nantong, Jiangsu, China.

Abstract (171 words)

Spinal microglia change their phenotype and proliferate after nerve injury, contributing to neuropathic pain. We have characterized for the first time the electrophysiological properties of microglia and the potential role of microglial potassium channels in the spared nerve injury (SNI) model of neuropathic pain. We observed a strong increase of microglial inward currents restricted at 2 days after injury associated with hyperpolarization of the resting membrane potential (RMP) of microglial cells compared to later timepoints and naive animals. We identified pharmacologically the current as being Kir2.1-dependent and its modification as caused by increase of this channel at the cell membrane 2 days after SNI. Kir2.1 blockade with ML133 reversed the RMP hyperpolarization and strongly reduced currents of microglial cells 2 days after SNI. These electrophysiological changes occurred coincidentally to the peak of microglial proliferation following nerve injury. Finally, spinal injection of ML133 significantly attenuated the proliferation of microglia and neuropathic pain behaviors after nerve injury. In summary, our data implicate Kir2.1-mediated microglial proliferation as an important therapeutic target in neuropathic pain.

Introduction

Pain is an unpleasant sensory and emotional experience associated with actual or potential tissue damage. Its main purpose is to prevent injuries from harmful insults. This protective function is altered in chronic pain conditions, especially in neuropathic pain. Neuropathic pain is a debilitating condition, defined as pain caused by a lesion or disease of the somatosensory nervous system by the International Association for the Study of Pain (IASP). Affecting up to 10% of the population, it can be generated by direct trauma to the nerve, metabolic diseases, or infectious agents (Attal et al. 2008, Colloca et al. 2017). Neuropathic pain symptoms include spontaneous or evoked pain such as allodynia and hyperalgesia. Allodynia is characterized by painful reactions to non-noxious stimuli, whereas hyperalgesia is characterized by enhanced pain responses to mild noxious stimuli (Koltzenburg 1998, Martinez et al. 2010). Current treatments of neuropathic pain mostly target neuronal pathways with only a third of the patients claiming a satisfactory decrease in pain symptoms (Colloca et al. 2017).

Microglia and astrocytes are the most abundant cell types in the central nervous system (CNS), with microglia alone representing 10% of all the cells (Salter and Beggs 2014). These glial cells are emerging as new potential targets in neuropathic pain as involvement of glia in fibromyalgia and low back pain has recently been revealed also in humans (Loggia et al. 2015, Albrecht et al. 2018). Microglia are macrophage-like cells in the immune system in the CNS. They can react to modification in the CNS but also to peripheral lesion as seen in nerve injury models of neuropathic pain (Chen et al. 2018, Gattlen et al. 2016, Kettenman et al. 2011).

Different features of microglial reactivity, globally termed microgliosis, can be recognized, such as marker expression, morphological changes and proliferation (Chen et al. 2018). The multiple phenotypes acquired in vivo by reactive microglia after an injury goes far beyond the M1 and M2 classification, respectively pro and anti-inflammatory phenotype in which they are sometimes restrained (Ransohoff 2016, Song and Colonna 2018). Microgliosis evolves over time and each characteristic of activation needs to be studied in

a timecourse to unravel its true evolution (Gattlen et al. 2016). Proliferation of microglia in the spinal cord was described as peaking 3 days after sciatic nerve constriction (Echeverry et al. 2011) and 2 to 3 days after spared nerve injury model (Suter et al. 2007, Gattlen et al. 2016) in rats, but the number of cells stayed elevated for longer periods.

Microglia also show modification of their electrophysiological properties mostly described as inward or outward currents using patch clamp techniques (Nguyen et al. 2017). These currents were measured in different microglia phenotypes elicited by lipopolysaccharides (LPS), cytokines, chemokines, in *in-vitro* or *ex-vivo* models (Nguyen et al. 2017, Moussaud et al. 2009, Deftu et al. 2018, Lam et al. 2017). Different receptors have been involved in these current changes, mostly ion channels (Kir2.1, KCa1.1, KCa3.1, Kv1.3, P2X4x, Orai1, TRPs) but also GPCRs (P2Y12) (Nguyen et al. 2017) depending on the trigger. Blocking voltage-gated potassium channels (Kvs) with the broad range potassium channel blocker 4-aminopyridine (4-AP) reduced microglial activation following amyloid-β injection in rat hippocampus and reduced neuronal death (Franciosi et al. 2006). Kv1.3 enhances cytokine production leading to neurotoxic effects in rat pups brain microglial culture (Fordyce et al. 2005). Kv1.5 forms heteromers with Kv1.3 to reduce microglial proliferation in mouse pups brain microglial culture (Pannasch et al. 2006). P2X12 is linked to morphological changes of microglia (Gu et al. 2016). The inwardly rectifying potassium channel Kir2.1 is involved in cell conformation changes in brain microglial culture of mouse pups (Muessel et al. 2013). In neonatal rat brain microglial culture, Kir2.1 is important for homeostatic functions such as proliferation and migration via Ca^{2+}-signaling and Ca^{2+}-release activated Ca^{2+}channels (CRAC/Orai1) (Lam et al. 2015). Furthermore, modifications of membrane ion channels are linked to microglial membrane potential (Chung et al. 1999).

Microglia also have protective roles therefore a subtle modulation of the unwanted pathways in microglial reactivity should be sought instead of their full inhibition. Indeed, inactivating or deleting microglia in acute injury is seldom associated with a beneficial outcome, which suggests that microglia also harbor important protective/repair function. This might change in chronic disease as neuropathic pain (Chen et al. 2018, Biber et al. 2014).

We aim here for a description of timecourse of electrophysiological changes in microglia in the spinal cord dorsal horn in a model of peripheral nerve injury pain model. We therefore want to unravel new ways of modulating microglia phenotype in pain therapy.

Results

Inward microglial currents are increased 2 days after SNI.

We first examined whether microglia developed any changes in their electrophysiological properties in response to a voltage pulse protocol (insert Fig 1.B) after spared nerve injury (SNI). We observed a significant increase of inward current 2 days after SNI in freshly dissociated microglia from the spinal cord (Fig 1. A, B and C). Current density at -100 mV went from -27.9 ± 17.4 pA/pF for cells from naive to -59.4 ± 41.9 pA/pF from SNI D2 animals ($p<0.01$). At day 4 and 7 after SNI no more significant differences were seen compared to naive animals (Fig 1. A, B and C). The same pattern was noticed in microglial cells from spinal cord slices (Fig. 1 D) with current densities at -100 mV going from -5.60 ± 4.09 in naïve to -14.0 ± 13.5 pA/pF in SNI D2 cells ($p<0.01$). Only very low outward currents at depolarized pulses were recorded for both naive and SNI D2 microglia.

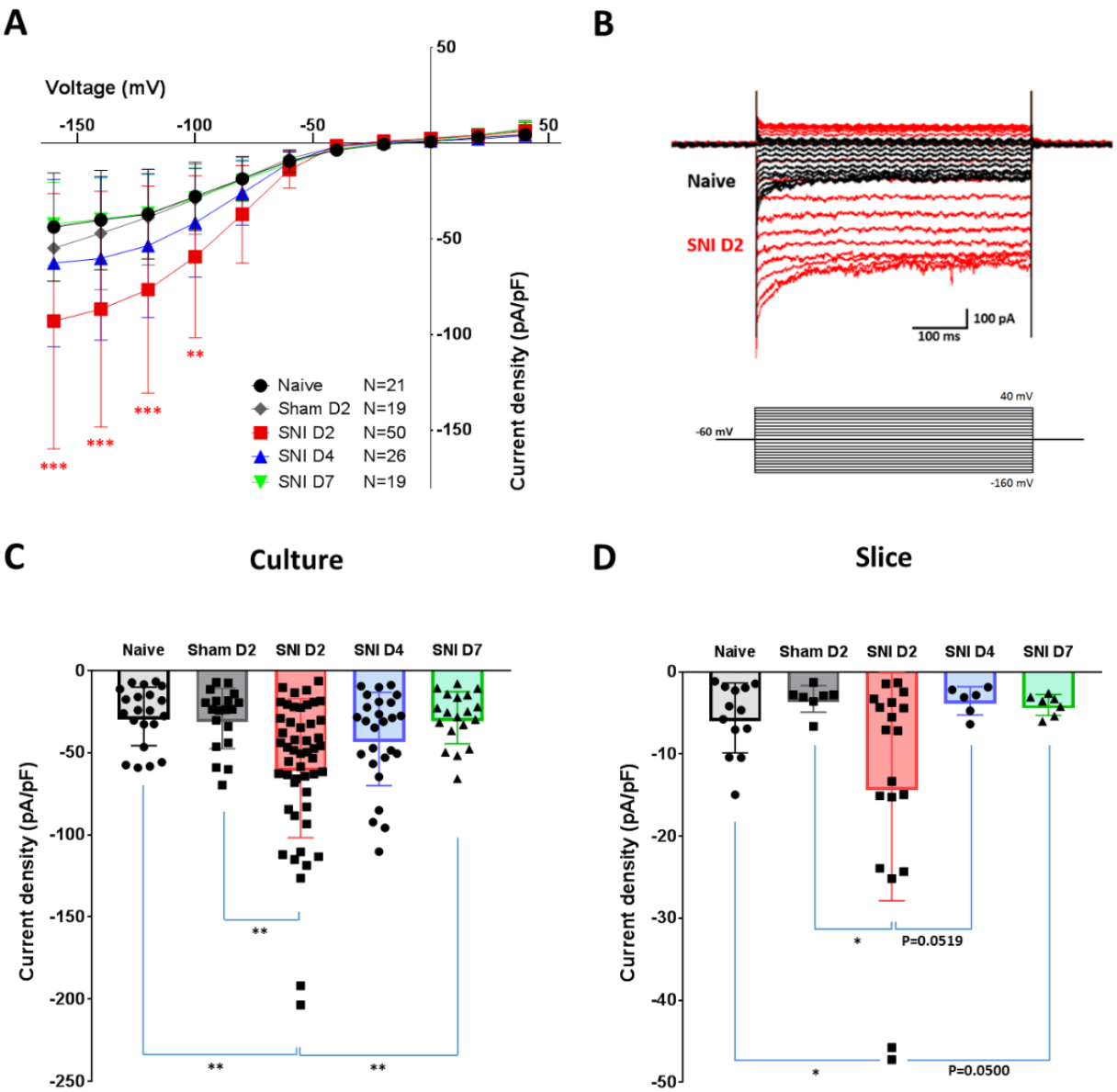

Fig. 1: Spinal cord dorsal horn microglial current densities recorded after SNI. (A) I-V curve showing current densities recorded in freshly dissociated microglia with 20 mM K^+ in extracellular solution. **(B)** Representative traces of naive (black) and SNI D2 cells (red) when applying voltage steps from -160 to +40 mV with 10 mV increments. Inset represents the stimulation protocol. **(C)** Histograms showing current densities generated by freshly dissociated cells with 20 mM K^+ in extracellular solution at a voltage of -100 mV. **(D)** Histograms showing current densities generated by microglial cells in spinal cord slices with 5 mM K^+ in extracellular solution at a voltage of -100 mV. Mean ± SD. *: $p < 0.05$, **: $p < 0.01$, ***: $p < 0.001$.

Kir2.1 is responsible for inward microglial currents.

To characterize the origin of that current, we first showed that the current is potassium-dependent by modifying the extracellular potassium concentration to 20, 5 or 0 mM K^+ (Fig. 2 A). We then used 20 mM K^+ for pharmacological trials and controlled the most interesting findings with the more physiological 5mM K^+ concentration. We then gradually inhibited the current with increasing concentration of both barium (Fig. 2 B) and cesium (Suppl. Fig. 1), two broad-range potassium channel blockers.

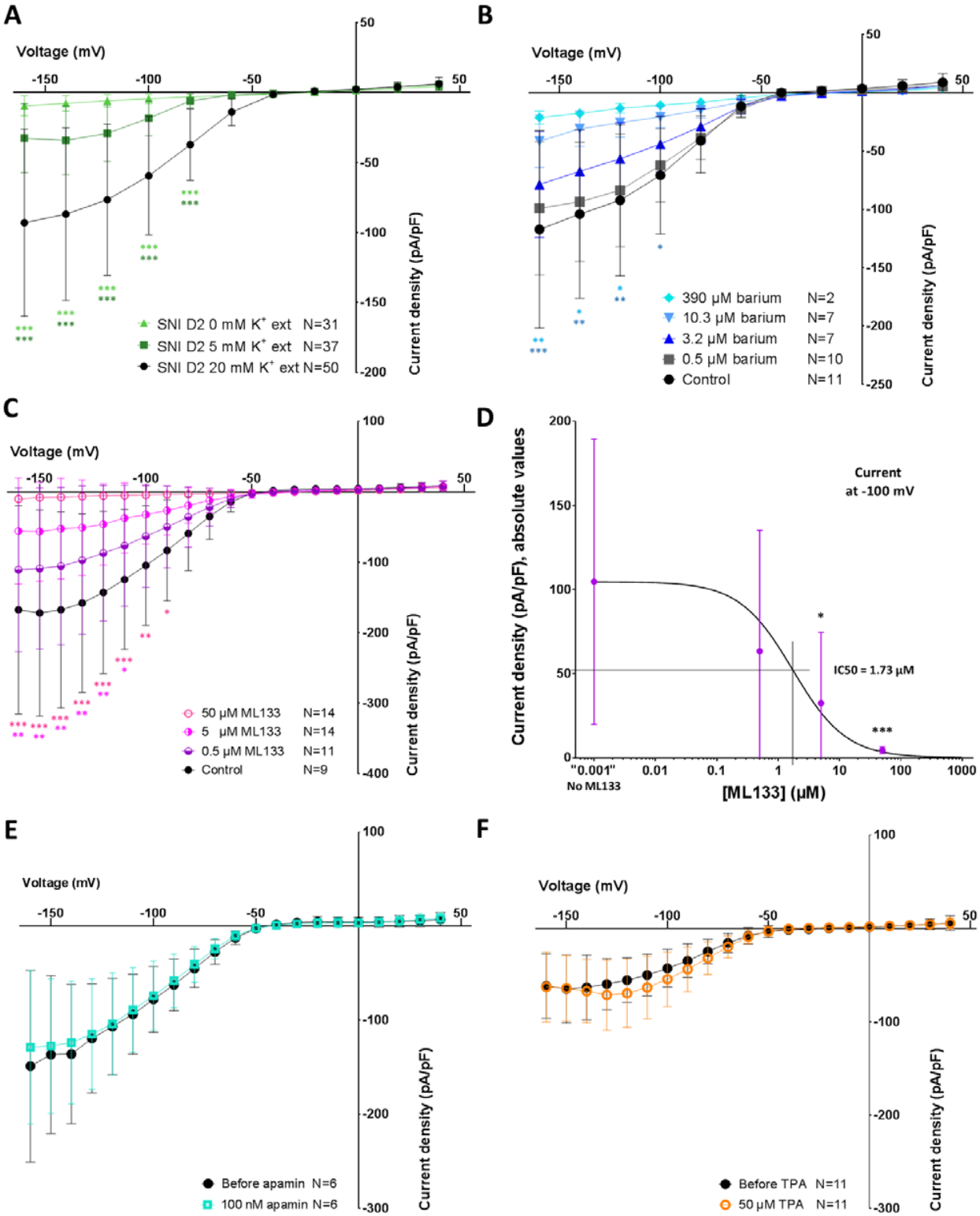

Fig. 2: Pharmacological response of dorsal horn microglial current densities after SNI. (A) I-V curve showing current densities recorded in freshly dissociated microglia from SNI D2 mice with either 0, 5 or 20 mM K^+ in extracellular solution. I-V curve of SNI D2 microglia blocked with increasing concentrations of barium **(B)** or ML133**,** a specific blocker of the Kir2.x channel family **(C)**. **(D)** Dose-response curve for ML133. IC50 is 1.73 µM. **(E, F)** I-V curves of SNI D2 microglia blocked with respectively 100 nM apamin, a SK1, SK2 and SK3 channel blocker or 50 µM TPA, a two-pore potassium channel (THIK-1) blocker. Mean ± SD. *: $p < 0.05$, **: $p < 0.01$, ***: $p < 0.001$.

We then specifically blocked different K^+ channels known to be expressed in microglia and potentially responsible for inward currents: inward rectifying potassium channels (Kir2.x channels) with ML133 (Lam et al. 2015), small conductance calcium activated potassium channels (SK) with apamin (Schlichter et al. 2010, Kettenmann et al. 2011) and two-pore potassium channels, from which Two-pore domain TWIK-related Halothane-Inhibited K^+ channels (THIK) have been highlighted as important, with tetrapenthyl-ammonium (TPA) (Madry et al. 2018).

ML133 induced a dose-dependent block of the SNI D2 K^+ current densities with maximal inhibition obtained with 50 µM ML133: -4.66 ± 1.91 pA/pF at -100 mV (Fig. 2 C and D) and an IC50 determined at 1.73 µM. Apamin as a blocker of SK1, SK2, and SK3 channels induced no significant change at a concentration of 100 nM (Fig. 2 E). TPA did not induce any difference in currents at 50 µM (Fig. 2 F).

Although Kir2.2, Kir2.3 and Kir2.4 mRNA are detectable in mouse microglia, their expression is very weak compared to Kir2.1 (Lam et al. 2017). Moreover, Kir2.5 is electrically silent and Kir2.6 is only expressed in skeletal muscles (Ryan et al. 2010). Thus, we assume that the currents we measured are generated by Kir2.1.

The microglial RMP is hyperpolarized 2 days after SNI.

We also examined the resting membrane potential of microglial cells after SNI. In freshly dissociated microglia with 20 mM extracellular K^+, the RMP was significantly hyperpolarized from -17.0 ± 12.7 mV in naive animals and -20.3 ± 7.8 mV in sham D2 animals to -30.5 ± 17.4 mV in SNI D2 animals ($p < 0.001$ and $p < 0.05$ respectively). At SNI D4 and D7, RMP values were -21.3 ± 9.0 and -22.2 ± 8.8 mV respectively, no more different from naive and sham D2 levels (Fig. 3 B).

In spinal cord slices with a 5 mM K^+ extracellular solution, the RMP was hyperpolarized from -16.9 ± 5.6 mV in sham D2 animals to -45.0 ± 21.1 mV in SNI D2 animals ($p < 0.001$). Naive microglia had a RMP of -20.4 ± 10.2 mV ($p < 0.01$ vs SNI D2). RMP went back to naive or sham D2 levels at SNI D7 (-28.4 ± 9.9 mV) (Fig. 3 C).

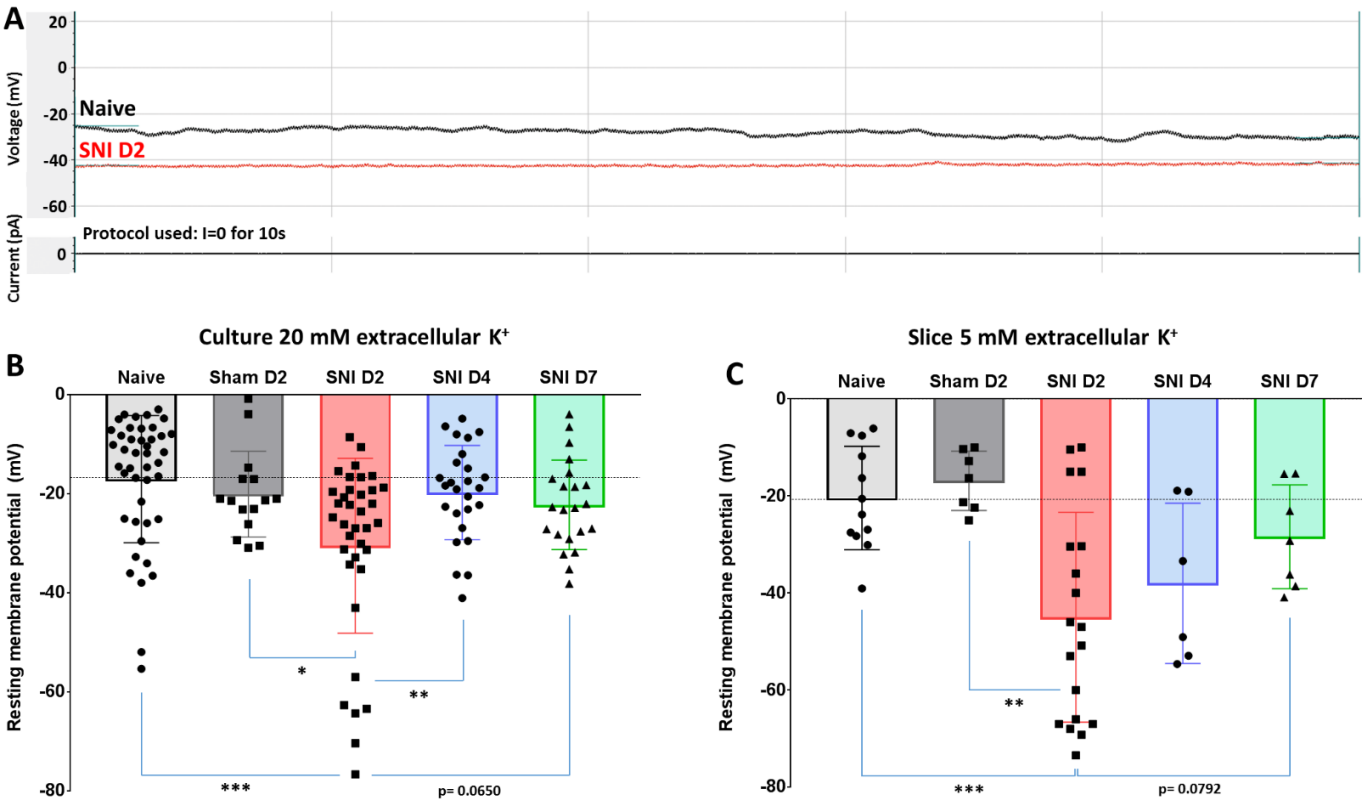

Fig. 3: Resting membrane potential (RMP) of spinal cord dorsal horn microglia after SNI. (A) Representative traces of current clamped microglial cells. **(B)** Histograms showing RMPs of freshly dissociated microglia with 20 mM K^+ in extracellular solution. **(C)** Histograms showing RMPs of microglial cells in spinal cord slices with 5 mM K^+ in extracellular solution. Mean ± SD. *: $p < 0.05$, **: $p < 0.01$, ***: $p < 0.001$.

The microglial RMP is regulated by Kir2.1.

ML133 at a concentration of 50 µM depolarized the RMP of SNI D2 microglia from -36.9 ± 14.3 mV before to -9.00 ± 6.36 mV ($p < 0.001$) after perfusion with an extracellular concentration of 20 mM K^+. Naive cells were also depolarized from -21.2 ± 13.8 mV to -4.29 ± 5.42 mV ($p < 0.01$) by Kir2.1 blockade. Apamin, however, did not significantly change the RMPs (Fig. 4 A). No sham D2 animals were used as currents and RMPs were similar to naive.

The result was replicated with a 5 mM extracellular K^+ solution to be closer to physiological state. There ML133 depolarized SNI D2 microglia from -49.4 ± 22.6 mV before to -4.81 ± 9.27 mV ($p < 0.001$) after the block. Naive cells were also depolarized by Kir2.1 blockade: going from -27.5 ± 17.8 mV to -4.82 ± 9.28 ($p < 0.001$) with ML133 (Fig. 4 B).

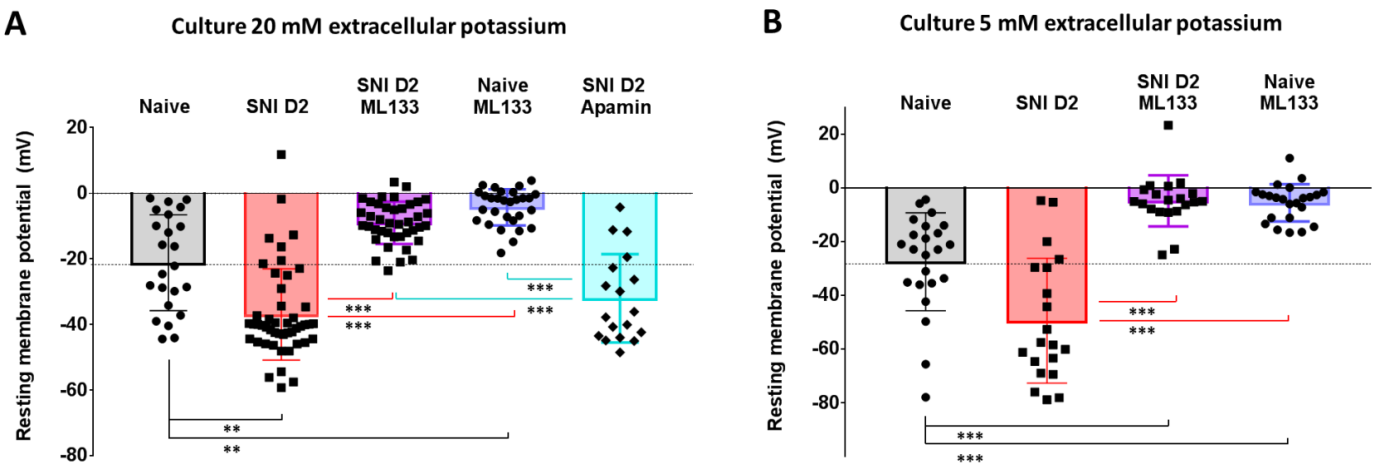

Fig. 4: Effect of pharmacological blockade on RMP of spinal cord dorsal horn microglia after SNI. (A) Histograms showing RMPs of freshly dissociated microglia with 20 mM K^+ in extracellular solution with 50 µM ML133 or 100 nM apamin block. **(B)**. Histograms showing RMPs of freshly dissociated microglia with 5 mM K^+ in extracellular solution with 50 µM ML133. Mean ± SD. *: $p < 0.05$, **: $p < 0.01$, ***: $p < 0.001$.

When isolating the Kir2.1 component, an increase of Kir2.1 outward currents is seen in SNI D2 microglia.

To link the increase in inward current at much hyperpolarized voltage steps to RMP modifications, we analyzed the isolated Kir2.1 component (ML133 sensitive component) in the physiological window of RMP and observed an expected small outward current.

The K^+ equilibrium potentials according to the Nernst equation in our conditions are: -83.4 mV for 5 mM of extracellular K^+ and -47.9 mV for 20 mM of extracellular K^+, which correspond to Kir2.1 isolated reversal potentials (Fig. 5).

Analyzing the data with two-way ANOVAs from the K^+ reversal potential (-80 mV for A, -50 mV for B) to 0 mV, we noticed a higher Kir2.1 isolated currents in SNI D2 than in naive animals.

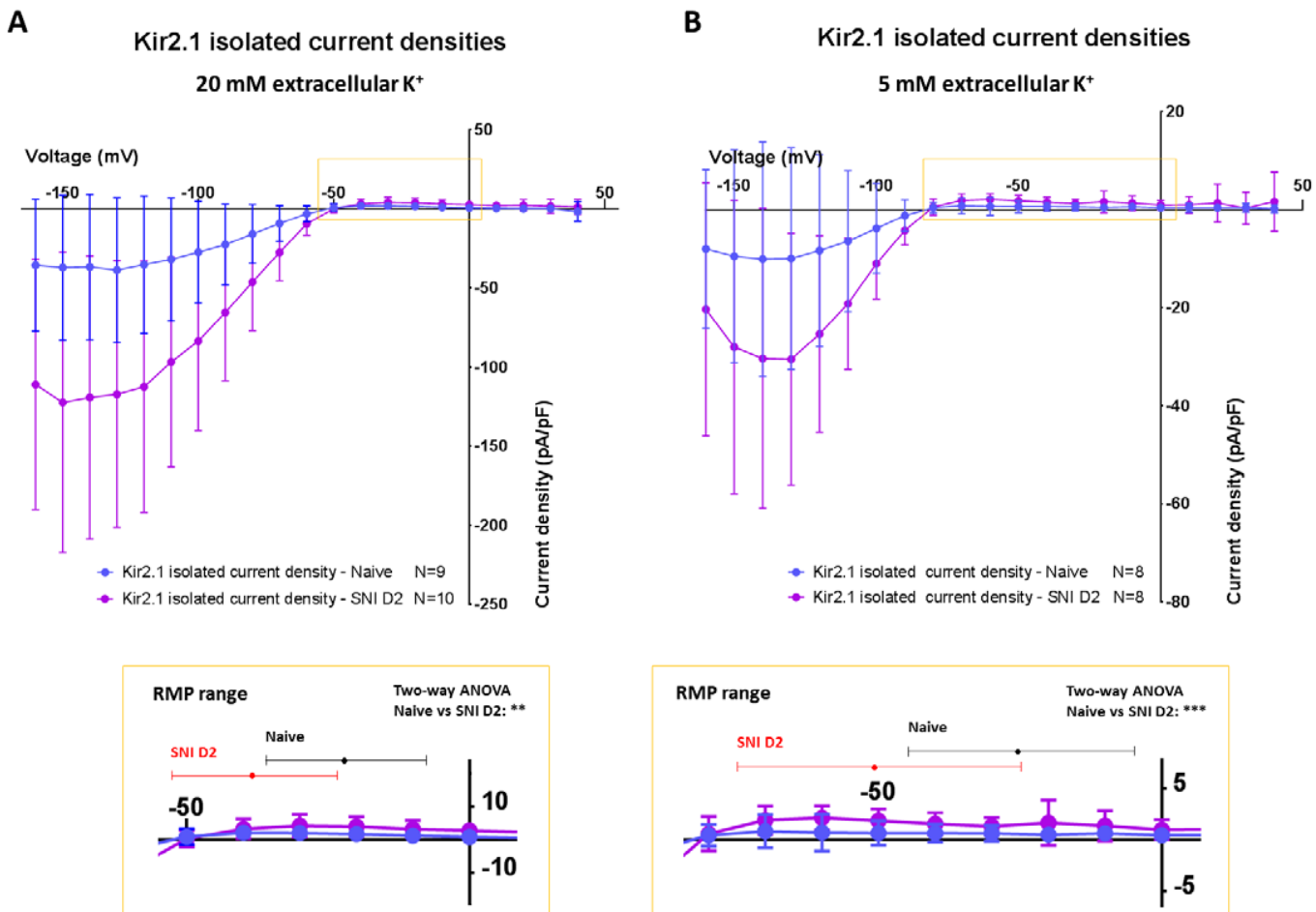

Fig. 5: Kir2.1 isolated current densities of spinal cord dorsal horn microglia. I-V curves of naive and SNI D2 Kir2.1 isolated current densities (ML133 sensitive) with an extracellular solution containing 20 mM K^+ **(A)** or 5 mM K^+ **(B)**. Inserts represent highlighted parts from the K^+ reversal potential of I-V curves to 0 mV. The ranges of RMPs measured in Fig. 4 are mentioned as horizontal bars. Mean ± SD. *: $p < 0.05$, **: $p < 0.01$, ***: $p < 0.001$.

Kir2.1 membrane expression is increased 2 days after SNI.

To explain the increase in Kir2.1-induced current, we labelled the cells with Kir2.1 antibodies with both intracellular and extracellular epitopes. Using the Kir2.1 intracellular epitope and cell permeabilization, we showed that almost every microglia were labelled, both in naive and SNI D2 conditions (Fig. 6 A). With an antibody against an extracellular epitope of Kir2.1, only 23.2 % of our naive microglia were stained without permeabilization, whereas over twice more cells were stained (49.3 %) in SNI D2 microglia (Fig. 6 B).

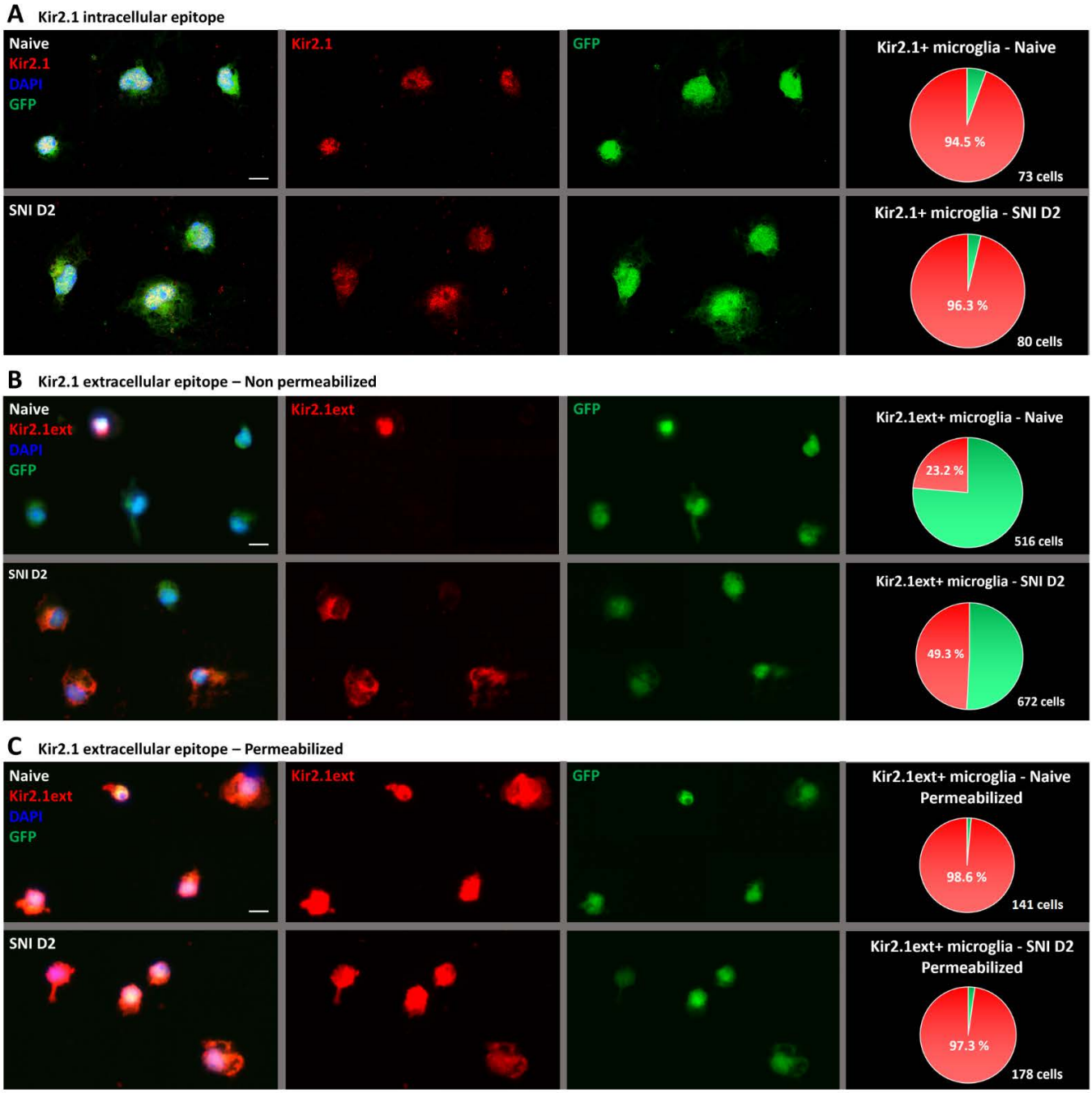

Fig. 6: Distribution of Kir2.1 at the membrane of spinal cord dorsal horn microglia after SNI. (A, B and C) Immunofluorescence images showing naive or SNI D2 freshly dissociated microglia stained with antibodies against Kir2.1 - intracellular epitope (permeabilized) **(A)**, Kir2.1 - extracellular epitope, non-permeabilized **(B)** or Kir2.1 - extracellular epitope, permeabilized **(C)**. **(D)** Histogram showing the blind counting of Kir2.1 - extracellular epitope antibody, non-permeabilized (shown in **B**) cells out of microglia cells. N=3 animals per group. Scale bars represent 10 µm. Mean ± SD. *: $p < 0.05$, **: $p < 0.01$, ***: $p < 0.001$.

After cell permeabilization, the antibody against the Kir2.1 extracellular epitope stained almost every microglia as for the antibody against the Kir2.1 intracellular epitope, in both naive and SNI D2 conditions (Fig. 6 C). We noticed that both SNI D4 and SNI D7 cells have similar Kir2.1 membrane expression as the naive condition, correlating to our electrophysiology experiments (Fig.6 D).

Microglia proliferation in the spinal cord dorsal horn peaks 2 days after SNI.

In response to peripheral nerve injury, spinal microglia undergo morphological hypertrophy and proliferation in rats (Gattlen et al. 2016). To assess whether the same is true in mice, microglia proliferation was then evaluated in the ipsilateral dorsal horn (DHi) after SNI by counting CX3CR1-EGFP positive cells as well as the cells stained with Ki-67 marker of proliferation (Fig. 7).

We observed an increasing number of microglial cells after SNI from naive to D7 (Fig. 7 A). However, the Ki-67 proliferation marker, peaked at 2 days after SNI, decreased at D4 and was no more visible in SNI D7 slices. No proliferation was seen in both naive and sham D7 (Fig. 7 B).

Fig. 7 C shows a representative image of a SNI day 7 spinal cord, with the insert marking the region where the counting was performed.

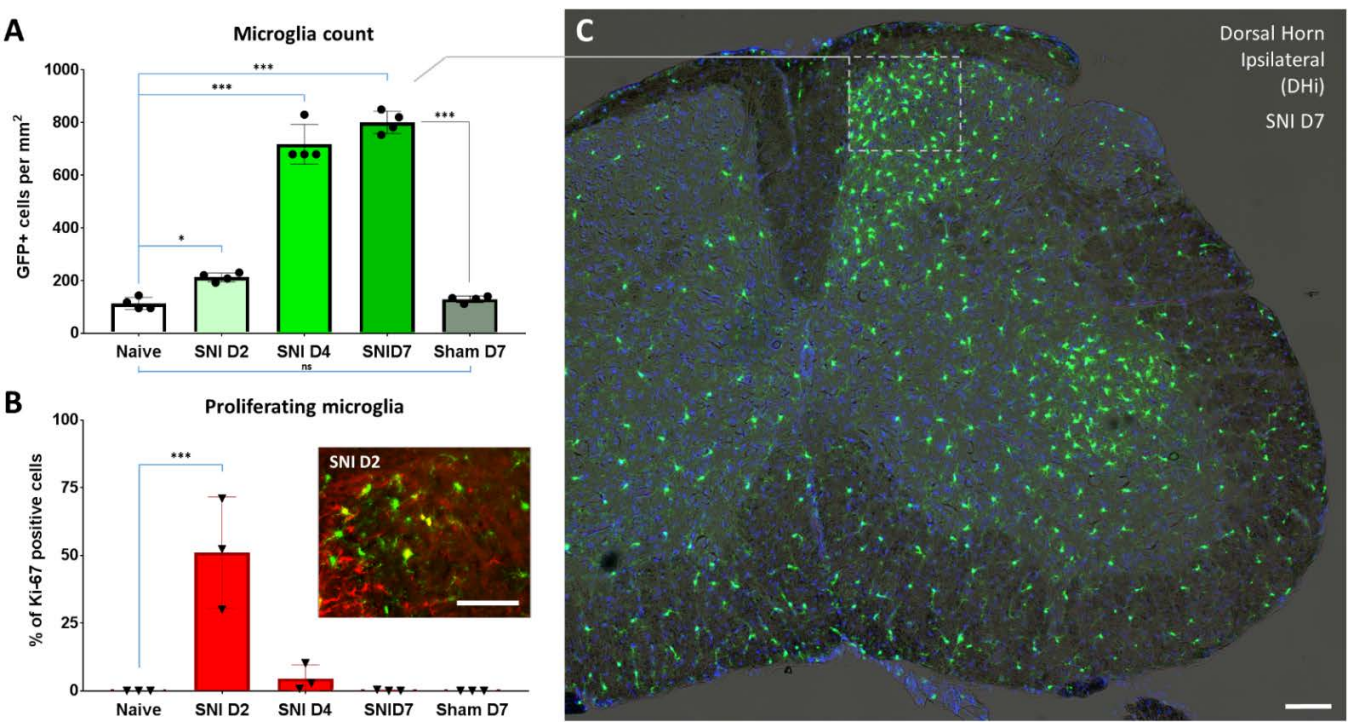

Fig. 7: Spinal cord dorsal horn microglial proliferation after SNI. (A) CX3CR1-EGFP cell count (microglia). N=4 animals **(B)** Cells count for the proliferation marker Ki-67. Only cells labelled for both CX3CR1 and Ki-67 were counted. A representative image of a Ki-67 staining is shown for SNI D2. N=3 animals. (**C**) Image showing a spinal cord slice; with an increase of microglia in the DHi to the surgery in green. DAPI staining appears in blue. Scale bars represent 100 µm. Here we compared against naive and sham D7 for (**A**) and against naive for (**B**). Mean ± SD. *: $p < 0.05$, **: $p < 0.01$, ***: $p < 0.001$.

ML133 strongly reduces proliferation in BV2 microglial cell line

Microglial proliferation and modification of electrophysiological properties by Kir2.1 both peak at day 2. It has been shown that RMP varies during cell cycle in cancer cells and that K^+ channels regulate proliferation (Yang and Brackenbury 2013, Urrego et al. 2014). We therefore investigated the link between Kir2.1, RMP modification and microglial proliferation by testing the effect of ML133 on an immortalized murine microglial cell line (BV2). ML133 at the same concentration as for electrophysiology, 50 µM, reduced number of cells as well as the proportion of proliferating (Ki-67 positive) cells at 2 and 4 days of culture (Fig. 8). There was no significant difference in the number of cells between 4h, D2 and D4 when we apply ML133 (Fig. 8 B).

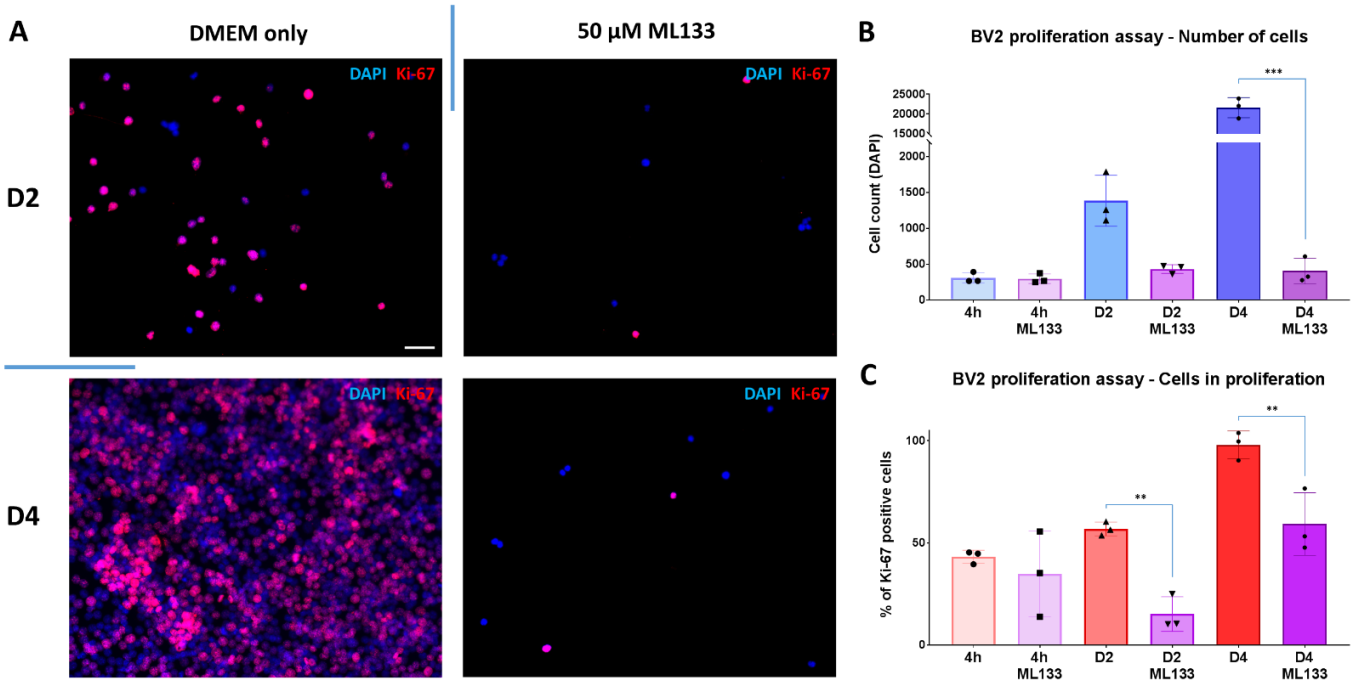

Fig 8: BV2 microglial cell line proliferation assay with ML133 by immunofluorescence. (A) Merged images of BV2 cells stained with DAPI (in blue) and with the proliferation marker Ki-67 (in red) cultured either in DMEM only or in DMEM with 50 µM ML133 for 2 or 4 days. Representative images taken in the center of the chamber. **(B)** Automatic cell count for using the DAPI nucleus staining with ImageJ software. **(C)** Percentage of cells counted for the proliferation marker Ki-67 out of the DAPI counted cells. 2000 cells per well were seeded in each well. After 2h of incubation at 37°C for the cells to attach, DMEM medium was changed with medium with or without ML133. The scale bar represents 50 µm. Mean ± SD. *: $p < 0.05$, **: $p < 0.01$, ***: $p < 0.001$.

ML133 reduces pain hypersensitivity and proliferation after intrathecal injection in mice

Our in vitro data suggests that Kir2.1 is essential in controlling the proliferation of BV2 cells. As our freshly dissociated microglia did not proliferate once in culture, we next examined directly in vivo for both the effect on microglial proliferation and behavioral changes.

We intrathecally injected either phosphate buffered saline (PBS) or ML133 in mice twice daily starting before SNI surgery. ML133 reduced both mechanical static allodynia tested by Von Frey and dynamic allodynia tested with a brush, at 1 and 2 days after SNI assessed (Fig. 9 A-D). The effect of ML133 is not significantly different just before or after the injection. Therefore, we can conclude that this drug has no acute effect but a preventive effect by modulating microglia.

The proliferation of microglia was evaluated at 2 days following SNI with the proliferation marker Ki-67 and the microglial marker Iba1 (Fig. 9 E). A reduction of the number of Ki-67 positive cells after intrathecal injection of ML133 was observed (Fig. 9 F).

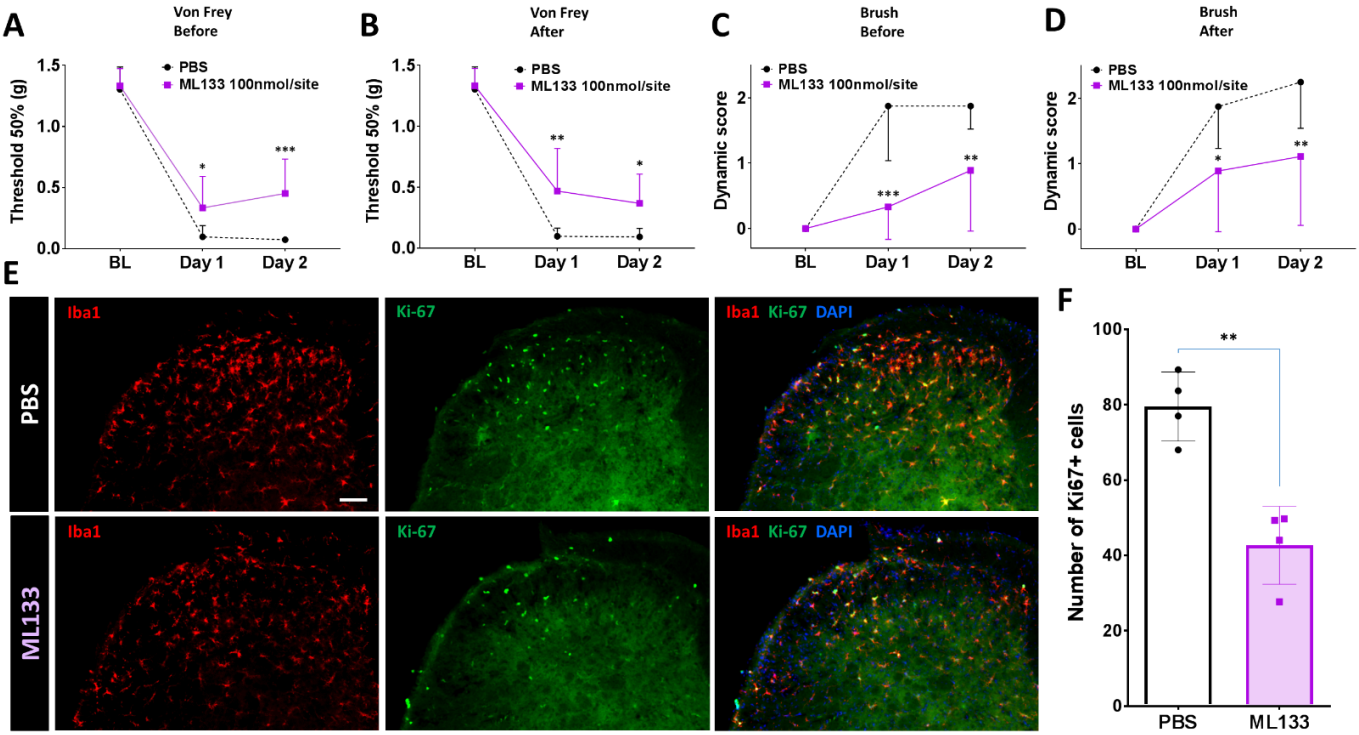

Fig. 9: ***In vivo*** **effects of intrathecal ML133 on spinal cord dorsal horn microglia.** Intrathecal injection twice per day starting before SNI of either 100 nM of ML133 or PBS in CD1 mice. **(A and B)** Mechanical hypersensitivity assessed with Von Frey before **(A)** and after **(B)** the second daily injection. **(C and D)** Dynamic allodynia measured by brush before **(C)** and after **(D)** the second daily injection. **(E)** Dorsal horn immunofluorescence of mice injected with PBS or ML133**.** The microglial marker Iba1 appears in red and the proliferation marker Ki-67 in green and the nucleus staining DAPI in blue. **(F)** Graph bars representing the Ki-67 positive cells in PBS or ML133 injected mice. N=8 animals per groups for behavior, N=4 animals per groups for immunostainings, with 4 images counted per animals. The scale bar represents 100 µm. Mean ± SD. *: $p < 0.05$, **: $p < 0.01$, ***: $p < 0.001$.

Discussion

In the current study, we report a novel function of the potassium channel Kir2.1 in the proliferation of microglia, by which microglia play an essential role in the pathogenesis of neuropathic pain. To our knowledge, this report is the first to identify this channel as a potential microglial target for the treatment of neuropathic pain. Our data reveal that following a peripheral nerve injury, the electrophysiological profile of microglia drastically changes. Two days after peripheral nerve injury, we observed an increase of Kir2.1-induced current and a hyperpolarization of the membrane potential of microglia, both of them coming back at their naive level at day 7. This coincides with the proliferation of microglia in spinal cord and the development of neuropathic pain behavior. Blocking Kir2.1 channel inhibited the increase in current, reestablished the membrane potential, reduced proliferation of microglia (in cultured cell-line and *in vivo*) and alleviated neuropathic pain behavior.

Electrophysiological modifications of microglia after SNI

We observed an increase of inward current at low voltage steps 2 days after SNI, but we did not see an outward current at positive potentials as often described in when challenging microglia. However a strong increase in outward current associated with a reduction of the inward current is mostly described when specific triggers mimicking pathogen-induced activation are applied such as lipopolysaccharide (LPS), pneumococcal cell walls (PCW) or HIV-TAT protein (De Simoni et al. 2008, Seifert 2011, Scheffel et al. 2012). When tissue-damaging procedures such as hypoxia (MCAO) or stab wound are used, a strong inward current with very low outward current is described, as in our model (Lyons et al. 2000, Seifert 2011, Richter et al. 2014). Injection of chemokine CXCL1 also induced inward current (Deftu et al. 2018). One study using facial axotomy of the facial nerve showed an increase of inward current followed by an outward current and finally return to baseline of both (Boucsein et al. 2000).

The inward current is caused by Kir2.1.

We first showed that the current is dependent on potassium concentration and inhibited by the broad blockers barium and cesium. The absence of effect of apamin excludes SK channels. IC50 for SK2 and SK3 are 27 pM and 4 nM respectively, far below the concentration we used (Grunnet et al. 2001). SK1 may not be fully blocked with the 100 nM of apamin of our experiment (IC50 of 704 pM and 196 nM for SK1, due to a biphasic block), however its impact in potassium currents in microglia is rather small since its expression in microglia is low compared to SK3 (Schlichter et al. 2010) or even undetected (Khanna et al. 2001). Mostly SK3 was shown to play a major role in microglia-induced neurotoxicity. Its Inhibition reduced reactive oxygen species and neuronal death in hippocampus (Schlichter et al. 2010).

TPA, a specific blocker of two-pore K^+ channels also showed no effect. We did not use blocker of Kvs, in the absence of outward current. For barium, the channel with the IC50 nearest to our results is Kir2.1 (IC50 of 3.2 µM). Kir2.2 (IC50 of 0.5 µM) should be more sensitive and Kir2.3 (IC50 of 10.3 µM) and Kir2.4 (IC50 of 390 µM) less sensitive (Hibino et al. 2010). ML133, the specific Kir2.x family blocker strongly reduced our currents. ML133 is to our knowledge the most selective Kir2.x blocker available with an EC50 of 1.8 µM for Kir2.1, 2.9 µM for Kir2.2, 4.0 µM for Kir2.3 and 2.8 µM for Kir2.6 at pH 7.4. Yet, ML133 can inhibit other channels. It has an IC50 of 7.7 µM for Kir6.2, 32.9 µM for Kir7.1, 76 µM for Kir4.1, and more than 300 µM for Kir1.1 at pH 7.4 (Wang HR et al. 2011). Lam and colleagues 2017 demonstrated that Kir2.1 is the main Kir2.x member expressed in microglia in both Sprague Dawley rats and C57BL6 mice compared to Kir2.2, Kir2.3 and Kir2.4. We therefore concluded the increased inward current at the low-voltage steps as Kir2.1-dependent.

Two transcriptomic analysis studies could not highlight an increase of Kir2.1 in microglia after stimulation (Zhang et al. 2014, Hickman et al. 2014). We could not conclude on an increased expression of the channel at the RNA level. However, we showed that an increased proportion of channels migrate to cell membrane. Using extracellular antibodies against Kir2.1 without permeabilization, we found that Kir2.1 is expressed at the membrane twice more often in SNI D2 than in naive. Kir2.1 externalization in SNI D4 and SNI D7 cells were not different from naive cells. This pattern coincides with our electrophysiological data of Kir2.1-induced increase in current.

Kir2.1 modulates membrane potential.

RMPs of our microglia were measured between -17 and -24 mV in naive condition, which is close to the range of resting state values described in the literature, comprised between -18 and -37 mV (Chung et al. 1998-9, Schilling et al. 2015, Gu et al. 2016). Two days after SNI, these potentials became hyperpolarized. Surprisingly, hyperpolarization was seen in most studies of reactive microglia, whatever the current modification observed: outward or inward. The RMP was rescued by blocking the increased current, both inward or outward (Chung et al. 1998-9, Blomster et al. 2016). Kir2.1 is an important channel for regulation of the membrane potential of microglia. When blocking Kir2.1 channels with ML133, the resting membrane potential is depolarized in both naive and SNI D2 cells. Hyperpolarization of the membrane potential associated to an increase of spinal cord microglial Kir currents was previously observed after intrathecal injection of the pro-inflammatory cytokine CXCL1 (Deftu et al. 2018).

Madry and colleagues 2018 observed a hyperpolarization of microglial membrane potential following ATP injection in extracellular space via micropipette. They showed a reduction of current when they used TPA or isoflurane to block the potassium currents of their microglia which they identified as dependent on the two pore K^+ channel - THIK-1. They also observed a rescue of the resting membrane potential from highly hyperpolarized with the ATP perfusion, to a level similar to control when blocking those channels with TPA or isoflurane. However in our model, TPA did not affect currents or RMPs.

At physiological levels, the membrane potential is more depolarized than the reversal potential of potassium. Kir2.1 channels are also able to generate small outward currents in this situation. Due to their size, those currents are difficult to detect unless subtracting the current remaining after blocking Kir2.1 from the total current and therefore revealing the Kir2.1-sensitive current. At more depolarized potentials, there is no further increase of the outward current despite the higher electrochemical driving force because of the intrinsic properties of Kir channels, which have a lower conductance at higher potential. Kir2.x channels are key

channels for the regulation of cell membrane potential, in excitable and non-excitable cells (Hibino et al. 2010) and this small outward current at membrane potential explains the hyperpolarization of microglial cells.

Resting membrane potential and proliferation in SNI microglia

Two days after SNI, the RMP was hyperpolarized and microglia proliferation was at its peak. A link between RMP and cell cycle has been previously observed (Yang and Brackenbury 2013, Urrego et al. 2014). The broad K^+ channel blocker barium has been shown to reduce M-CSF induced microglial proliferation (Schlichter et al. 1996). High level of K^+ efflux has been observed long ago during the M phase of proliferating cancer cells (Mills and Tupper 1976, Boonstra et al. 1981). More recently, Wang W et al. 2014 showed that blocking voltage-gated potassium channels such as Kv1.3 and Kv3.1 would arrest the cell cycle before the M phase in myeloma cancer cells. In our freshly dissociated microglia, no proliferation was observed and we therefore tested the link between Kir2.1 channels and proliferation on BV2 microglia which constantly multiply. ML133 greatly reduced the proliferation in those cells. To exclude a toxic effect of ML133, the drug was washed out and proliferation was encountered again, proving viability of the cells (Suppl. fig. 2). Finally, we could show that microglial proliferation was reduced in vivo when applying ML133. We can therefore hypothesize that the RMP hyperpolarization caused by Kir2.1 is necessary for microglial proliferation.

ML133 reduced allodynia after SNI.

Using the SNI model of neuropathic pain allowed us to evaluate effect on behavior and we could show that intrathecal injection of ML133 reduced mechanical static and dynamic allodynia following the injury. To our knowledge, there is only one previous published study on ML133 and pain (Shi et al. 2018) which could also demonstrate that it prevented dynamic but not static allodynia when injected before SNI with a dose-dependent effect for 5 days after SNI. ML133 also reversed dynamic but not static allodynia in 2 days when given after SNI. Their focus was on neurons. They saw no increase in total Kir2.1 protein in spinal cord, and no change in Kir2.1 current in neurons, but claimed a colocalization of Kir2.1 with neuronal markers in the dorsal horn of the spinal cord.

In conclusion, this study provides a new insight into mechanisms underlying the electrophysiological properties and proliferation of microglia in response to a peripheral nerve injury. Although further studies are necessary for a comprehensive understanding of these mechanisms, we unravel a new path for a currently unmet medical need: treatment of neuropathic pain, occurring via Kir2.1 channels induced microglial RMP modulation.

Material and methods

Animals

Adult transgenic male C57BL/6 mice (20–24 g) expressing Enhanced Green Fluorescent Protein under the control of the endogenous CX3CR1 locus (*CX3CR1*^{EGFP}Mice (B6.129P-*Cx3cr1*^{tm1Litt}/J) Jackson Laboratory, USA) were used to allow recordings on CX3CR1-Green Fluorescent Protein-labeled microglia. The handling of animals was in accordance with the European Union Directive 2010/63/EU and the ethical guidelines of the University of Lausanne.

For intrathecal injection of ML133, male CD1 mice (8-10 weeks) from Charles River were used as indicated for behavioral and biochemical experiments. Mice were housed four per cage at 22 ± 0.5°C under a controlled 12 hours light/dark cycle with free access to food and water. After surgery, the mice were observed in the home cage until they were able to take food and water. All efforts were made to minimize animal suffering, reduce the number of animals used, and use alternatives to *in vivo* techniques, in accordance with the International Association for the Study of Pain, the National Institutes of Health Office of Laboratory Animal Welfare Guide for the Care and Use of Laboratory Animals and with animal welfare guidelines established by the University of Cincinnati Institutional Animal Care and Use Committee.

SNI model

SNI surgery mouse model was performed as described previously (Decosterd and Woolf 2000). Briefly, mice were anesthetized with isoflurane. A skin and muscle incision was made in the thigh to expose the sciatic nerve on one side. Then, the tibial and common

peroneal nerves were ligated and transected distal to the ligature. The third branch, the sural nerve, was left intact and stretch or contact carefully avoided.

Solutions

Patch-clamp recordings were made in an extracellular solution (ES) containing (in mM): 120 NaCl, 20 KCl, 2 $CaCl_2$, 1 $MgCl_2$, 10 HEPES, and 10 D-glucose. The potassium-free solution was similar to the ES, except for the KCl, which was replaced with 20 mM choline chloride. For the 5 mM K^+ ES, the same but the 5 mM of K^+ was completed by 15 mM of choline chloride. The pH was adjusted to 7.4 with NaOH at room temperature and the osmolarity was 300 mOsm/kg. The intracellular solution contained (in mM): 5 NaCl, 130 KCl, 1 $CaCl_2$, 2 $MgCl_2$, 10 HEPES, 10 EGTA, with a pH of 7.4 adjusted with KOH and an osmolarity of 290 mOsm/kg. Barium solutions (0.5, 2.3, 10.3, and 390 µM), Cesium solutions (0.01, 0.1, 0.5, 1, and 5 nM), ML133 solutions (0.5, 5 and 50 µM), TPA solution (50 µM) and apamin solution (100 nM) were prepared in either 20 mM or 5 mM K^+ ESs.

Microglia primary culture

Mice were terminally anesthetized by intraperitoneal (i.p) injection of pentobarbital, and then decapitated. The spinal column was removed and the spinal cord was flushed out with PBS injected from its sacral part of the column. The tissue was transferred into a petri dish containing extracellular solution (ES) used for electrophysiology, and the lumbar region was separated under a stereomicroscope (Zeiss, Jena, Germany). The ipsilateral dorsal horn (DHi) of the L3-L5 region was collected, placed in DMEM with papain (2 mg/mL, Sigma) and incubated at 30°C for 30 min on a shaker. The tissue was triturated 3–4 times in 2 mL fresh culture medium: DMEM supplemented with 10% heat inactivated fetal bovine serum (BSA) and 1% Penicillin-streptomycin (PS) and allowed to settle for 2 min. The supernatant containing the cell suspension was transferred, and the procedure was repeated two times. The resulting cell suspension was centrifuged at 400*g* for 5 min at room temperature. After discarding the supernatant, the sediment was re-suspended in a culture medium and plated on 12 mm coverslips in 35 mm petri dishes containing 2 mL of culture medium or in 8-chamber slides (Nunc) containing 300 µl of culture medium. After 24 h incubation at 37°C and 5% CO_2, immunofluorescence or patch-clamp recordings were performed.

BV2 cell Culture

BV2 cells are immortalized C57BL/6 mice murine brain cells (IRCCS Ospedale Policlinico San Martino (ICLC, Genova)). Cells were cultured in T75 flasks, passed once a week. For experiments, cells were harvested and plated in 8-chamber slides. Culture medium was DMEM + 10% FBS + 1% PS. If not otherwise mentioned, all reagents were from Gibco, Life Technologies.

Electrophysiology

Fire-polished borosilicate glass pipettes with filament (World precision Instruments -TW150 F-4) were pulled using a DMZ-Universal Puller (Zeitz-Instruments) to a resistance near 5 MΩ. A MultiClamp 700B amplifier and a Digidata 1440A with the pClamp 10.3 software (Molecular Devices, Sunnyvale, CA, USA) were used for recordings. The cells were clamped at a holding potential of –60 mV and fast, slow and whole-cell compensation were made with a correction of 70%, a bandwidth of 5 kHz and a low-pass filter of 10 kHz. The whole-cell recordings were made under an Olympus BX51WI microscope (Tokyo, Japan) with a fluorescent lamp X-Cite 120PC-Q (Excelitas Technologies, Waltham, MA, SUA) and a digital acquisition camera ORCA-Flash2.8 (Hamamatsu Photonics, Shizuoka, Japan).

Immunofluorescence

Mice were terminally anesthetized by i.p injection of pentobarbital and perfused with ice cold PBS for 1 min followed by 4% paraformaldehyde (PFA) in PBS for 4 min. The sciatic nerve ipsilateral to the injury was dissected up to the L3–L5 spinal nerves to identify the corresponding level of the spinal cord. L3-L5 level of spinal cord was then collected and post-fixed overnight in 4% PFA at 4°C then transferred into 20% sucrose during 24h for cryoprotection and rapidly frozen. Slices of 18 µm thickness were cut on a cryostat and placed on slides for staining. For dissociated cells the same protocol as for electrophysiology was used. Twenty-four hours after plating, cells were fixed with 4% PFA for 10 min. After washing, cells or slices were incubated for 45 min in a 5% BSA, 0.1% triton X-100 PBS blocking solution and overnight with the primary antibody. If no permeabilization was needed, no triton X-100 was used during all the procedure. As primary antibodies, we used rabbit anti-Kir2.1 intracellular (1:300, Alomone Labs, Israel), rabbit anti-Kir2.1 extracellular (1:500, Alomone Labs, Israel) or rabbit anti-Ki-67 (1:750, Abcam, USA) for experiments depicted in Fig. 6, 7 and 8.

After PBS washing, cells or slices were incubated in the blocking solution for one hour at room temperature with the secondary antibody. Donkey anti-rabbit Cy3 (1:500, Jackson, USA) was used for experiments depicted in Fig. 6, 7 and 8. DAPI (4',6-diamidino-2-phenylindole) was applied on the slices for nuclear labelling before the final PBS wash. Lumbar spinal cord sections were then mounted on slides with Mowiol mounting medium and stored at 4 °C.

Pictures of 4 Ki-67-labelled lumbar sections for each naïve, SNI and sham operated animals were taken with the 40× objective using an Axio Imager Z1 fluorescence microscope (Zeiss, Oberkochen, Germany). Field was placed on the edge of the grey matter as shown in Fig. 7 C. Fluorescence intensity and exposure time were kept constant. An investigator blinded to the sample identity counted the positive cells.

For Kir2.1 extracellular labelling, tile scans of 8x8 mm were taken with a 10× objective on a Leica DMi8 Inverted fluorescence microscope. Fluorescence intensity and exposure time were kept constant for each picture. Cells were counted by an investigator blinded to the treatment. An intensity threshold of 10'000 intensity units (image J) in a 182 area square was chosen to select positives cells. One dot in Fig. 6 D represents the mean of 2 tile scans per animal each containing around 100 microglia.

For Kir2.1 intracellular epitope, images were taken with a Zeiss LSM 780 Quasar Confocal Microscope.

For the BV2 cell counting, the same amount of cells was plated in each chamber of 8-chambers slides. After tile scan acquisition, DAPI and Ki-67 positive cells were automatically counted with the ImageJ software.

For *in vivo* experiments, immunohistochemistry of spinal cord sections were carried out as follows. Mice were terminally anesthetized and perfused with PBS, followed by 4% paraformaldehyde in PBS (PFA solution) and lumbar spinal cords were collected two days after SNI surgery. Tissues were post-fixed in PFA solution overnight and subsequently transferred into 30% sucrose in PBS for 24h. Spinal cords were sliced into 40 µm sections and collected in PBS. Free floating sections were then blocked for 1h at room temperature with 1% BSA with 0.2% Triton X-100 in PBS (BSA solution). Subsequently, sections were incubated with Iba1 (goat, 1:1000, cat# NB100-1028, Novus) and Ki-67 primary antibody (rabbit, 1:50, cat# NB600-1252, Novus) overnight at 4°C, followed by incubation with the secondary antibody donkey anti-goat Alexa Fluor® 555 and donkey anti-rabbit Alexa Fluor® 488 (1:1000, Thermo Fisher Scientific) for 1 h at room temperature. Sections were mounted on slides and DAPI (Thermo Fisher Scientific) was used for counterstaining. Quantification of images from multiple sections of each SC, selected at random, were captured under an Olympus BX63 fluorescent microscope using cellSens imaging acquisition software (Olympus, Center Valley, PA). All image capture and quantification were performed comparing samples from all experimental groups, prepared with the same staining solutions, and then measured using identical display parameters.

Behavioral testing

Static mechanical allodynia was assessed as the hind paw withdrawal response to von Frey hair stimulation using the up-and-down method, as previously described (Chaplan et al. 1994). Briefly, the mice were first acclimatized (1 hour) in individual clear Plexiglas boxes on an elevated wire mesh platform to facilitate access to the plantar surface of the hind paws. Subsequently, a series of von Frey hairs (0.02, 0.07, 0.16, 0.4, 0.6, 1.0, and 1.4 g; Stoelting CO., Wood Dale, IL) were applied perpendicular to the plantar surface of the hind paw. A test began with the application of the 0.6 g hair. A positive response was defined as a clear paw withdrawal or shaking. Whenever a positive response occurred, the next lower hair was applied, and whenever a negative response occurred, the next higher hair was applied. The testing consisted of 6 stimuli, and the pattern of response was converted to a 50% von Frey threshold, using the method described previously (Dixon 1980), by an investigator blinded to treatment.

Dynamic allodynia was assessed as the response to a light stroke on the lateral plantar region of the paw with a paintbrush, in the heel-to-toe direction. The paintbrush was prepared by smoothing the tip and removing the outer layer of hairs. An average of three tests at 10-s intervals was obtained for each mouse. The scoring system was as follows: 0: walking away or occasional, very brief paw lifting within 1 s (as for normal touch behavior); 1: sustained lifting (> 2 s) of the stimulated paw toward the body; 2: strong lateral paw lift above the level of the body; 3: multiple flinching or licking of the stimulated paw (Shi et al. 2018).ML133 (S2825; Selleckchem, Houston, TX) was dissolved in dimethylsulfoxide (200 nmol/ µL) and diluted in PBS to the final concentrations of 100 nmol/site before intrathecal administration in a 5 µL volume, one hour before surgery, followed by two daily i.t. injections.

Analysis

Patch clamp data were analyzed with Clampfit 10.3 (Molecular Devices). Statistical analyses were performed with Prism 7 software (GraphPad, San Diego, CA, USA). For I-V curves, two-way ANOVAs with Sidak correction on post-hoc tests were performed on the inward current densities from -160 to -70 mV. For behavior, two-way ANOVAs with Sidak correction on post-hoc tests were performed. For the I-V curves of Kir2.1 Isolated current densities, two-way ANOVAs were performed from the reversal potential to 0 mV.

For Fig. 1 D, 3, 6, and Suppl. fig. 2, one-way ANOVAs with Dunett's correction on post-hoc tests were used because all groups were compared to one. For Fig. 7 and 8, one-way ANOVAs with Sidak correction on post-hoc tests were used because groups were compared all together or 2 by 2 (Fig. 8). For Fig 9 F, t-test was used. For Fig. 1 C, 2 D, and 4, the non-parametric Kruskal-Wallis test with Dunn's correction on post-hoc tests was applied because normality (Shapiro-Wilk test) was not met and differences between SDs (Brow-Forsythe test) were found.

Values were represented as mean ± SD and $p < 0.05$ was considered significant. Thresholds were represented as follows: *: $p < 0.05$, **: $p < 0.01$, ***: $p < 0.001$. Only biological replicates are presented in the figures.

STAR ⋆ METHODS

KEY RESOURCES TABLE

REAGENT or RESOURCE	SOURCE	IDENTIFIER
Antibodies		
Rabbit anti-Kir2.1 intracellular	Alomone Labs, Israel	APC-026
Rabbit anti-Kir2.1 extracellular	Alomone Labs, Israel	APC-159
Rabbit anti-Ki-67	Abcam, UK	Ab15580
Donkey anti-rabbit Cy3	Jackson, USA	711-165-151
Goat anti-Iba1	Novus, USA	NB100-1028
Rabbit anti-Ki-67	Novus, USA	NB600-1252
Donkey anti-rabbit Alexa Fluor® 488	Thermo Fisher	A-27034
Donkey anti-goat Alexa Fluor® 555	Thermo Fisher	A-21432
Chemicals, Peptides, and Recombinant Proteins		
Apamin	Alomone Labs, Israel	STA-200
Barium	Sigma-Aldrich	342920
Cesium	Sigma-Aldrich	289329
ML-133	Sigma-Aldrich	SML0190
ML-133	Selleckchem, USA	S2825
TPA	Sigma-Aldrich	258962
Diamidinophenylindole (DAPI)	Thermo Fisher	D-3571
Experimental Models: Organisms/Strains		
CX3CR1^{EGFP}Mice (B6.129P-*Cx3cr1*^{tm1Litt}/J) Characterized by Jung S. et al. 2000	Jackson, USA	005582
CD1 mice	Charles River, USA	CD-1 IGS
BV2 microglial cell line created from C57BL/6 mouse brain.	IRCCS Ospedale Policlinico San Martino (ICLC, Genova)	ICLC catalog code: ATL03001
Software and Algorithms		
ImageJ	imagej.net	N/A
Axiovision	Zeiss	rel.4.6
Las X	Leica microsystems	N/A
pClamp10	Molecular Devices	10.3
GraphPad Prism	GraphPad Softwares	v. 7
Zen	Zeiss	Blue / black

Other		
Isoflurane	Provet	2222
Pentobarbital (Esconarkon)	Streuli Pharma	V102013
8-chamber slides	Nunc	4808
Micropipette Puller	Zeitz-Instruments	DMZ-universal puller
Borosillicate tubes with filament	World precision Instruments	TW150 F-4

Acknowledgments:

We thank Pr. Christian Kern, Head of department of anesthesiology, Lausanne University Hospital (CHUV), for his support and Pr. Anita Lüthi for the use some laboratory infrastructure. We thank Marie Pertin, Guylène Kirschmann and Ludovic Gillet for technical help and advice. This study is supported by the European Society of Anaesthesiology ESA Project Grants 2014 (MRS), the Swiss National Science Foundation grants 310030A_124996 (ID) and 33CM30-124117 (ID), the 2015 IASP Collaborative grant (MRS and VR), the NIH grant NS106264 (TB) and the SCIEX 12.366 grant (ID).

Author Contributions: Christophe Gattlen designed the experiments, performed the electrophysiology, immunostainings except for the *in vivo* part, analyzed data and drafted the first manuscript. Alexandru F. Deftu designed and performed electrophysiology experiments. Violeta Ristoiu designed and supervised electrophysiology experiments. Raquel Tonello and Yuejuan Liu designed and performed the behavior and the immunostaining from the *in vivo* part. Temugin Berta and Isabelle Decosterd supervised the experiments and design and corrected the manuscript. Marc R. Suter designed and supervised the experiments and the whole study and wrote the final manuscript.

Conflicts of Interest: The authors declare no conflict of interest.

References

Albrecht DS, Forsberg A, Sandstrom A, Bergan C, Kadetoff D, Protsenko E, Lampa J, Lee YC, Hoglund CO, Catana C, Cervenka S, Akeju O, Lekander M, Cohen G, Halldin C, Taylor N, Kim M, Hooker JM, Edwards RR, Napadow V et al. (2018) Brain glial activation in fibromyalgia - A multi-site positron emission tomography investigation. Brain, behavior, and immunity 75: 72-83

Attal N, Fermanian C, Fermanian J, Lanteri-Minet M, Alchaar H, Bouhassira D (2008) Neuropathic pain: are there distinct subtypes depending on the aetiology or anatomical lesion? Pain 138: 343-53

Biber K, Owens T, Boddeke E (2014) What is microglia neurotoxicity (Not)? Glia 62: 841-54

Blomster LV, Strobaek D, Hougaard C, Klein J, Pinborg LH, Mikkelsen JD, Christophersen P (2016) Quantification of the functional expression of the Ca2+ -activated K+ channel KCa 3.1 on microglia from adult human neocortical tissue. Glia 64: 2065-2078

Boonstra J, Mummery CL, Tertoolen LG, Van Der Saag PT, De Laat SW (1981) Cation transport and growth regulation in neuroblastoma cells. Modulations of K+ transport and electrical membrane properties during the cell cycle. Journal of cellular physiology 107: 75-83

Boucsein C, Kettenmann H, Nolte C (2000) Electrophysiological properties of microglial cells in normal and pathologic rat brain slices. The European journal of neuroscience 12: 2049-58

Chen G, Zhang YQ, Qadri YJ, Serhan CN, Ji RR (2018) Microglia in Pain: Detrimental and Protective Roles in Pathogenesis and Resolution of Pain. Neuron 100: 1292-1311

Chaplan SR, Bach FW, Pogrel JW, Chung JM, Yaksh TL (1994) Quantitative assessment of tactile allodynia in the rat paw. Journal of neuroscience methods 53: 55-63

Chung S, Joe E, Soh H, Lee MY, Bang HW (1998) Delayed rectifier potassium currents induced in activated rat microglia set the resting membrane potential. Neuroscience letters 242: 73-6

Chung S, Jung W, Lee MY (1999) Inward and outward rectifying potassium currents set membrane potentials in activated rat microglia. Neuroscience letters 262: 121-4

Colloca L, Ludman T, Bouhassira D, Baron R, Dickenson AH, Yarnitsky D, Freeman R, Truini A, Attal N, Finnerup NB, Eccleston C, Kalso E, Bennett DL, Dworkin RH, Raja SN (2017) Neuropathic pain. Nature reviews Disease primers 3: 17002

De Simoni A, Allen NJ, Attwell D (2008) Charge compensation for NADPH oxidase activity in microglia in rat brain slices does not involve a proton current. The European journal of neuroscience 28: 1146-56

Decosterd I, Woolf CJ (2000) Spared nerve injury: an animal model of persistent peripheral neuropathic pain. Pain 87: 149-58

Deftu AF, Ristoiu V, Suter MR (2018) Intrathecal Administration of CXCL1 Enhances Potassium Currents in Microglial Cells. Pharmacology 101: 262-268

Dixon WJ (1980) Efficient analysis of experimental observations. Annual review of pharmacology and toxicology 20: 441-62

Echeverry S, Shi XQ, Rivest S, Zhang J (2011) Peripheral nerve injury alters blood-spinal cord barrier functional and molecular integrity through a selective inflammatory pathway. The Journal of neuroscience : the official journal of the Society for Neuroscience 31: 10819-28

Fordyce CB, Jagasia R, Zhu X, Schlichter LC (2005) Microglia Kv1.3 channels contribute to their ability to kill neurons. The Journal of neuroscience: the official journal of the Society for Neuroscience 25: 7139-49

Franciosi S, Ryu JK, Choi HB, Radov L, Kim SU, McLarnon JG (2006) Broad-spectrum effects of 4-aminopyridine to modulate amyloid beta1-42-induced cell signaling and functional responses in human microglia. The Journal of neuroscience: the official journal of the Society for Neuroscience 26: 11652-64

Gattlen C, Clarke CB, Piller N, Kirschmann G, Pertin M, Decosterd I, Gosselin RD, Suter MR (2016) Spinal Cord T-Cell Infiltration in the Rat Spared Nerve Injury Model: A Time Course Study. International journal of molecular sciences 17: 352

Grunnet M, Jensen BS, Olesen SP, Klaerke DA (2001) Apamin interacts with all subtypes of cloned small-conductance Ca2+-activated K+ channels. Pflugers Archiv : European journal of physiology 441: 544-50

Gu N, Eyo UB, Murugan M, Peng J, Matta S, Dong H, Wu LJ (2016) Microglial P2Y12 receptors regulate microglial activation and surveillance during neuropathic pain. Brain, behavior, and immunity 55: 82-92

Heo DK, Lim HM, Nam JH, Lee MG, Kim JY (2015) Regulation of phagocytosis and cytokine secretion by store-operated calcium entry in primary isolated murine microglia. Cellular signalling 27: 177-86

Hibino H, Inanobe A, Furutani K, Murakami S, Findlay I, Kurachi Y (2010) Inwardly rectifying potassium channels: their structure, function, and physiological roles. Physiological reviews 90: 291-366

Hickman SE, Kingery ND, Ohsumi TK, Borowsky ML, Wang L-c, Means TK, El Khoury J (2013) The microglial sensome revealed by direct RNA sequencing. Nature neuroscience 16: 1896

International Association for the Study of Pain (IASP)

Jung S, Aliberti J, Graemmel P, Sunshine MJ, Kreutzberg GW, Sher A, Littman DR (2000) Analysis of fractalkine receptor CX(3)CR1 function by targeted deletion and green fluorescent protein reporter gene insertion. Molecular and cellular biology 20: 4106-14

Kettenmann H, Hanisch UK, Noda M, Verkhratsky A (2011) Physiology of microglia. Physiological reviews 91: 461-553

Khanna R, Roy L, Zhu X, Schlichter LC (2001) K+channels and the microglial respiratory burst. American journal of physiology Cell physiology 280

Koltzenburg M (1998) Painful neuropathies. Current opinion in neurology 11: 515-21

Lam D, Schlichter LC (2015) Expression and contributions of the Kir2.1 inward-rectifier K(+) channel to proliferation, migration and chemotaxis of microglia in unstimulated and anti-inflammatory states. Frontiers in cellular neuroscience 9: 185

Lam D, Lively S, Schlichter LC (2017) Responses of rat and mouse primary microglia to pro- and anti-inflammatory stimuli: molecular profiles, K(+) channels and migration. Journal of neuroinflammation 14: 166

Loggia ML, Chonde DB, Akeju O, Arabasz G, Catana C, Edwards RR, Hill E, Hsu S, Izquierdo-Garcia D, Ji RR, Riley M, Wasan AD, Zurcher NR, Albrecht DS, Vangel MG, Rosen BR, Napadow V, Hooker JM (2015) Evidence for brain glial activation in chronic pain patients. Brain : a journal of neurology 138: 604-15

Lyons SA, Pastor A, Ohlemeyer C, Kann O, Wiegand F, Prass K, Knapp F, Kettenmann H, Dirnagl U (2000) Distinct physiologic properties of microglia and blood-borne cells in rat brain slices after permanent middle cerebral artery occlusion. Journal of cerebral blood flow and metabolism : official journal of the International Society of Cerebral Blood Flow and Metabolism 20: 1537-49

Madry C, Kyrargyri V, Arancibia-Carcamo IL, Jolivet R, Kohsaka S, Bryan RM, Attwell D (2018) Microglial Ramification, Surveillance, and Interleukin-1beta Release Are Regulated by the Two-Pore Domain K(+) Channel THIK-1. Neuron 97: 299-312.e6

Martinez V, Attal N, Bouhassira D, Lantéri-Minet M (2010) Les douleurs neuropathiques chroniques: diagnostic, évaluation et traitement en médecine ambulatoire. Recommandations pour la pratique clinique de la Société française d'étude et de traitement de la douleur. Douleurs : Evaluation - Diagnostic - Traitement 11: 3-21

Mills B, Tupper JT (1976) Cell cycle dependent changes in potassium transport. Journal of cellular physiology 89: 123-32

Moussaud S, Lamodière E, Savage C, Draheim HJ (2009) Characterization of K+ current in microglia cell line, Cell Physiol Biochem 2009;24:141-152

Muessel MJ, Harry GJ, Armstrong DL, Storey NM (2013) SDF-1alpha and LPA modulate microglia potassium channels through rho gtpases to regulate cell morphology. Glia 61: 1620-8

Nguyen HM, Blomster LV, Christophersen P, Wulff H (2017) Potassium channel expression and function in microglia: Plasticity and possible species variations. Channels (Austin, Tex) 11: 305-315

Nguyen HM, Grossinger EM, Horiuchi M, Davis KW, Jin LW, Maezawa I, Wulff H (2017) Differential Kv1.3, KCa3.1, and Kir2.1 expression in "classically" and "alternatively" activated microglia. Glia 65: 106-121

Pannasch U, Farber K, Nolte C, Blonski M, Yan Chiu S, Messing A, Kettenmann H (2006) The potassium channels Kv1.5 and Kv1.3 modulate distinct functions of microglia. Molecular and cellular neurosciences 33: 401-11

Ransohoff RM (2016) A polarizing question: do M1 and M2 microglia exist? Nature neuroscience 19: 987-91

Ryan DP, da Silva MR, Soong TW, Fontaine B, Donaldson MR, Kung AW, Jongjaroenprasert W, Liang MC, Khoo DH, Cheah JS, Ho SC, Bernstein HS, Maciel RM, Brown RH, Jr., Ptacek LJ (2010) Mutations in potassium channel Kir2.6 cause susceptibility to thyrotoxic hypokalemic periodic paralysis. Cell 140: 88-98

Salter MW, Beggs S (2014) Sublime microglia: expanding roles for the guardians of the CNS. Cell 158: 15-24

Scheffel J, Regen T, Van Rossum D, Seifert S, Ribes S, Nau R, Parsa R, Harris RA, Boddeke HW, Chuang HN, Pukrop T, Wessels JT, Jurgens T, Merkler D, Bruck W, Schnaars M, Simons M, Kettenmann H, Hanisch UK (2012) Toll-like receptor activation reveals developmental reorganization and unmasks responder subsets of microglia. Glia 60: 1930-43

Schilling T, Eder C (2015) Microglial K(+) Channel Expression in Young Adult and Aged Mice. Glia 63: 664-672

Schlichter LC, Sakellaropoulos G, Ballyk B, Pennefeather PS, Phipps DJ (1996) Properties of K+ and Cl- channels and their involvement in proliferation of rat microglia. GLIA 17:225-236

Schlichter LC, Kaushal V, Moxon-Emre I, Sivagnanam V, Vincent C (2010) The Ca2+ activated SK3 channel is expressed in microglia in the rat striatum and contributes to microglia-mediated neurotoxicity in vitro. Journal of neuroinflammation 7: 4-4

Seifert S (2011) Electrophysiological properties and intracellular calcium recordings of microglial cells from the adult brain, d-nb.info

Shi Y, Chen Y, Wang Y (2018) Kir2.1 Channel Regulation of Glycinergic Transmission Selectively Contributes to Dynamic Mechanical Allodynia in a Mouse Model of Spared Nerve Injury. Neuroscience bulletin

Song WM, Colonna M (2018) The identity and function of microglia in neurodegeneration. Nature immunology 19: 1048-1058

Suter MR, Wen YR, Decosterd I, Ji RR (2007) Do glial cells control pain? Neuron glia biology 3: 255-68

Urrego D, Tomczak AP, Zahed F, Stuhmer W, Pardo LA (2014) Potassium channels in cell cycle and cell proliferation. Philosophical transactions of the Royal Society of London Series B, Biological sciences 369: 20130094

Wang HR, Wu M, Yu H, Long S, Stevens A, Engers DW, Sackin H, Daniels JS, Dawson ES, Hopkins CR, Lindsley CW, Li M, McManus OB (2011) Selective inhibition of the K(ir)2 family of inward rectifier potassium channels by a small molecule probe: the discovery, SAR, and pharmacological characterization of ML133. ACS chemical biology 6: 845-56

Wang W, Fan Y, Wang S, Wang L, He W, Zhang Q, Li X (2014) Effects of voltage-gated K+ channel on cell proliferation in multiple myeloma. TheScientificWorldJournal 2014: 785140

Yang M, Brackenbury WJ (2013) Membrane potential and cancer progression. Frontiers in physiology 4: 185

Zhang Y, Chen K, Sloan SA, Bennett ML, Scholze AR, O'Keeffe S, Phatnani HP, Guarnieri P, Caneda C, Ruderisch N, Deng S, Liddelow SA, Zhang C, Daneman R, Maniatis T, Barres BA, Wu JQ (2014) An RNA-sequencing transcriptome and splicing database of glia, neurons, and vascular cells of the cerebral cortex. The Journal of neuroscience : the official journal of the Society for Neuroscience 34: 11929-4

Supplementary material

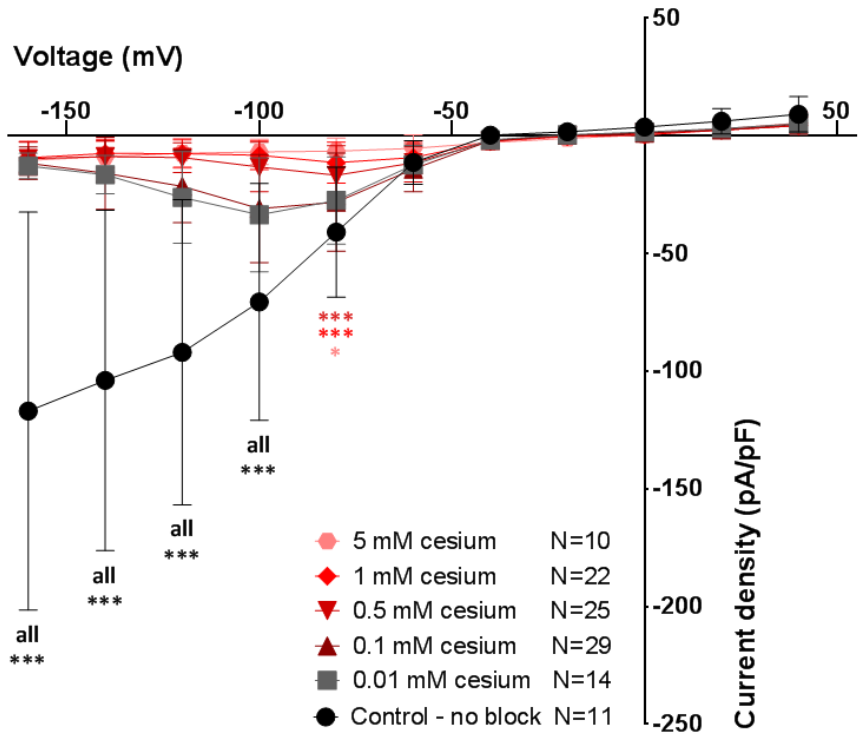

Suppl. fig. 1: Pharmacological response of dorsal horn microglial current densities after SNI. I-V curve showing currents densities recorded in freshly dissociated microglia from SNI D2 mice in 20 mM K^+ extracellular solution blocked with different concentrations of cesium**,** a broad K^+ blocker**.** Mean ± SD, *: $p < 0.05$, **: $p < 0.01$, ***: $p < 0.001$. All groups were compared to control – no block.

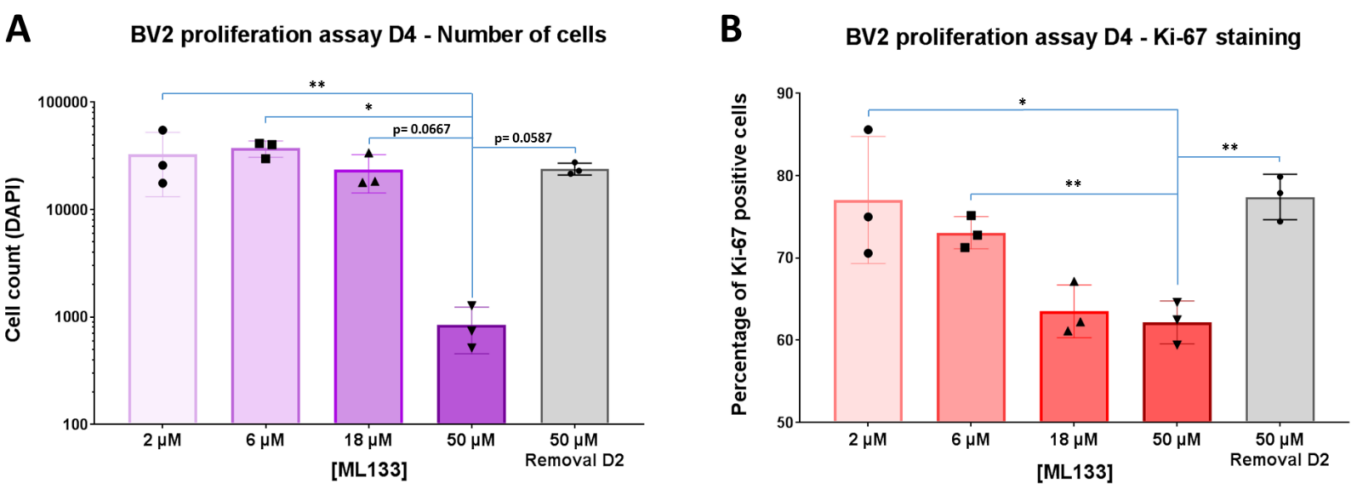

Suppl. fig. 2: ML133 dose-dependency effect on proliferation of BV2 cells: (A) Effect of increasing concentration of ML133 during 4 days on proliferation of BV2. For Removal D2 column (in grey) ML133 was removed after 2 days to show viability of the cells; automatic cell count with ImageJ software using DAPI nucleus staining. **(B)** Percentage of positive cells for the proliferation marker Ki-67 out of the DAPI counted cells. Automatic cell count with ImageJ software using Ki-67 marker. Mean ± SD, *: $p < 0.05$, **: $p < 0.01$, ***: $p < 0.001$.

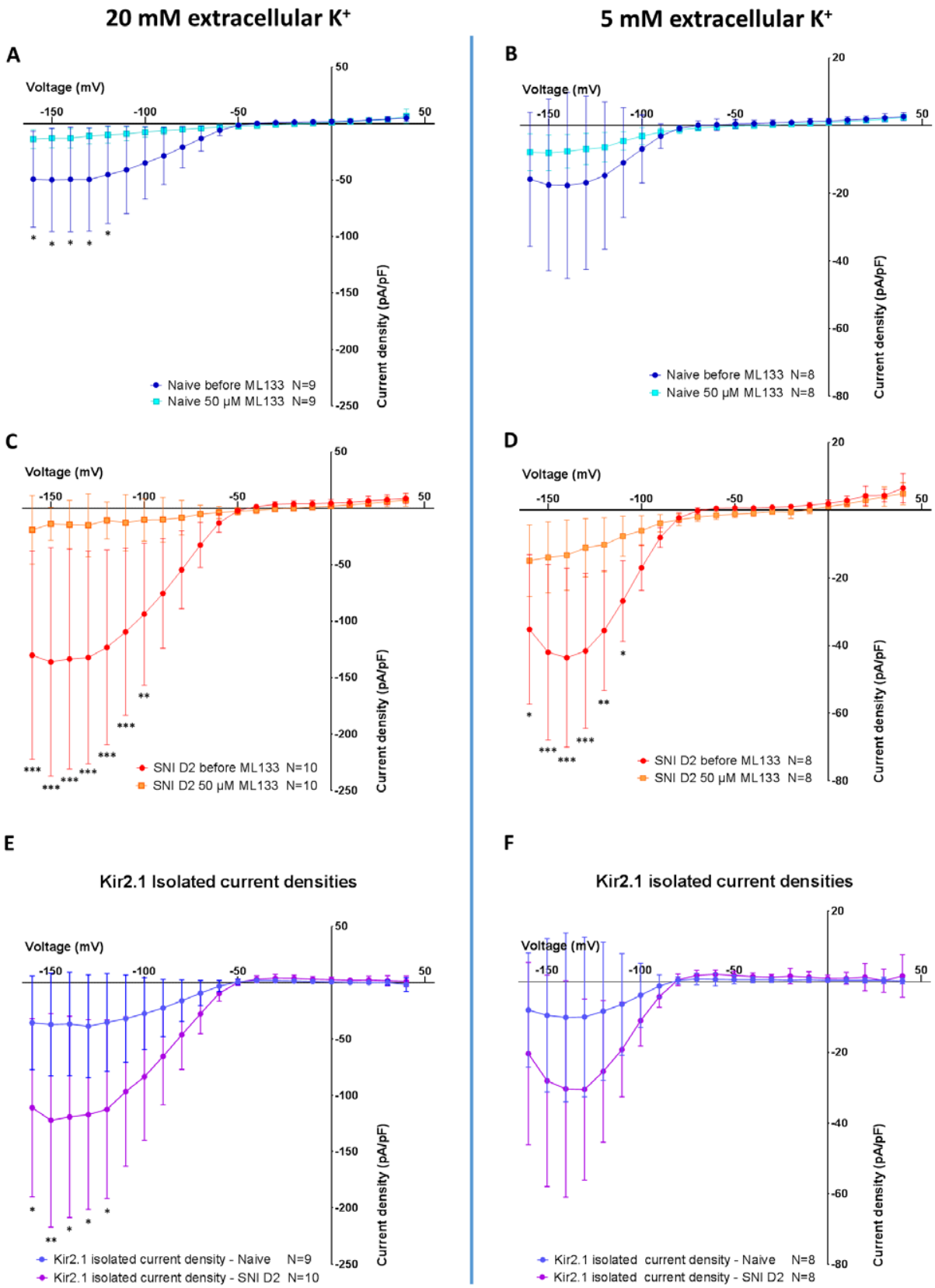

Suppl. fig. 3: Detail of ML133 sensitive current densities: I-V curves of freshly dissociated microglia before and after ML133 in naive (**(A)**, 20 mM extracellular K^+; **(B)** 5 mM extracellular K^+) and SNI D2 (**(C)** 20 mM extracellular K^+; **(D)** 5 mM extracellular K^+). **(E and F)** I-V curves of naive and SNI D2 Kir2.1 isolated current (ML133 sensitive), with 20 mM K^+ and 5 mM K^+ in extracellular solution respectively. These curves are obtained by subtraction of the value before and after ML133 of each **A**, **B**, **C** and **D**. Mean ± SD, *: $p < 0.05$, **: $p < 0.01$, ***: $p < 0.001$.

Discussion

1. Microglial activation

We can observe similarities in microglial activation between different neuropathic pain models: first, there is a rapid increase in the number of microglia over the first week after the injury. (Hu and McLachlan 2006). The amount of microglia then either remains stable or lowers slowly during next week depending on the studies. The hypersensitivity caused by the neuropathic pain model follows the same trend. It peaks early: often two days after peripheral injury and then stabilizes or lowers slowly (Kim et al. 2007, Clark et al. 2007, Cao and De Leo 2008, Dominguez et al 2008, Guasti et al 2009, Zhuang et al. 2007, Feng and Dubner 2008, Gattlen et al. 2016)

The inflammation models cause more an acute reaction. Microglial reactivity is also reported early: at day 2 sometimes before, at day 1 for intraplantar capsaicin injection (Chen et al. 2008). Huxtable and colleagues 2013 even showed increase of ROS inducing genes and cyclooxygenase gene upregulation in microglia 3 hours after systemic injection of LPS. Similarly, Svensson et al. 2003 showed spinal microglial activation of p38 MAPK pathway already ten minutes after substance P intrathecal injection. However, few effects remained after one week, except for formalin and CFA, which generated a strong inflammation. Still, the hypersensibility caused by those models did not last more than 2 weeks. Yong-hui 2012 showed that protein synthesis from activated microglia is reduced to naive level at day 14.

When injected intraplantar, intra-articular or in the hind paw the inflammatory agent, induced microglial reactivity in the dorsal horn ipsilaterally to the injection site. Following injection in the spinal cord or even systemically the effect on the microglia was the same but in the whole spinal cord (references Table 2).

2. Gene profiling of activated microglia

With the first article, we investigated the gene profile of the dorsal horn of the spinal cord: the location where most microglial reaction after the SNI were described. We investigated 96 genes of interest in the context of inflammation, pathogen pattern recognition receptors such as toll-like receptors (TLR) and downstream effectors of cellular signaling such as MYD88 and NF-κB.

There was a clear increase in gene expression of TLRs and complement components over all the timecourse. These genes are related to pathogen detection for the TLRs and opsonisation via the complement. Even in the absence of pathogen in the SNI, microglia use this pathway to induce a phenotype in response to peripheral nerve injury.

We also showed that pro-inflammatory cytokines such as IL-6, IL-18, CCL4, CCL12, CXCL11 and TNF-α genes were upregulated in early time points D2 to D10. Later on their amount was reduced, quickly for some with already a drop at D4 (TNF-α, CCL4, CCL12, CXCL11), and later - D10 - for others (IL-6, IL-18).

We also noticed an increase of anti-inflammatory agents in the later timepoints. At D21, we observed a strong increase in gene expression of CCL1, CCL22 and IL-10.

Together with the decrease of pro-inflammatory agents until D21, we observed a switch from pro-inflammatory to anti-inflammatory phenotype of the genes expressed in the spinal cord, which might reflect a change of microglia activation phenotype. This process seems to start at least 2 weeks from the nerve injury, then microglia change slowly to an anti-inflammatory phenotype.

We can correlate this hypothesis with the results of these studies:

Griffin et al. 2017 showed an increase of different pro-inflammatory genes in spinal cord adult microglia 7 days after SNI: IL-18, CCR5, CCL13, CXCL13 were upregulated. They also observe the same increase in the complement genes.

In a later time point, Andreou et al. 2017 revealed that in a mouse model of breast cancer brain metastasis, their microglia expressed the mannose receptor C-type 1 and arginase 1: two anti-inflammatory marker only at day 21.

What would have caused this microglial phenotypic switch from pro- to anti-inflammatory? The response could be an interaction with astrocytes: studies have shown that they are also modified after nerve injury (Hu et al 2006, Wei et al. 2008, Cui et al. 2011), maybe with a delay.

Indeed, it seems that astrocytic activation is late by a few days compared to the microglial activation, peaking at D7 while D2 for microglia (Kim et al. 2007), but all these timecourse will depend on the marker which is studied.

In addition, Sun et al. 2017 showed that IL-17 is a key activator of astrocytes and that its expression is not increased at D3 but strongly increased at D7, when the number of astrocytes is also high. Interestingly, they mention this cytokine as possibly induced by microglial TLR2 activation.

Another study that goes in this direction is the work of Liddelow et al. 2017, showing that purified activated microglia is capable of inducing reactive astrocytes.

Faulkner and colleagues 2004 showed in the SCI that reactive astrocytes have a shielding role towards neurons and oligodendrocytes and that there was an increase in inflammation after the removal of reactive astrocytes.

Shinozaki et al. 2017 showed similar results using the traumatic brain injury (TBI) model: the brain version of the SCI. There also astrocytes had a protective role, creating a scar formation around the injury. Interestingly they showed that those astrocytes were activated by microglia via downregulation of astrocytic P2Y1 purinergic receptors.

The general hypothesis would be that activated microglia would make astrocytes react. Those activated astrocyte would by their cytokine secretions cause a microglial phenotypic switch toward an anti-inflammatory phenotype.

3. Immune cell infiltration

In the first article, we also looked for the contribution of infiltrating lymphocytes. From our work, it appeared that unless a breach of the BBB occurs, only few T-lymphocytes infiltrate the CNS. Thus, the neuroinflammation seemed to be caused mostly by the cells in place: glia.

Others arrived to the same conclusion we did. Kim et al. 2011 showed that there was no macrophage, neutrophils, dendritic cells, T lymphocytes or even B lymphocytes following partial sciatic nerve ligation neuropathic pain surgery. Austin and colleagues 2012 found only very few lymphocytes infiltrated in the dorsal or ventral horn after CCI: they could count 0 to 2 cells per part analyzed. Yet, some studies observed lymphocytes infiltrated in the dorsal horn ipsilateral to the nerve injury (Costigan et al. 2009, Cao and De Leo 2008). Echeverry et al. 2011 reported that monocyte chemo-attractant protein 1 (MCP-1) caused a transient permeabilization of the blood spinal cord barrier after nerve injury – the equivalent of the BBB for spinal cord. They also noted that TGF-β and IL-10 had the opposing effect. One could hypothesize that depending on the cytokine balance the blood spinal cord barrier is more or less permeable to immune cells. Still, what exactly allows infiltration remains unclear.

There is a possibility for macrophages to infiltrate the CNS after neuroinflammation. As resident macrophages and microglia do not express the CCR2 receptor, genetic labeling with CCR2-RFP transgenic mice can repertory only circulating macrophages. In SNI however, such labelling revealed only very few amount in spinal cord 7 days after SNI (Smith et al. 2018).

4. Electrophysiological properties of microglia

Electrophysiological modifications in microglia with currents induced by voltage step protocols have been shown in many models of microglial activation, whether be it inward, outward or even both.

After reviewing them (Table 4), the different types of currents measured seem not to be species-dependent: rats, mice, and even human microglia showed similar current patterns. The tissue of origin of microglia (brain or spinal cord) was also not a differentiating factor. The most important factors were the age of the organism and the type of microglial activator/trigger.

Resting currents pattern differs a lot between ages : embryo have low inward and intermediate outward currents, newborns have high inward low outward current, juveniles (20 days old for mice) have the same pattern as newborns, adults (8 weeks and more for mice) present low inward and low outward currents.

When activated with a specific trigger microglia often shows similar patterns: pathogen induced activation via LPS, PCW or HIV-TAT protein all show a strong increase of outward current, while the inward current is reduced compared to the resting state (De Simoni et al. 2008, Seifert 2011, Scheffel et al. 2012).

However, if microglia is activated by a tissue damaging procedure such as hypoxia (MCAO), Status epilepticus (SE), or stab wound, they exhibit strong inward currents, while keeping very low outward current (Lyons et al. 2000, Menteyneet al. 2009, Seifert 2011, Richter et al. 2014). I also observed this pattern after SNI in the second study.

Activation with interleukins often used to induce an alternative type of activation (IL-4, IL-10), ATP, or other chemicals gave unique patterns difficult to classify.

Microglia in slices tend to have an overall lower current both in resting state and in activated state than dissociated and freshly cultured microglia.

The resting membrane potential of microglia is comprised between -18 and -40 mV in resting state. Few studies investigated the RMP of their microglia before and after treatment, however they mostly observed a hyperpolarization of the microglial RMP after activation of around 20 mV. A surprising fact is that this happened whether the increased current was inward or outward and the RMP was rescued by blocking the increased current either way. (Inward Chung et al 1999, outward Chung et al. 1998, Blomster et al. 2016)

In my study, I observed similar RMP with a range between -18 and -24 mV in naive condition. Two days after SNI, microglia showed increased inward currents together with a hyperpolarized RMP. Using ML133, the inward current was fully blocked and the microglial RMP depolarized beyond its resting level.

The inward current of Kir2.1 is seen when hyperpolarized voltages of the step protocol are applied. It does not explain the change of the membrane potential since the entry of positive potassium ions would depolarize the membrane, not hyperpolarize it.

At physiological levels, the potentials, is more depolarized than the reversal potential of potassium, Kir2.1 channels will generate small outward currents. Those currents are difficult to detect unless subtracting the current remaining after blocking Kir2.1 from the total current and therefore revealing the Kir2.1 sensitive current (Figure 5 of second article). At even more depolarized potential, there is no increase of the outward current because of the intrinsic properties of Kir channels, which have a lower conductance at higher potential.

Once Kir2.1 was blockedwith ML133, this ion flux was stopped and more K^+ remained in the cell – causing the observed depolarization of the RMP.

In several studies, there is an increase of outward current and a hyperpolarization of the RMP measured in activated microglia (Chung et al. 1998-9, Blomster et al. 2016). This exit of K+ ions is causing a hyperpolarization of the RMP, as fewer cations remains in the cell. Pharmacological blockade of this efflux, led to a return to a more depolarized RMP.

Aside of barium and cesium, we used the most specific pharmacological blockers commercially available. However, a Kir2.1 specific inhibitor has not been discovered yet, so we used the Kir2.x family blocker ML133. Here is a table of the blockers we used and their target.

Blocker	Channel targeted	Effects	Source	Identifier	References
Barium Cesium	K+ channels	Block all potassium channels due to their larger size. When in extracellular solution it blocks inward potassium currents: stopping the ion flux by getting stuck in pores of potassium channels. When put in intracellular solution the outward current by the same mechanism. High concertation must be applied for a full block.	Sigma-Aldrich for both	342920 for barium 289329 for cesium	**Schlichter et al. 1996**
ML133 We used 50 µM	Kir2.1	Blocks the whole Kir2.x family from the intracellular side with high selectivity. ML133 blockade is not voltage dependant and gets more potent with lower pH. IC50 at pH 7.4: 1.8 µM for Kir2.1 7.7 µM for Kir6.2 2.9 µM for Kir2.2 32.9 µM for Kir7.1 4.0 µM for Kir2.3 76 µM for Kir4.1 2.8 µM for Kir2.6 more than 300 µM for Kir1.1	Sigma-Aldrich	SML0190	**Lam et al. 2015** **Wang et al. 2011**
TPA (tetrapentyl-ammonium) We used 50 µM	THIK-1	Blocks two-pore domain TWIK-related potassium channels from the intracellular side. No values were found for THIK-1 IC50, thus we used the same amount as Madry and al. 2018. From their results we could extrapolate it between 0.5 and 5 µM . For other channels members of this family - IC50: 0.3 µM for TRESK 10.5 µM for TREK-1 8.5 µM for TASK-3	Sigma-Aldrich	258962	**Madry et al. 2018** **Piechotta et al. 2011**
Apamin We used 100 nM	SK channels	Blocks selectively SK1, SK2, and SK3 channels. IC50: 27 pM for SK2 4 nM for SK3 704 pM and 196 nM for SK1 due to biphasic blockade	Alomone Labs	STA-200	**Khanna et al. 2001** **Grunnet et al. 2001**

Table 5: Pharmacological blockers used on microglial channels.

5. Impact of membrane potential on proliferation

In cancer cells, depolarizations or hyperpolarizations of the membrane potential of cells cause proliferation. Several Kir channels are involved in this. In addition, there is a high K^+ efflux during M phase of the cell cycle, hyperpolarizing the membrane (Yang and Brackenbury 2013).

Several study report that membrane hyperpolarization at the G1/S checkpoint is necessary for S phase initiation. For instance depolarizing the cell membrane stops G1/S progression in glia (Canady et al. 1990), Schwann cells (Wilson and Chiu 1993), Lymphocytes (Price et al. 1989) and several other cells.

Previously, Schlichter and colleagues 1996 reduced proliferation of CSF-1 cultivated microglia, Wether using the broad K^+ channel blocker barium or different chloride channel.

They show aswell a reduction of inward currents with the barium block. With chloride channel blockade, they stopped the inward Cl^- flux, which could depolarize the cell, as no Cl^- would diffuse in the cell anymore.

Considering outward currents, many studies using LPS for instance had impressive outward currents generated. Once determined as potassium current via broad blockers such as barium or cesium, few candidates were to be discriminated: Kv1.1, Kv1.2, Kv1.3, Kv1.5 and Kv1.6 (Kotecha and Schlichter 1999). Following the use of diverse potassium channel blocker, Menteyne et al. 2009 determined that the current was originating from Kv1.3 and Kv1.5.

Later, several studies managed to fully block their outward current with Agitoxin-2 or PAP1: both selective blocker of Kv1.3. This relayed Kv1.5 to less importance. Still the important point is that when the induced outward current was blocked with 4-AP, the RMP of microglia was depolarized to resting levels (Chung et al 1998).

With the studies on outward microglial current, I could extend my conclusion to any channel that would have a major impact in the current of activated microglia. Thus, the modulation of the RMP would be the key for the activity state of microglia: if the microglial RMP is hyperpolarized, the microglia is activated, if the RMP is depolarized, the microglia is quiescent. Any channel having an effect on controlling RMP could therefore be targeted to regulate microglial membrane potential and therefore reactivity.

In my second study, proliferation of microglia peaked at D2, at the same time as the change in RMP.

I used ML133 on BV2 cell line and managed to stop the proliferation of cells. With this proof of concept, we decided to inject ML133 intrathecally for a delivery in the spinal cord microglia. In order to gain time, we collaborated with the lab of Temugin Berta, our former colleagues now based in the USA for this in vivo experiment. Intrathecal injection of ML133 did lower the proliferation of microglia 2 days after SNI.

6. ML133 effect on neuropathic pain

Using in vivo model allowed us to evaluate effect on behavior and we could show that intrathecal injection of ML133 reduced mechanical static and dynamic allodynia following SNI. To our knowledge, there is only one previous published study on ML133 and pain (Shi and colleagues 2018). They also used the SNI model and could demonstrate that ML133 prevents dynamic but not static allodynia when injected before SNI with a dose-dependent effect for 5 days and reversed dynamic but not static allodynia in 2 days when given after SNI. However, their clained mechanism is different as they focused on neurons as the target for ML133. They saw no increase in total Kir2.1 protein in spinal cord, and no change in Kir2.1 current in neurons, but claim a colocalization of Kir2.1 with neuronal markers in the dorsal horn of the spinal cord. They used a dose slightly inferior to ours, which could explain the absence of effect on static allodynia.

Before intrathecally injecting an inhibitor of Kir2.x channel and knowing Kir channels could also be neuronal, we tested ML133 on few neurons with a multi electrode array (MEA) device. No intensive firing was triggered. This indicates that there are probably others channels regulating the RMP in neurons, or that another mechanism compensated the role on RMP of the blocked Kir2.x. Another explanation would be that the RMP of the cell is depolarized to a point that most of voltage gated sodium channels are inactivated. In this situation, no action potential could be triggered.

Shi and colleagues' theory is interesting: they mention that Kir2.1 regulates the activity of lamina 1 neurons of the dorsal horn of the spinal cord where the gating process takes place. Their goal is to increase activity of glycinergic inhibitory neurons.

All this data together, I could formulate the following conclusion: Kir2.1 is the main regulator of membrane potential in SNI activated microglia. Its blockade by ML133 reversed the SNI induced hyperpolarization of microglial RMP. ML133 also blocked BV2 microglial proliferation. It also reduced proliferation and mechanical hypersensibility when injected in SNI mice.

7. Limitations of this study

The antibodies we used for Kv1.3, Kv1.5 and Kir2.1 were specific according to our tests against each other with specific plasmid on HEK cells. However, the quality of staining on slices was poor due to a lot of background noise. This is why we stained freshly dissociated primary microglia. We cannot completely exclude the presence of other Kir2.x channels in spinal cord slices from our immunostaining

For this study, we used male mice only. As several studies have shown differences in microglial activation or drugs response between male and female (Sorge et al. 2015, Doyle et al. 2017, Chen et al. 2018, Villa et al 2018), Our conclusions do not apply to female unless we repeat the experiment in the other sex. Besides differential link between microglial reactivity and neuropathic pain between both sex, oestrogens were shown to be involved in the regulation of Kir2.1 by inhibiting it (Wu et al. 2016), emphasizing the need to be cautious not to transfer the result to female blindly.

The intrathecal injection is performed in the lumbar region, high concentration of intrathecal ML133 could result in blockade of the whole spinal cord Kir2.x channels. The behavioral effect might therefore not be driven by the inhibition of microglial proliferation but by other targets of ML133 in the spinal cord or in DRG cells. There is a reduction in microglial proliferation, but the direct causal link between this and the behavioral effect is not proven. We should then refine our experiments; this will be discussed in the perspectives.

The qPCR and the western blots have been performed on quarters of spinal cord. We expected a difference in channels expression due to SNI strong enough to be detectable in this tissue. Unfortunately, it was not the case. This could be explained by the fact that in a quarter of spinal cord, there is only around 10% of microglial cells, and the changes specific to microglia can have been diluted. Using FACS and specialized RNA extraction kits, we should reach for a purified microglia population for gene and protein profiling. This would give us a precise answer to the change of potassium channel expression in microglia.

8. Perspectives and applications

To have a more specific approach than by intrathecal injection of ML133, we should use specific knock out of Kir2.1 via viral vector (AAV). The virus would silence the Kir2.1 (*KCNJ2*) gene by fully or partially removing it through homologous recombination. We would need a virus that infects specifically the targeted cells – here microglia. With the AAV6 specific for microglia that has been engineered by Rosario et al. 2016 for instance. After few weeks of infection, no Kir2.1 protein should remain in the infected microglia and behavioral assay following SNI could be performed.

We could use transgenic mice with microglial specific knock out of Kir2.1, also by homologous recombination. The downsize compared to the virus is that it takes more time and that absence of Ki2.1 in microglia since birth might impede development. However once the lineage is available it might be more convenient than virus production.

To investigate the implication of the RMP as the final important factor and not Kir2.1 is the oher aspect of interest and could be achieved by using Designer Receptors Exclusively Activated by Designer Drugs (DREADDs). Those receptors allow the activation of a GPCR when activated by clozapine, a drug that can be taken orally with little side effects at low dose.

For expressing DREADDs specifically in microglia (as for the Kir2.1 KO), we would need double transgenic mice: floxed DREADDs (or floxed Kir2.1) transgenic mice crossed with CX3CR1-CRE transgenic mice. Then in the pups of this breeding, the CRE recombinase expressed in microglia due to the specific CX3CR1 promoter would interact with the floxed DREADDs (or take out the Kir2.1) and make it active.

Here we have the choice to use the activator DREADDs or the inhibitor DREADDs transgenic mice. Both DREADDS receptor type are interesting but they answer different questions.

9. Conclusion

We have highlighted several pro-inflammatory genes increased during the first timepoints that were reduced overtime, while anti-inflammatory cytokines were expressed later on.

Even in a neuropathic pain model such as the SNI, microglia does switch to an anti-inflammatory phenotype, although the process takes several weeks. I propose here a timeline of microglial activation to illustrate the situation after nerve injury (Figure 22).

Nevertheless, although microglia switches to an anti-inflammatory phenotype, neuroinflammation is only lowered and there is not a return to basal level. There is still a lot of work to do to understand what sustains this inflammation. Maybe the microglial switch takes much longer than its first apparition, maybe the inflammation soup installed in the intracellular space is much harder to resorb than we would expect, and even anti-inflammatory microglia struggle to stabilize the situation. Maybe also only a part of the microglia actually switches to anti-inflammatory as we could observe that while most pro-inflammatory genes were reduced, few reached their basal level again.

We could also suppose that anti-inflammatory microglia have only few effects on neurons. The damaged nerve cells would keep their ectopic firing and their release ATP and CSF-1 even after the microglial phenotypic switch. This could keep a part of the microglia in a pro-inflammatory state and reduce the efficacy of anti-inflammatory cytokines.

Concerning potassium channels and microglial activation, I was convinced that Kv1.3 would be the ideal candidate: specific to microglia, this channel elicited impressive outward potassium currents in numerous microglial activations.

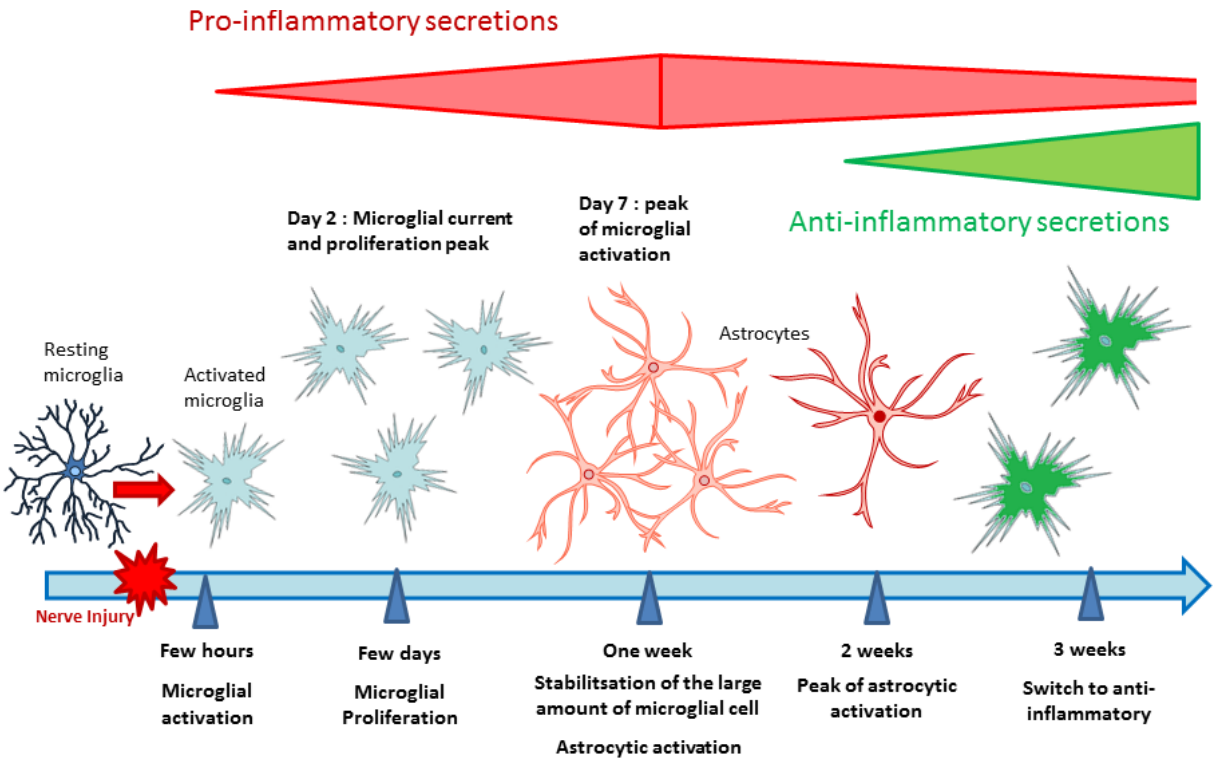

Figure 22: Proposed timeline of microglial activation after nerve injury. Once microglia is activated, it proliferates quickly in the first days and activates a serial of pro-inflammatory genes whose expression peaks after a week. Astrocytes also activate few days after microglia. Their activation peaks after 2 weeks. We observe a reduction of pro inflammatory gene expression after few weeks, but it seems not to stop completely. In addition, an anti-inflammatory gene expression is observed after 3 weeks.

Yet, it appeared that this channel is not involved in the SNI neuropathic pain model. Possibly because the reaction of microglia is different in neuropathic pain model from an acute inflammation via LPS injection for instance – where this channel would probably be the best track to investigate.

While studying our electrophysiology results, I noticed a remarkable change in the membrane potential of activated microglia, which reversed to a resting state value when the potassium current was blocked. The next objective would be to understand the function of microglial RMP ML133 has indeed a therapeutic potential, however might not be used systemically, nor at high concentration beacause of potential side effect on other Kir

channels. Targeting directly the RMP might be the answer and specifically in phase as postoperative period where a neuroinflammation transiently appears

I also show that we can modulate microglial reactivity through its RMP. Following my hypothesis: depolarizing microglia via the blockade of Kir2.1 channels, our colleagues managed to reduce the proliferation and the hypersensitivity of SNI animals. There is still more research to do on the subject but I believe I could provide the idea for a new therapeutic approach against neuropathic pain targeting microglial membrane potential.

References

Andreou KE, Soto MS, Allen D, Economopoulos V, de Bernardi A, Larkin JR, Sibson NR (2017) Anti-inflammatory Microglia/Macrophages As a Potential Therapeutic Target in Brain Metastasis. Frontiers in oncology 7: 251

Ansel JC, Brown JR, Payan DG, Brown MA (1993) Substance P selectively activates TNF-alpha gene expression in murine mast cells. Journal of immunology (Baltimore, Md : 1950) 150: 4478-85

Apkarian AV, Bushnell MC, Treede RD, Zubieta JK (2005) Human brain mechanisms of pain perception and regulation in health and disease. European journal of pain (London, England) 9: 463-84

Arnoux I, Hoshiko M, Sanz Diez A, Audinat E (2014) Paradoxical effects of minocycline in the developing mouse somatosensory cortex. Glia 62: 399-410

Attal N, Fermanian C, Fermanian J, Lanteri-Minet M, Alchaar H, Bouhassira D (2008) Neuropathic pain: are there distinct subtypes depending on the aetiology or anatomical lesion? Pain 138: 343-53

Austin PJ, Kim CF, Perera CJ, Moalem-Taylor G (2012) Regulatory T cells attenuate neuropathic pain following peripheral nerve injury and experimental autoimmune neuritis. Pain 153: 1916-31

Babbedge RC, Soper AJ, Gentry CT, Hood VC, Campbell EA, Urban L (1996) In vitro characterization of a peripheral afferent pathway of the rat after chronic sciatic nerve section. Journal of neurophysiology 76: 3169-77

Bachstetter AD, Morganti JM, Jernberg J, Schlunk A, Mitchell SH, Brewster KW, Hudson CE, Cole MJ, Harrison JK, Bickford PC, Gemma C (2011) Fractalkine and CX 3 CR1 regulate hippocampal neurogenesis in adult and aged rats. Neurobiology of aging 32: 2030-44

Baker M, Bostock H (1992) Ectopic activity in demyelinated spinal root axons of the rat. The Journal of physiology 451: 539-552

Banks WA (2009) Characteristics of compounds that cross the blood-brain barrier. BMC neurology 9 Suppl 1: S3-S3

Bannister K, Dickenson AH (2016) What do monoamines do in pain modulation? Current opinion in supportive and palliative care 10: 143-8

Basbaum AI, Bautista DM, Scherrer G, Julius D (2009) Cellular and molecular mechanisms of pain. Cell 139: 267-84

Baumann N, Pham-Dinh D (2001) Biology of oligodendrocyte and myelin in the mammalian central nervous system. Physiological reviews 81: 871-927

Beggs S, Salter MW (2007) Stereological and somatotopic analysis of the spinal microglial response to peripheral nerve injury. Brain, behavior, and immunity 21: 624-33

Benarroch EE (2011) Nitric oxide: A pleiotropic signal in the nervous system. Neurology 77: 1568-76

Blomster LV, Strobaek D, Hougaard C, Klein J, Pinborg LH, Mikkelsen JD, Christophersen P (2016) Quantification of the functional expression of the Ca2+ -activated K+ channel KCa 3.1 on microglia from adult human neocortical tissue. Glia 64: 2065-2078

Boucsein C, Zacharias R, Farber K, Pavlovic S, Hanisch UK, Kettenmann H (2003) Purinergic receptors on microglial cells: functional expression in acute brain slices and modulation of microglial activation in vitro. The European journal of neuroscience 17: 2267-76

Brain SD, Williams TJ (1989) Interactions between the tachykinins and calcitonin gene-related peptide lead to the modulation of oedema formation and blood flow in rat skin. British journal of pharmacology 97: 77-82

Burchiel KJ (1980) Abnormal impulse generation in focally demyelinated trigeminal roots. Journal of neurosurgery 53: 674-83

Cao L, DeLeo JA (2008) CNS-infiltrating CD4+ T lymphocytes contribute to murine spinal nerve transection-induced neuropathic pain. European journal of immunology 38: 448-58

Canady KS, Ali-Osman F, Rubel EW (1990) Extracellular potassium influences DNA and protein syntheses and glial fibrillary acidic protein expression in cultured glial cells. Glia 3: 368-74

Caterina MJ, Schumacher MA, Tominaga M, Rosen TA, Levine JD, Julius D (1997) The capsaicin receptor: a heat-activated ion channel in the pain pathway. Nature 389: 816-24

Chen Y, Willcockson HH, Valtschanoff JG (2009) Influence of the vanilloid receptor TRPV1 on the activation of spinal cord glia in mouse models of pain. Experimental neurology 220: 383-90

Chen YJ, Nguyen HM, Maezawa I, Grossinger EM, Garing AL, Kohler R, Jin LW, Wulff H (2015) The potassium channel KCa3.1 constitutes a pharmacological target for neuroinflammation associated with ischemia/reperfusion stroke. Journal of cerebral blood flow and metabolism : official journal of the International Society of Cerebral Blood Flow and Metabolism

Chessell IP, Hatcher JP, Bountra C, Michel AD, Hughes JP, Green P, Egerton J, Murfin M, Richardson J, Peck WL, Grahames CB, Casula MA, Yiangou Y, Birch R, Anand P, Buell GN (2005) Disruption of the P2X7 purinoceptor gene abolishes chronic inflammatory and neuropathic pain. Pain 114: 386-96

Cheung G, Kann O, Kohsaka S, Faerber K, Kettenmann H (2009) GABAergic activities enhance macrophage inflammatory protein-1alpha release from microglia (brain macrophages) in postnatal mouse brain. The Journal of physiology 587: 753-68

Chiu IM, von Hehn CA, Woolf CJ (2012) Neurogenic inflammation and the peripheral nervous system in host defense and immunopathology. Nature neuroscience 15: 1063-7

Chung S, Joe E, Soh H, Lee MY, Bang HW (1998) Delayed rectifier potassium currents induced in activated rat microglia set the resting membrane potential. Neuroscience letters 242: 73-6

Chung S, Jung W, Lee MY (1999) Inward and outward rectifying potassium currents set membrane potentials in activated rat microglia. Neuroscience letters 262: 121-4

Clark AK, Yip PK, Grist J, Gentry C, Staniland AA, Marchand F, Dehvari M, Wotherspoon G, Winter J, Ullah J, Bevan S, Malcangio M (2007) Inhibition of spinal microglial cathepsin S for the reversal of neuropathic pain. Proceedings of the National Academy of Sciences of the United States of America 104: 10655-60

Colloca L, Ludman T, Bouhassira D, Baron R, Dickenson AH, Yarnitsky D, Freeman R, Truini A, Attal N, Finnerup NB, Eccleston C, Kalso E, Bennett DL, Dworkin RH, Raja SN (2017) Neuropathic pain. Nature reviews Disease primers 3: 17002

Costigan M, Moss A, Latremoliere A, Johnston C, Verma-Gandhu M, Herbert TA, Barrett L, Brenner GJ, Vardeh D, Woolf CJ, Fitzgerald M (2009) T-cell infiltration and signaling in the adult dorsal spinal cord is a major contributor to neuropathic pain-like hypersensitivity. The Journal of neuroscience : the official journal of the Society for Neuroscience 29: 14415-22

Coull JA, Beggs S, Boudreau D, Boivin D, Tsuda M, Inoue K, Gravel C, Salter MW, De Koninck Y (2005) BDNF from microglia causes the shift in neuronal anion gradient underlying neuropathic pain. Nature 438: 1017-21

Cuadros MA, Navascues J (1998) The origin and differentiation of microglial cells during development. Progress in neurobiology 56: 173-89

Cui J, He W, Yi B, Zhao H, Lu K, Ruan H, Ma D (2014) mTOR pathway is involved in ADP-evoked astrocyte activation and ATP release in the spinal dorsal horn in a rat neuropathic pain model. Neuroscience 275: 395-403

Dallenbach KM (1939) Pain: History and present status. American Journal of Psychology 52:331–347. doi:10.2307/1416740.

De Simoni A, Allen NJ, Attwell D (2008) Charge compensation for NADPH oxidase activity in microglia in rat brain slices does not involve a proton current. The European journal of neuroscience 28: 1146-56

Chen G, Luo X, Qadri MY, Berta T, Ji RR (2018) Sex-Dependent Glial Signaling in Pathological Pain: Distinct Roles of Spinal Microglia and Astrocytes. Neuroscience bulletin 34: 98-108

Decosterd I, Woolf CJ (2000) Spared nerve injury: an animal model of persistent peripheral neuropathic pain. Pain 87: 149-58

Deftu AF, Ristoiu V, Suter MR (2018) Intrathecal Administration of CXCL1 Enhances Potassium Currents in Microglial Cells. Pharmacology 101: 262-268

Del Puerto A, Wandosell F, Garrido JJ (2013) Neuronal and glial purinergic receptors functions in neuron development and brain disease. Frontiers in cellular neuroscience 7

Descartes R (1644) Treatise of Man

Deumens R, Bozkurt A, Meek MF, Marcus MA, Joosten EA, Weis J, Brook GA (2010) Repairing injured peripheral nerves: Bridging the gap. Progress in neurobiology 92: 245-76

Devor M (2013) Neuropathic pain: pathophysiological response of nerves to injury. Chapter 61. In: S.L. McMahon, M. Koltzenburg, I. Tracey and D.C. Turk (Eds.), Wall and Melzack's Textbook of Pain, 6th edition, Churchill Livingstone, London, pp861-888.

Di Lucente J, Nguyen HM, Wulff H, Jin LW, Maezawa I (2018) The voltage-gated potassium channel Kv1.3 is required for microglial pro-inflammatory activation in vivo. Glia

Dominguez E, Rivat C, Pommier B, Mauborgne A, Pohl M (2008) JAK/STAT3 pathway is activated in spinal cord microglia after peripheral nerve injury and contributes to neuropathic pain development in rat. Journal of neurochemistry 107: 50-60

Doyle HH, Eidson LN, Sinkiewicz DM, Murphy AZ (2017) Sex Differences in Microglia Activity within the Periaqueductal Gray of the Rat: A Potential Mechanism Driving the Dimorphic Effects of Morphine. The Journal of neuroscience : the official journal of the Society for Neuroscience

Dries E (2010) Minocycline-conditioning brings surveying and reactive microglial cells to an alerted state according to their potassium channel profile hdl.handle.net/1942/12566

Dubin AE, Patapoutian A (2010) Nociceptors: the sensors of the pain pathway. The Journal of clinical investigation 120: 3760-3772

Echeverry S, Shi XQ, Rivest S, Zhang J (2011) Peripheral nerve injury alters blood-spinal cord barrier functional and molecular integrity through a selective inflammatory pathway. The Journal of neuroscience : the official journal of the Society for Neuroscience 31: 10819-28

Eder C, Fischer HG, Hadding U, Heinemann U (1995) Properties of voltage-gated currents of microglia developed using macrophage colony-stimulating factor. Pflugers Archiv : European journal of physiology 430: 526-33

Ferreira AC, Sousa N, Bessa JM, Sousa JC, Marques F (2018) Metabolism and adult neurogenesis: Towards an understanding of the role of lipocalin-2 and iron-related oxidative stress. Neuroscience and biobehavioral reviews 95: 73-84

Ferreira R, Lively S, Schlichter LC (2014) IL-4 type 1 receptor signaling up-regulates KCNN4 expression, and increases the KCa3.1 current and its contribution to migration of alternative-activated microglia. Frontiers in cellular neuroscience 8: 183

Finnerup NB, Haroutounian S, Kamerman P, Baron R, Bennett DL, Bouhassira D, Cruccu G, Freeman R, Hansson P, Nurmikko T, Raja SN, Rice AS, Serra J, Smith BH, Treede RD, Jensen TS (2016) Neuropathic pain: an updated grading system for research and clinical practice. Pain 157: 1599-606

Fordyce CB, Jagasia R, Zhu X, Schlichter LC (2005) Microglia Kv1.3 channels contribute to their ability to kill neurons. The Journal of neuroscience : the official journal of the Society for Neuroscience 25: 7139-49

Fried K, Govrin-Lippmann R, Rosenthal F, Ellisman MH, Devor M (1991) Ultrastructure of afferent axon endings in a neuroma. Journal of neurocytology 20: 682-701

Fumagalli M, Lecca D, Abbracchio MP (2011) Role of purinergic signalling in neuro-immune cells and adult neural progenitors. Frontiers in bioscience (Landmark edition) 16: 2326-41

Gattlen C, Clarke CB, Piller N, Kirschmann G, Pertin M, Decosterd I, Gosselin RD, Suter MR (2016) Spinal Cord T-Cell Infiltration in the Rat Spared Nerve Injury Model: A Time Course Study. International journal of molecular sciences 17: 352

Gemes G, Koopmeiners A, Rigaud M, Lirk P, Sapunar D, Bangaru ML, Vilceanu D, Garrison SR, Ljubkovic M, Mueller SJ, Stucky CL, Hogan QH (2013) Failure of action potential propagation in sensory neurons: mechanisms and loss of afferent filtering in C-type units after painful nerve injury. The Journal of physiology 591: 1111-1131

Ginhoux F, Greter M, Leboeuf M, Nandi S, See P, Gokhan S, Mehler MF, Conway SJ, Ng LG, Stanley ER, Samokhvalov IM, Merad M (2010) Fate mapping analysis reveals that adult microglia derive from primitive macrophages. Science (New York, NY) 330: 841-5

Gold MS, Gebhart GF (2010) Nociceptor sensitization in pain pathogenesis. Nature medicine 16: 1248-57

Gold MS, Shuster MJ, Levine JD (1996) Characterization of six voltage-gated K+ currents in adult rat sensory neurons. Journal of neurophysiology 75: 2629-46

Gottschalk A, Smith DS (2001) New concepts in acute pain therapy: preemptive analgesia. American family physician 63: 1979-84

Gould E (2007) How widespread is adult neurogenesis in mammals? Nature reviews Neuroscience 8: 481-8

Govrin-Lippmann R, Devor M (1978) Ongoing activity in severed nerves: source and variation with time. Brain research 159: 406-10

Graeber MB, Streit WJ (2010) Microglia: biology and pathology. Acta neuropathologica 119: 89-105

Griffin RS, Costigan M, Brenner GJ, Ma CH, Scholz J, Moss A, Allchorne AJ, Stahl GL, Woolf CJ (2007) Complement induction in spinal cord microglia results in anaphylatoxin C5a-mediated pain hypersensitivity. The Journal of neuroscience : the official journal of the Society for Neuroscience 27: 8699-708

Gu N, Eyo UB, Murugan M, Peng J, Matta S, Dong H, Wu LJ (2016) Microglial P2Y12 receptors regulate microglial activation and surveillance during neuropathic pain. Brain, behavior, and immunity 55: 82-92

Guan Z, Kuhn JA, Wang X, Colquitt B, Solorzano C, Vaman S, Guan AK, Evans-Reinsch Z, Braz J, Devor M, Abboud-Werner SL, Lanier LL, Lomvardas S, Basbaum AI (2016) Injured sensory neuron-derived CSF1 induces microglial proliferation and DAP12-dependent pain. Nature neuroscience 19: 94-101

Guasti L, Richardson D, Jhaveri M, Eldeeb K, Barrett D, Elphick MR, Alexander SP, Kendall D, Michael GJ, Chapman V (2009) Minocycline treatment inhibits microglial activation and alters spinal levels of endocannabinoids in a rat model of neuropathic pain. Molecular pain 5: 35

Grunnet M, Jensen BS, Olesen SP, Klaerke DA (2001) Apamin interacts with all subtypes of cloned small-conductance Ca2+-activated K+ channels. Pflugers Archiv : European journal of physiology 441: 544-50

Harriott AM, Gold MS (2009) Contribution of primary afferent channels to neuropathic pain. Current pain and headache reports 13: 197-207

Hertz L, Zielke HR (2004) Astrocytic control of glutamatergic activity: astrocytes as stars of the show. Trends in neurosciences 27: 735-43

Hildebrand ME, Xu J, Dedek A, Li Y, Sengar AS, Beggs S, Lombroso PJ, Salter MW (2016) Potentiation of Synaptic GluN2B NMDAR Currents by Fyn Kinase Is Gated through BDNF-Mediated Disinhibition in Spinal Pain Processing. Cell reports 17: 2753-2765

Hu B, Xu G, Zhang X, Xu L, Zhou H, Ma Z, Shen X, Zhu J, Shen R (2018) Paeoniflorin Attenuates Inflammatory Pain by Inhibiting Microglial Activation and Akt-NF-kappaB Signaling in the Central Nervous System. Cellular physiology and biochemistry : international journal of experimental cellular physiology, biochemistry, and pharmacology 47: 842-850

Hu P, Bembrick AL, Keay KA, McLachlan EM (2007) Immune cell involvement in dorsal root ganglia and spinal cord after chronic constriction or transection of the rat sciatic nerve. Brain, behavior, and immunity 21: 599-616

Huxtable AG, Smith SM, Vinit S, Watters JJ, Mitchell GS (2013) Systemic LPS induces spinal inflammatory gene expression and impairs phrenic long-term facilitation following acute intermittent hypoxia. Journal of applied physiology (Bethesda, Md : 1985) 114: 879-87

Ilschner S, Ohlemeyer C, Gimpl G, Kettenmann H (1995) Modulation of potassium currents in cultured murine microglial cells by receptor activation and intracellular pathways. Neuroscience 66: 983-1000

Inoue K, Tsuda M (2018) Microglia in neuropathic pain: cellular and molecular mechanisms and therapeutic potential. Nature reviews Neuroscience 19: 138-152

International Association for the Study of Pain (IASP)

Kajander KC, Bennett GJ (1992) Onset of a painful peripheral neuropathy in rat: a partial and differential deafferentation and spontaneous discharge in A beta and A delta primary afferent neurons. Journal of neurophysiology 68: 734-44

Karperien A, Ahammer H, Jelinek HF (2013) Quantitating the subtleties of microglial morphology with fractal analysis. Frontiers in cellular neuroscience 7: 3

Kawasaki Y, Zhang L, Cheng JK, Ji RR (2008) Cytokine mechanisms of central sensitization: distinct and overlapping role of interleukin-1beta, interleukin-6, and tumor necrosis factor-alpha in regulating synaptic and neuronal activity in the superficial spinal cord. The Journal of neuroscience : the official journal of the Society for Neuroscience 28: 5189-94

Kettenmann H, Hanisch UK, Noda M, Verkhratsky A (2011) Physiology of microglia. Physiological reviews 91: 461-553

Kettenmann H, Hoppe D, Gottmann K, Banati R, Kreutzberg G (1990) Cultured microglial cells have a distinct pattern of membrane channels different from peritoneal macrophages. Journal of neuroscience research 26: 278-287

Khakh BS, North RA (2012) Neuromodulation by extracellular ATP and P2X receptors in the CNS. Neuron 76: 51-69

Khanna R, Roy L, Zhu X, Schlichter LC (2001) K+ channels and the microglial respiratory burst Am J Physiol Cell Physiol 280: C796–C806, 2001.

Kim CF, Moalem-Taylor G (2011) Detailed characterization of neuro-immune responses following neuropathic injury in mice. Brain research 1405: 95-108

Kim D, Kim MA, Cho IH, Kim MS, Lee S, Jo EK, Choi SY, Park K, Kim JS, Akira S, Na HS, Oh SB, Lee SJ (2007) A critical role of toll-like receptor 2 in nerve injury-induced spinal cord glial cell activation and pain hypersensitivity. The Journal of biological chemistry 282: 14975-83

Kobayashi K, Yamanaka H, Fukuoka T, Dai Y, Obata K, Noguchi K (2008) P2Y12 receptor upregulation in activated microglia is a gateway of p38 signaling and neuropathic pain. The Journal of neuroscience : the official journal of the Society for Neuroscience 28: 2892-902

Kokoeva MV, Yin H, Flier JS (2007) Evidence for constitutive neural cell proliferation in the adult murine hypothalamus. The Journal of comparative neurology 505: 209-20

Komm B, Beyreis M, Kittl M, Jakab M, Ritter M, Kerschbaum HH (2014) Glycine modulates membrane potential, cell volume, and phagocytosis in murine microglia. Amino acids 46: 1907-17

Konno M, Shirakawa H, Iida S, Sakimoto S, Matsutani I, Miyake T, Kageyama K, Nakagawa T, Shibasaki K, Kaneko S (2012) Stimulation of transient receptor potential vanilloid 4 channel suppresses abnormal activation of microglia induced by lipopolysaccharide. Glia 60: 761-70

Kotecha SA, Schlichter LC (1999) a kv1.5 to kv1.3 switch in endogenous hippocampal microglia, The Journal of Neuroscience, 9(24):10680–10693

Lam D, Lively S, Schlichter LC (2017) Responses of rat and mouse primary microglia to pro- and anti-inflammatory stimuli: molecular profiles, K(+) channels and migration. Journal of neuroinflammation 14: 166

Lam D, Schlichter LC (2015) Expression and contributions of the Kir2.1 inward-rectifier K(+) channel to proliferation, migration and chemotaxis of microglia in unstimulated and anti-inflammatory states. Frontiers in cellular neuroscience 9: 185

Levy D, Zochodne DW (2000) Increased mRNA expression of the B1 and B2 bradykinin receptors and antinociceptive effects of their antagonists in an animal model of neuropathic pain. Pain 86: 265-71

Li K, Tan YH, Light AR, Fu KY (2013) Different peripheral tissue injury induces differential phenotypic changes of spinal activated microglia. Clinical & developmental immunology 2013: 901420

Li Y, Du XF, Du JL (2013) Resting microglia respond to and regulate neuronal activity in vivo. Communicative & integrative biology 6: e24493

Liddelow SA, Guttenplan KA, Clarke LE, Bennett FC, Bohlen CJ, Schirmer L, Bennett ML, Münch AE, Chung W-S, Peterson TC, Wilton DK, Frouin A, Napier BA, Panicker N, Kumar M, Buckwalter MS, Rowitch DH, Dawson VL, Dawson TM, Stevens B et al. (2017) Neurotoxic reactive astrocytes are induced by activated microglia. Nature 541: 481-487

Linton S (2005) Models of Pain Perception. Elsevier Health, 2005. Print.

Liu CN, Wall PD, Ben-Dor E, Michaelis M, Amir R, Devor M (2000) Tactile allodynia in the absence of C-fiber activation: altered firing properties of DRG neurons following spinal nerve injury. Pain 85: 503-21

Liu J, Xu P, Collins C, Liu H, Zhang J, Keblesh JP, Xiong H (2013) HIV-1 Tat protein increases microglial outward K(+) current and resultant neurotoxic activity. PloS one 8: e64904

Lopez-Alvarez VM, Puigdomenech M, Navarro X, Cobianchi S (2018) Monoaminergic descending pathways contribute to modulation of neuropathic pain by increasing-intensity treadmill exercise after peripheral nerve injury. Experimental neurology 299: 42-55

Lyons SA, Pastor A, Ohlemeyer C, Kann O, Wiegand F, Prass K, Knapp F, Kettenmann H, Dirnagl U (2000) Distinct physiologic properties of microglia and blood-borne cells in rat brain slices after permanent middle cerebral artery occlusion. Journal of cerebral blood flow and metabolism : official journal of the International Society of Cerebral Blood Flow and Metabolism 20: 1537-49

Ma C, LaMotte RH (2007) Multiple sites for generation of ectopic spontaneous activity in neurons of the chronically compressed dorsal root ganglion. The Journal of neuroscience : the official journal of the Society for Neuroscience 27: 14059-68

Madry C, Kyrargyri V, Arancibia-Carcamo IL, Jolivet R, Kohsaka S, Bryan RM, Attwell D (2018) Microglial Ramification, Surveillance, and Interleukin-1beta Release Are Regulated by the Two-Pore Domain K(+) Channel THIK-1. Neuron 97: 299-312

Magistretti PJ, Allaman I (2018) Lactate in the brain: from metabolic end-product to signalling molecule. Nature Reviews Neuroscience 19: 235

Meldrum M (2011) A History of Pain Management. Opioids: Past, Present and Future. Journal of the American Medical Association.

Melzack R, Bromage PR (1973) Experimental phantom limbs. Experimental neurology 39: 261-9

Melzack R, Wall PD (1965) Pain mechanisms: a new theory. Science (New York, NY) 150: 971-9

Mendell LM (2014) Constructing and deconstructing the gate theory of pain. Pain 155: 210-6

Menteyne A, Levavasseur F, Audinat E, Avignone E (2009) Predominant functional expression of Kv1.3 by activated microglia of the hippocampus after Status epilepticus. PloS one 4

Mergenthaler P, Lindauer U, Dienel GA, Meisel A (2013) Sugar for the brain: the role of glucose in physiological and pathological brain function. Trends in neurosciences 36: 587-597

Mikami N, Matsushita H, Kato T, Kawasaki R, Sawazaki T, Kishimoto T, Ogitani Y, Watanabe K, Miyagi Y, Sueda K, Fukada S, Yamamoto H, Tsujikawa K (2011) Calcitonin gene-related peptide is an important

regulator of cutaneous immunity: effect on dendritic cell and T cell functions. Journal of immunology (Baltimore, Md : 1950) 186: 6886-93

Mizumura K, Sugiura T, Katanosaka K, Banik RK, Kozaki Y (2009) Excitation and sensitization of nociceptors by bradykinin: what do we know? Experimental brain research 196: 53-65

Moussaud S, Lamodière E, Savage C, Draheim HJ (2009) Characterization of K+ current in microglia cell line, Cell Physiol Biochem 2009;24:141-152

Muessel MJ, Harry GJ, Armstrong DL, Storey NM (2013) SDF-1alpha and LPA modulate microglia potassium channels through rho gtpases to regulate cell morphology. Glia 61: 1620-8

Nagel MA, Gilden DH (2007) The protean neurologic manifestations of varicella-zoster virus infection. Cleveland Clinic journal of medicine 74: 489-94, 496, 498-9

Navratilova E, Atcherley CW, Porreca F (2015) Brain Circuits Encoding Reward from Pain Relief. Trends in neurosciences 38: 741-750

Nedelec B, Hou Q, Sohbi I, Choiniere M, Beauregard G, Dykes RW (2005) Sensory perception and neuroanatomical structures in normal and grafted skin of burn survivors. Burns : journal of the International Society for Burn Injuries 31: 817-30

Nguyen HM, Blomster LV, Christophersen P, Wulff H (2017) Potassium channel expression and function in microglia: Plasticity and possible species variations. Channels (Austin, Tex) 11: 305-315

Nguyen HM, Grossinger EM, Horiuchi M, Davis KW, Jin LW, Maezawa I, Wulff H (2017) Differential Kv1.3, KCa3.1, and Kir2.1 expression in "classically" and "alternatively" activated microglia. Glia 65: 106-121

Nimmerjahn A, Kirchhoff F, Helmchen F (2005) Resting microglial cells are highly dynamic surveillants of brain parenchyma in vivo. Science (New York, NY) 308: 1314-8

Nörenberg W, Gebicke-Haerter PJ, Illes P (1994) Voltage-dependent potassium channels in activated rat microglia. The Journal of physiology 475: 15-32

Obermeier B, Daneman R, Ransohoff RM (2013) Development, maintenance and disruption of the blood-brain barrier. Nature medicine 19: 1584-1596

Okun E, Griffioen KJ, Mattson MP (2011) Toll-like receptor signaling in neural plasticity and disease. Trends in neurosciences 34: 269-81

Panatier A, Robitaille R (2012) The soothing touch: microglial contact influences neuronal excitability. Developmental cell 23: 1125-6

Pannasch U, Farber K, Nolte C, Blonski M, Yan Chiu S, Messing A, Kettenmann H (2006) The potassium channels Kv1.5 and Kv1.3 modulate distinct functions of microglia. Molecular and cellular neurosciences 33: 401-11

Paolicelli RC, Bolasco G, Pagani F, Maggi L, Scianni M, Panzanelli P, Giustetto M, Ferreira TA, Guiducci E, Dumas L, Ragozzino D, Gross CT (2011) Synaptic pruning by microglia is necessary for normal brain development. Science (New York, NY) 333: 1456-8

Parkhurst CN, Yang G, Ninan I, Savas JN, Yates JR, 3rd, Lafaille JJ, Hempstead BL, Littman DR, Gan WB (2013) Microglia promote learning-dependent synapse formation through brain-derived neurotrophic factor. Cell 155: 1596-609

Penas C, Navarro X (2018) Epigenetic Modifications Associated to Neuroinflammation and Neuropathic Pain After Neural Trauma. Frontiers in cellular neuroscience 12: 158

Peng Y, Lu K, Li Z, Zhao Y, Wang Y, Hu B, Xu P, Shi X, Zhou B, Pennington M, Chandy KG, Tang Y (2014) Blockade of Kv1.3 channels ameliorates radiation-induced brain injury. Neuro-oncology 16: 528-39

Pfrieger FW, Barres BA (1995) What the fly's glia tell the fly's brain. Cell 83: 671-4

Piechotta PL, Rapedius M, Stansfeld PJ, Bollepalli MK, Ehrlich G, Andres-Enguix I, Fritzenschaft H, Decher N, Sansom MS, Tucker SJ, Baukrowitz T (2011) The pore structure and gating mechanism of K2P channels. The EMBO journal 30: 3607-19

Price M, Lee SC, Deutsch C (1989) Charybdotoxin inhibits proliferation and interleukin 2 production in human peripheral blood lymphocytes. Proceedings of the National Academy of Sciences of the United States of America 86: 10171-5

Pogatzki-Zahn E, Segelcke D, Zahn P (2018) Mechanisms of acute and chronic pain after surgery: update from findings in experimental animal models. Current opinion in anaesthesiology 31: 575-585

Prinz M, Kann O, Draheim HJ, Schumann RR, Kettenmann H, Weber JR, Hanisch U-K (1999) Microglial Activation by Components of Gram-Positive and -Negative Bacteria: Distinct and Common Routes to the Induction of Ion Channels and Cytokines. Journal of Neuropathology & Experimental Neurology 58: 1078-1089

Richler E, Chaumont S, Shigetomi E, Sagasti A, Khakh BS (2008) Tracking transmitter-gated P2X cation channel activation in vitro and in vivo. Nature methods 5: 87-93

Richter N, Wendt S, Georgieva PB, Hambardzumyan D, Nolte C, Kettenmann H (2014) Glioma-associated microglia and macrophages/monocytes display distinct electrophysiological properties and do not communicate via gap junctions. Neuroscience letters 583: 130-5

Rivera C, Li H, Thomas-Crusells J, Lahtinen H, Viitanen T, Nanobashvili A, Kokaia Z, Airaksinen MS, Voipio J, Kaila K, Saarma M (2002) BDNF-induced TrkB activation down-regulates the K+-Cl- cotransporter KCC2 and impairs neuronal Cl- extrusion. The Journal of cell biology 159: 747-752

Rogers JT, Morganti JM, Bachstetter AD, Hudson CE, Peters MM, Grimmig BA, Weeber EJ, Bickford PC, Gemma C (2011) CX3CR1 deficiency leads to impairment of hippocampal cognitive function and synaptic plasticity. The Journal of neuroscience : the official journal of the Society for Neuroscience 31: 16241-50

Rosario AM, Cruz PE, Ceballos-Diaz C, Strickland MR, Siemienski Z, Pardo M, Schob K-L, Li A, Aslanidi GV, Srivastava A, Golde TE, Chakrabarty P (2016) Microglia-specific targeting by novel capsid-modified AAV6 vectors. Molecular therapy Methods & clinical development 3: 16026-16026

Salter MW, Beggs S (2014) Sublime microglia: expanding roles for the guardians of the CNS. Cell 158: 15-24

Salter MW, Stevens B (2017) Microglia emerge as central players in brain disease. Nature medicine 23: 1018-1027

Samuels SE, Lipitz JB, Dahl G, Muller KJ (2010) Neuroglial ATP release through innexin channels controls microglial cell movement to a nerve injury. The Journal of general physiology 136: 425-42

Saria A (1984) Substance P in sensory nerve fibres contributes to the development of oedema in the rat hind paw after thermal injury. British journal of pharmacology 82: 217-222

Schafer DP, Lehrman EK, Kautzman AG, Koyama R, Mardinly AR, Yamasaki R, Ransohoff RM, Greenberg ME, Barres BA, Stevens B (2012) Microglia sculpt postnatal neural circuits in an activity and complement-dependent manner. Neuron 74: 691-705

Scheffel J, Regen T, Van Rossum D, Seifert S, Ribes S, Nau R, Parsa R, Harris RA, Boddeke HW, Chuang HN, Pukrop T, Wessels JT, Jurgens T, Merkler D, Bruck W, Schnaars M, Simons M, Kettenmann H, Hanisch UK (2012) Toll-like receptor activation reveals developmental reorganization and unmasks responder subsets of microglia. Glia 60: 1930-43

Schilling T, Eder C (2015) Microglial K(+) Channel Expression in Young Adult and Aged Mice. Glia 63: 664-672

Schilling T, Lehmann F, Ruckert B, Eder C (2004) Physiological mechanisms of lysophosphatidylcholine-induced de-ramification of murine microglia. The Journal of physiology 557: 105-20

Schilling T, Quandt FN, Cherny VV, Zhou W, Heinemann U, Decoursey TE, Eder C (2000) Upregulation of Kv1.3 K(+) channels in microglia deactivated by TGF-beta. American journal of physiology Cell physiology 279: C1123-34

Schlichter LC, Sakellaropoulos G, Ballyk B, Pennefeather PS, Phipps DJ (1996) Properties of K+ and Cl- channels and their involvement in proliferation of rat microglia GLIA 17:225-236

Scholz J, Broom DC, Youn DH, Mills CD, Kohno T, Suter MR, Moore KA, Decosterd I, Coggeshall RE, Woolf CJ (2005) Blocking caspase activity prevents transsynaptic neuronal apoptosis and the loss of inhibition in lamina II of the dorsal horn after peripheral nerve injury. The Journal of neuroscience : the official journal of the Society for Neuroscience 25: 7317-23

Seifert S (2011) Electrophysiological properties and intracellular calcium recordings of microglial cells from the adult brain, d-nb.info

Seybold VS (2009) The role of peptides in central sensitization. Handbook of experimental pharmacology: 451-91

Shi Y, Chen Y, Wang Y (2018) Kir2.1 Channel Regulation of Glycinergic Transmission Selectively Contributes to Dynamic Mechanical Allodynia in a Mouse Model of Spared Nerve Injury. Neuroscience bulletin

Shinozaki Y, Shibata K, Yoshida K, Shigetomi E, Gachet C, Ikenaka K, Tanaka KF, Koizumi S (2017) Transformation of Astrocytes to a Neuroprotective Phenotype by Microglia via P2Y₁ Receptor Downregulation. Cell reports 19: 1151-1164

Smith BM, Whang J, Seenauth A, Scholz J (2018) Microglial signalling in the dorsal horn of the spinal cord after spared nerve injury, 17th world congress on pain IASP, PTS184

Sorge RE, Mapplebeck JC, Rosen S, Beggs S, Taves S, Alexander JK, Martin LJ, Austin JS, Sotocinal SG, Chen D, Yang M, Shi XQ, Huang H, Pillon NJ, Bilan PJ, Tu Y, Klip A, Ji RR, Zhang J, Salter MW et al. (2015) Different immune cells mediate mechanical pain hypersensitivity in male and female mice. Nature neuroscience 18: 1081-3

Sun C, Zhang J, Chen L, Liu T, Xu G, Li C, Yuan W, Xu H, Su Z (2017) IL-17 contributed to the neuropathic pain following peripheral nerve injury by promoting astrocyte proliferation and secretion of proinflammatory cytokines. Molecular medicine reports 15: 89-96

Suter MR, Berta T, Gao YJ, Decosterd I, Ji RR (2009) Large A-fiber activity is required for microglial proliferation and p38 MAPK activation in the spinal cord: different effects of resiniferatoxin and bupivacaine on spinal microglial changes after spared nerve injury. Molecular pain 5: 53

Svensson CI, Marsala M, Westerlund A, Calcutt NA, Campana WM, Freshwater JD, Catalano R, Feng Y, Protter AA, Scott B, Yaksh TL (2003) Activation of p38 mitogen-activated protein kinase in spinal microglia is a critical link in inflammation-induced spinal pain processing. Journal of neurochemistry 86: 1534-44

Talbot S, Dias JP, Lahjouji K, Bogo MR, Campos MM, Gaudreau P, Couture R (2012) Activation of TRPV1 by capsaicin induces functional kinin B(1) receptor in rat spinal cord microglia. Journal of neuroinflammation 9: 16

Tan YH, Li K, Chen XY, Cao Y, Light AR, Fu KY (2012) Activation of Src family kinases in spinal microglia contributes to formalin-induced persistent pain state through p38 pathway. The journal of pain : official journal of the American Pain Society 13: 1008-15

Taves S, Berta T, Liu DL, Gan S, Chen G, Kim YH, Van de Ven T, Laufer S, Ji RR (2016) Spinal inhibition of p38 MAP kinase reduces inflammatory and neuropathic pain in male but not female mice: Sex-dependent microglial signaling in the spinal cord. Brain, behavior, and immunity 55: 70-81

Taylor KS, Anastakis DJ, Davis KD (2010) Chronic pain and sensorimotor deficits following peripheral nerve injury. Pain 151: 582-91

Tominaga M, Caterina MJ (2004) Thermosensation and pain. Journal of neurobiology 61: 3-12

Tozaki-Saitoh H, Tsuda M, Miyata H, Ueda K, Kohsaka S, Inoue K (2008) P2Y12 receptors in spinal microglia are required for neuropathic pain after peripheral nerve injury. The Journal of neuroscience : the official journal of the Society for Neuroscience 28: 4949-56

Tremblay ME, Lowery RL, Majewska AK (2010) Microglial interactions with synapses are modulated by visual experience. PLoS biology 8: e1000527

Tsai KL, Chang HF, Wu SN (2013) The inhibition of inwardly rectifying K+ channels by memantine in macrophages and microglial cells. Cellular physiology and biochemistry : international journal of experimental cellular physiology, biochemistry, and pharmacology 31: 938-51

Tsuda M, Shigemoto-Mogami Y, Koizumi S, Mizokoshi A, Kohsaka S, Salter MW, Inoue K (2003) P2X4 receptors induced in spinal microglia gate tactile allodynia after nerve injury. Nature 424: 778-83

Villa A, Gelosa P, Castiglioni L, Cimino M, Rizzi N, Pepe G, Lolli F, Marcello E, Sironi L, Vegeto E, Maggi A (2018) Sex-Specific Features of Microglia from Adult Mice. Cell reports 23: 3501-3511

Visentin S, Renzi M, Levi G (2001) Altered outward-rectifying K(+) current reveals microglial activation induced by HIV-1 Tat protein. Glia 33: 181-90

Wake H, Moorhouse AJ, Jinno S, Kohsaka S, Nabekura J (2009) Resting microglia directly monitor the functional state of synapses in vivo and determine the fate of ischemic terminals. The Journal of neuroscience : the official journal of the Society for Neuroscience 29: 3974-80

Wall PD, Devor M (1983) Sensory afferent impulses originate from dorsal root ganglia as well as from the periphery in normal and nerve injured rats. Pain 17: 321-39

Wall PD, Gutnick M (1974) Ongoing activity in peripheral nerves: the physiology and pharmacology of impulses originating from a neuroma. Experimental neurology 43: 580-93

Wallace VC, Cottrell DF, Brophy PJ, Fleetwood-Walker SM (2003) Focal lysolecithin-induced demyelination of peripheral afferents results in neuropathic pain behavior that is attenuated by cannabinoids. The Journal of neuroscience : the official journal of the Society for Neuroscience 23: 3221-33

Wei F, Guo W, Zou S, Ren K, Dubner R (2008) Supraspinal glial-neuronal interactions contribute to descending pain facilitation. The Journal of neuroscience : the official journal of the Society for Neuroscience 28: 10482-95

Wilson GF, Chiu SY (1993) Mitogenic factors regulate ion channels in Schwann cells cultured from newborn rat sciatic nerve. The Journal of physiology 470: 501-20

Woolf CJ (2007) Central sensitization: uncovering the relation between pain and plasticity. Anesthesiology 106: 864-7

Woolf CJ, Ma Q (2007) Nociceptors--noxious stimulus detectors. Neuron 55: 353-64

Wu SY, Chen YW, Tsai SF, Wu SN, Shih YH, Jiang-Shieh YF, Yang TT, Kuo YM (2016) Estrogen ameliorates microglial activation by inhibiting the Kir2.1 inward-rectifier K(+) channel. Scientific reports 6: 22864

Yang M, Brackenbury WJ (2013) Membrane potential and cancer progression. Frontiers in physiology 4: 185

Yi HA, Yi SD, Jang BC, Song DK, Shin DH, Mun KC, Kim SP, Suh SI, Bae JH (2005) Inhibitory effects of glucosamine on lipopolysaccharide-induced activation in microglial cells. Clinical and experimental pharmacology & physiology 32: 1097-103

Zhang J, Shi XQ, Echeverry S, Mogil JS, De Koninck Y, Rivest S (2007) Expression of CCR2 in both resident and bone marrow-derived microglia plays a critical role in neuropathic pain. The Journal of neuroscience : the official journal of the Society for Neuroscience 27: 12396-406

Zhu W, Zheng H, Shao X, Wang W, Yao Q, Li Z (2010) Excitotoxicity of TNFalpha derived from KA activated microglia on hippocampal neurons in vitro and in vivo. Journal of neurochemistry 114: 386-96

Zhuang ZY, Kawasaki Y, Tan PH, Wen YR, Huang J, Ji RR (2007) Role of the CX3CR1/p38 MAPK pathway in spinal microglia for the development of neuropathic pain following nerve injury-induced cleavage of fractalkine. Brain, behavior, and immunity 21: 642-51